Non-platelet Purinergic Signaling and Tissue Factor Expression

by

Yiwei Liu

A dissertation submitted to the Graduate Faculty of
Auburn University
in partial fulfillment of the
requirements for the Degree of
Doctor of Philosophy

Auburn, Alabama
December 12th, 2015

Keywords: tissue factor; transcription; thrombosis; endothelium; cell signaling

Approved by

Jianzhong Shen, Chair, Associate Professor of Drug Discovery and Development
Vishnu Suppiramaniam, Professor of Drug Discovery and Development
Murali Dhanasekaran, Associate Professor of Drug Discovery and Development
Peter Panizzi, Assistant Professor of Drug Discovery and Development
Rajesh Amin, Assistant Professor of Drug Discovery and Development
Ya-Xiong Tao, Professor of Physiology

Abstract

Objective—Our group found previously that human coronary artery endothelial $P2Y_2$ receptor mediates tissue factor (TF) up-regulation at mRNA and protein levels. The exact mechanism remains unknown and can involve increased gene transcription, mRNA stability and protein stability. Other non-platelet tissues and cells, such as monocytes and microvascular endothelium, are also known to be actively involved in thrombosis and express inducible TF. Nevertheless, whether and how this induction can be regulated by purinergic stimulation is meagerly defined. The aim of this study was to determine how non-platelet purinergic stimulation affects TF transcription and mRNA stability.

Methods and Results—Here we show for the first time that endothelial $P2Y_2R$ mediated TF transcription up-regulation as well as mRNA stabilization. A new Evi-1 binding site was found but did not affect $P2Y_2R$ mediated endothelial TF expression as shown by luciferase assay. On the other hand, Evi-1 might play a role in monocyte differentiation and TNF-α signaling due to its changes shown by Western Blotting. New AP-1 binding site and subunits c-Jun, Fra-1 and ATF-2 were associated with TF transcription in human coronary artery endothelial cells (HCAEC) as demonstrated by luciferase assay, EMSA, Western Blotting, and ChIP assay. Of the three subunits, c-Jun and ATF-2 were under control of Rho/JNK pathway while Fra-1 was activated by Src/ERK1/2 axis. Among the three pathways, $P2Y_2R$/Src/ERK1/2/Fra-1 played a negative role on TF transcription as reflected by real-time PCR of TF pre-mRNA. p38/MK-2 pathway was suggested to stabilize TF mRNA through

AU-rich element binding proteins (AREBP) as shown by Western Blotting with pharmacological inhibitors. microRNA array screening yielded 44 microRNAs significantly changed by $P2Y_2R$ activation in HCAEC. Of them, down-regulation of microRNA-181a may contribute to higher TF mRNA stability. A primary profile of purinergic stimulation affecting induced TF expression in HCAEC, HUVEC, HMVEC, THP-1 cells and human primary monocytes was established by Western Blotting.

Conclusions—Purinergic induction of TF expression follows different patterns in various tissues. In HCAEC, under UTP stimulation, TF mRNA level is up-regulated due to both promoted transcription and improved mRNA stability. A novel AP-1 binding site was identified -1362 bp upstream of transcription starting site in TF promoter. Positive pathway $P2Y_2R$/Rho/JNK/c-Jun/ATF-2 and negative pathway $P2Y_2R$/Src/ERK1/2/Fra-1 orchestrate in the transcription up-regulation. Both AREBP and microRNAs are implied to contribute to improved mRNA stability. These insights into the TF induction mechanism shed lights on better understanding of nucleotide signaling and new antithrombotic therapy.

Acknowledgments

My thesis work would not have been possible without the guidance of my committee members, help from my labmates, support from my family, and numerous friends, to only some of whom it is possible to give particular mention here.

Above all, I would like to express my deepest and sincerest gratitude to my advisor, Dr. Jianzhong Shen, for his inspiring guidance, endless patience, attentive support, and the excellent atmosphere for research, which has been invaluable and gone beyond academic level.

I would like to thank all my committee members, Dr. Vishnu Suppiramaniam, Dr. Murali Dhanasekaran, Dr. Peter Panizzi, and Dr. Rajesh Amin, for their encouraging comments, thoughtful criticism, as well as their time and efforts. My thanks also go to Dr. Ya-Xiong Tao for acceptance to be university reader. I would also like to thank Dr. David Riese for providing systemic instructions in grant-writing.

I would like to thank my labmates Dr. Wanshu Ma, Ms. Lingxin Zhang, Mr. Chuan Wang, Mr. Thamer Alqurashi, and Mr. Mohammed Nasrullah as supportive, cheerful and generous friends. I would like to express my thanks to my department friend Dr. Gayani Nanayakkara for her help in luciferase assay. I have and will always cherish the friendships and wonderful memories with Dr. Richard Davis, Dr. Subhrajit Bhattacharya, Dr. Dwipayan Bhattacharya,

Ms. Shravanthi Mouli, Ms. Pattanin Yooket, Mr. Ahmed Alhowail, Mr. Abdullah Alasmari and Mr. Daniel Katz.

I would like to acknowledge the financial, academic, and technical support of the Harrison School of Pharmacy, Auburn University, and our staff that provided the indispensable supports for my life here.

There were numerous loving and caring people that accompanied me during my study in Auburn. Ms. Emily Ebner, Ms. Nesha Burch, the Lamberts, and Ms. Rachel Sedlacek embraced me as part of their families. Dr. Saranrat Wittayanukorn has been a friend with pungent personality, strong will, and perpetual support.

Finally, I would like to thank my parents for their unconditional love, selfless sacrifice to support my dream, and much more for which my mere expression of thanks likewise does not suffice. I hope what I did make them proud.

Table of Contents

List of Tables

List of Figures

List of Abbreviations

Coronary artery diseases (CAD)

Tissue factor (TF)

AU-rich element (ARE)

AU-rich element binding protein (AREBP)

Vascular adhesion molecule-1 (VCAM-1)

Intercellular adhesion molecule-1 (ICAM-1)

Lipopolysaccharide (LPS)

Ecotropic virus integration site 1 protein homolog (Evi-1)

Activator protein 1 (AP-1)

Phorbol myristate acetate (PMA)

Vascular endothelial growth factor (VEGF)

Human coronary artery endothelial cell (HCAEC)

Human umbilical vein endothelial cell (HUVEC)

Human microvascular endothelial cell adult dermis (HMVECad)

Tumor necrosis factor-α (TNF-α)

3'-untranslated region (3'-UTR)

Fetal bovine serum (FBS)

ATP binding cassette transporter (ABC transporter)

High-density lipoprotein-cholesterol (HDL-C)

Mitogen-activated protein kinase (MAPK)

Nitric oxide (NO)

Nuclear factor kappa B (NF-κB)

Extracellular signal-regulated kinase 1/2 (ERK)

Protein kinase B (AKT)

P38 mitogen-activated protein kinase (p38)

c-Jun N-terminal kinase (JNK)

Small interfering RNA (siRNA)

Human peripheral blood mononuclear cells (PBMCs)

Reverse transcription polymerase chain reaction (RT-PCR)

Glyceraldehyde 3-phosphate dehydrogenase (GAPDH)

Fluorescein isothiocyanate (FITC)

Immunoglobulin G (Ig G)

Phosphate buffered saline (PBS)

Immunohistochemistry (IHC)

Heterogeneous nuclear RNA (hnRNA)

Adenosine triphosphate (ATP)

Uridine-5'-triphosphate (UTP)

Uridine diphosphate (UDP)

Chapter 1. Introduction

1.1. Thrombosis

Thrombosis is the morbid formation of a blood clot (thrombus) inside a blood vessel, obstructing the flow of blood through the circulatory system. Hemostasis, or normal blood clotting, is beneficial for survival, while pathological thrombus poses significant health hazard. A pathological thrombus, formed when there is an imbalance in the blood coagulation system, can potentially obstruct blood flow, leading to a number of serious health (Viles-Gonzalez et al., 2004). Risk factors from three aspects contribute to the formation of thrombus, as postulated in Virchow's triad: 1) the hypercoagulability or thrombophilia status of blood composition, 2) change in vascular components (endothelium injury during surgery), and 3) blood flow disturbance, for example, one caused by atrial fibrillation (Furie and Furie, 2008; Wolberg et al., 2012). Two different types of thrombi can be formed: arterial thrombi and venous thrombi. Arterial thrombosis has long been held to be mainly a phenomenon of platelet activation, whereas venous thrombosis is largely a matter of activation of the clotting system (Prandoni, 2009).

The most common arterial thrombosis is a complication of atherosclerosis also termed as "atherothrombosis", and is a subject taking over in literature to describe an important facet of the disease other than hyperlipidemia and inflammation. Atherosclerosis is a pathological condition in which the artery wall thickens mainly due to the accumulation of lipids such as cholesterol and triglyceride in form of modified lipoproteins. Monocytes derived macrophages

scavenge the lipoproteins and become lipid-laden foam cells. This results in the formation of lesions or fatty streaks, which progress into complex plaques involving vascular smooth muscle cell (VSMC) migration and proliferation. VSMC deposits extracellular matrix during this process and form a fibrous cap for the plaque. At the same time, local leukocytes and resident vascular wall cells can secrete inflammatory cytokines and coagulation initiating tissue factor. The inflammatory mediators further induce expression of matrix-degrading proteinases that weaken fibrous cap of plaque. If fibrous cap ruptures at point of weakening, coagulation factors in blood can gain access to thrombogenic, tissue factor–containing lipid core, causing thrombosis, as shown in stage 5 in Figure 1.1. Thrombus formed as such may resorb by themselves. In some cases, occlusive thrombi arise not from fracture of fibrous cap but from superficial erosion of endothelial layer, resulting in mural thrombus, as shown in stage 7 in Figure 1.1. However, superficial erosions do not necessarily occur after fibrous cap rupture, as depicted in this idealized diagram. (Libby, 2001; Stary et al., 1995)

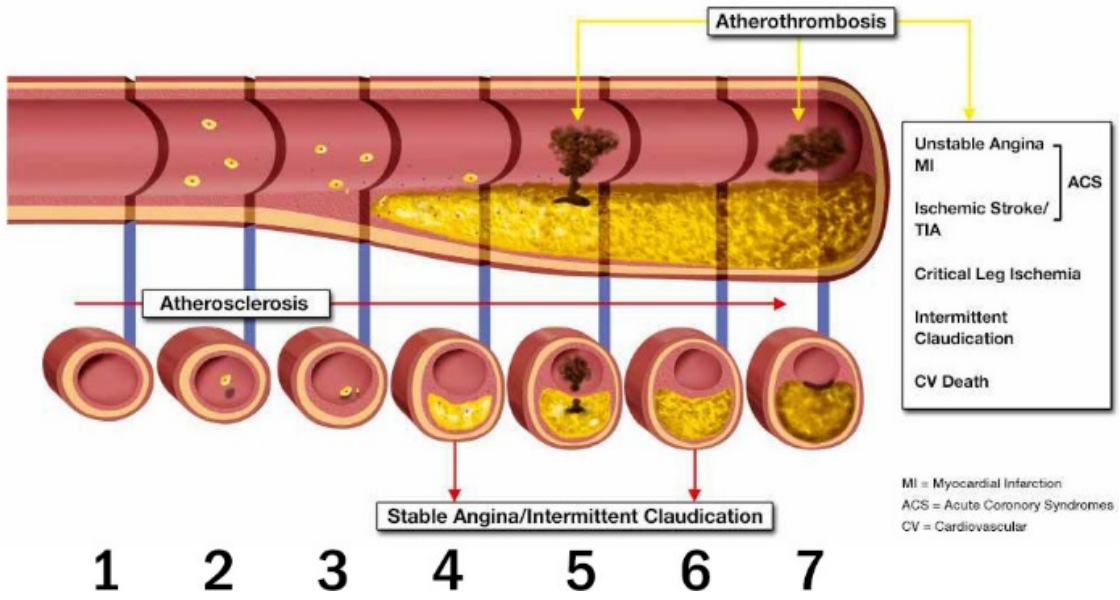

Figure 1.1. Scheme of atherosclerosis progression and atherothrombosis.

Adapted from Libby P. *Circulation*. 2001; 104: 365-372

Atherothrombosis is the underlying condition that results in serious disease and complications through different vascular territories. The three main clinical manifestations of atherothrombosis are coronary artery disease (CAD) (myocardial infarction and angina pectoris), cerebral ischaemia (stroke), and peripheral arterial disease (claudication). CAD, also called CHD (coronary heart disease), is the most common form of heart disease in the US and Europe, and is a serious health problem worldwide. It is characterized by a narrowing or an occlusion of the coronary arteries resulting in inadequate blood flow to the heart muscle itself, and preventing the heart from receiving enough blood and oxygen supply. Angina pectoris, characterized by temporary chest pain or discomfort due to reduced oxygen supply to the heart, is a symptom of CAD. Despite optimal medical treatment with modern medications, revascularization procedures with device therapy, and surgery, CAD is a leading cause of sudden death. The excessive mortality of CAD is primarily due to rupture and thrombosis of the atherothrombotic plaque. According to the American Heart Association, more than 13 million Americans have a history of CHD and 7.5 million have experienced an acute heart attack. The epidemical impact is still on the rise, occupying 17% of national health expenditure in the United States and is predicted to affect 40.5% of its population by 2030 (Heidenreich et al., 2011).

Revascularization procedures to treat CAD can further cause secondary thrombosis themselves. For example, patients receiving stent angioplasty and coronary bypass grafting are exposed to high risk of conditions of stent thrombosis and graft occlusion respectively (Farooq et al., 2013; Kappetein et al., 2011). Antiplatelet therapy can significantly prevent ischemic

complications involving the heart, brain, kidneys, and gastrointestinal tract after coronary bypass surgery (Mangano and Multicenter Study of Perioperative Ischemia Research, 2002).

1.2. Thrombosis Therapeutics

Both antithrombotics and fibrinolytic agents are used to prevent or treat thrombosis. Antithrombotics are further divided into antiplatelets, such as Aspirin and Plavix (Clopidogrel), and anticoagulants, such as direct thrombin inhibitor Dabigatran and direct Factor Xa inhibitor Rivaroxaban (Pudusseri et al., 2013).

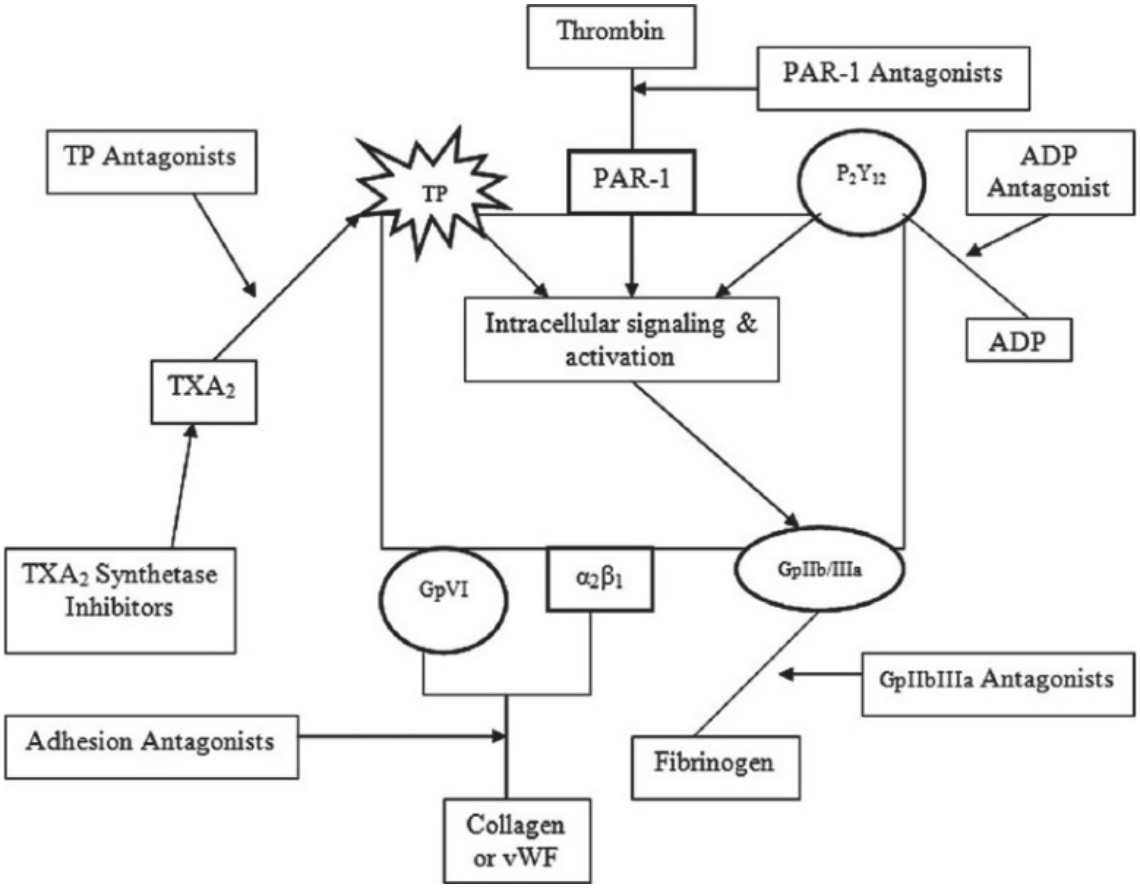

Figure 1.2. Site of action of various antiplatelet drugs.

Antiplatelets work by inhibiting 1) platelets' adhesion, 2) platelets' activation, 3) platelets' aggregation, and 4) platelet mediated links with inflammation.

Adapted from Sikka P and Bindra VK. *Indian Journal of Critical Care Medicine*. 2010

Since arterial thrombosis is dominant by platelet activation as stated earlier (Prandoni, 2009), antiplatelets are applied for this condition routinely. These drugs are classified on the basis of their site of action as shown in Figure 1.2. The first antiplatelet drug was aspirin, which has been used to relieve pain for more than 100 years. It is a cyclooxygenase (COX) inhibitor with selectivity preferring COX-1 over COX-2. In the mid-1960s, scientists showed that aspirin prevented platelets from clumping, and subsequent clinical trials showed that it reduces the risk of stroke and heart attack. In 1980, researchers showed that aspirin in very low doses (much lower than that required to relieve a headache) blocked the production of thromboxane A_2 (TXA2) in platelets that is required for platelet clumping due to its selectivity (Schror, 1997). During that time, better understanding of the process of platelet clumping allowed the development of designer antiplatelet drugs directed at specific targets. Now there are more potent antiplatelets on the market, such as Clopidogrel (ADP-receptor/P2Y12 antagonist), dipyridamole (phosphodiesterase inhibitor), and abciximab (GPIIb/Illa receptor antagonists). These drugs are used with aspirin or alone to effectively prevent heart attack and stroke. They also prolong the lives of patients who have already had a heart attack (Sikka and Bindra, 2010).

Clopidogrel is another potent antiplatelet drug acts by inhibiting ADP-induced platelet aggregation. Results of large clinical trials have demonstrated an overall benefit of clopidogrel over aspirin in the prevention of vascular ischemic events (myocardial infarction, stroke, vascular death) in patients with a history of symptomatic atherosclerotic disease. The antiaggregating effect of clopidogrel is attributed to an irreversible blockage of ADP binding to a purinergic receptor P2Y12 present at the platelet surface (Cattaneo, 2011). Clopidogrel is a

prodrug which requires CYP2C19 (at lower dose) and CYP3A4 (at higher dose) in liver for its activation (Zahno et al., 2010).

1.3. Tissue Factor

Tissue factor (TF), also known as factor III, is an integral transmembrane glycoprotein that is normally not exposed to circulation. TF is the initiator of the extrinsic coagulation pathway, which proceeds at the presence of Ca^{2+} to sequentially activate zymogens: FVII, factor X (FX), and prothrombin (FII) for the generation of coagulant mediators: FVIIa, FXa, and thrombin (FIIa), respectively. As a result, thrombin cleaves fibrinogen into fibrin that cross-link to produce insoluble blood clots. TF is found in the central nervous system (astrocytes), organ capsules, lungs (alveolar cells), and placenta (trophoblasts) at relatively high density (Drake et al., 1989; Fleck et al., 1990). In a normal blood vessel, TF is expressed mostly in tunica adventitia (fibroblasts and connective tissues), moderately in tunica media (smooth muscle cell), but undetectable in endothelium (Wilcox et al., 1989).

A diversity of stimuli can induce tissue factor in endothelium. Some are endogenous molecules, such as tumor necrosis factor-α (TNF-α), interlukin-1b, CD40 ligand (Steffel et al., 2006), or UTP; others are exogenous ones, such as endotoxin (Colucci et al., 1983) and caffeine (Gebhard et al., 2012); and still others are mechanic changes like shear stress (Houston et al., 1999). Monocytes, like endothelial cells, show very little to no basal expression of TF. Its expression can be induced by inflammatory stimuli such as C-reactive protein (Cermak et al., 1993), CD40 ligand (Mach et al., 1997), platelet-derived growth factor (PDGF), angiotensin II, and oxidized LDL (He et al., 2006; Wada et al., 1994); yet one of the most extensively studied

stimuli in this cell type is endotoxin, represented by lipopolysaccharide (LPS) (Guha and Mackman, 2002). In atherosclerosis plaque, foam cells transformed from monocyte-derived macrophages show increased TF expression as well (Meisel et al., 2002). Tissue factor is not only present in vascular cells or leukocytes but can also be detected in the bloodstream, referred to as circulating or blood-borne TF. This form of TF is mainly associated with microparticles originating from endothelial cells, vascular smooth muscle cells, circulating leukocytes, platelets, (Giesen et al., 1999) or even atherosclerosis plaques (Mallat et al., 2000). Thus, TF is a risk factor in thrombus formation both as a blood composition (TF in circulating cells and microparticles) and a vascular components (in subendothelial tissues and endothelium) (Butenas et al., 2009).

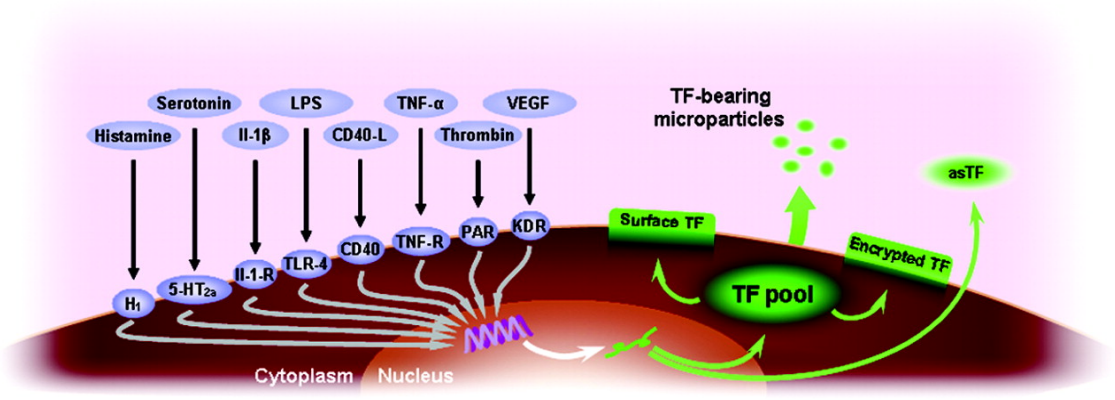

Figure 1.3. Induction of tissue factor expression and activity.

Adapted from Steffel J, Lüscher TF and Tanner FC. *Circulation.* 2006

Increased TF expression and activity is characterized in unstable atherosclerotic plaques and correlated with higher risk of atherothrombosis which will lead to myocardial infarction and ischemic stroke (34). Recent evidence suggests that inhibition of tissue factor or elements in the tissue factor pathway (e.g., factors VIIa and Xa, or thrombin) has the potential to further improve outcomes in atherothrombosis (Sambola et al., 2003). Elevated levels of TF are also

characterized in patients with other cardiovascular syndromes such as hypertension, diabetes and dyslipidemia (Steffel et al., 2006). In line with thrombosis occurrence, TF elevation is observed in other pathological conditions which possess inflammation and thrombosis propensity. TF, in the form of TF-FⅦa-PAR2 complex, is elevated in cancer, obesity, and type 2 diabetes mellitus (T2DM), and is attributed to metastasis (Ruf et al., 2011), weight gain (Badeanlou et al., 2011) and insulin resistance (Gerrits et al., 2011; Gerrits et al., 2009) respectively. Monoclonal inhibitory TF antibody saved baboons challenged with E.coli from septic shock (Taylor et al., 1991), indicating its critical role in disseminated intravascular coagulation (DIC).

In general, TF expression is mediated by activations of multiple intracellular signaling pathways. On signal transduction level, the MAP kinases p38, p44/42 (ERK), and c-jun terminal NH2-kinase (JNK), and protein kinase C are commonly discussed as positive pathways. In contrast, PI3K/Akt pathway is known to negatively regulate TF expression (19). On transcription level, endothelial tissue factor was shown to under concerted regulation of NF-κB, AP-1, and Sp-1 in porcine aortic cells by binding to sequences in a 300 bp region (Moll et al., 1995). Early growth response protein 1 (Egr-1) is also involved in TF transcription in mononuclear cells and affect process of diseases such as pulmonary fibrosis (Aljada et al., 2002; Yan et al., 1998).

1.4. Endothelial Function and Dysfunction

Vascular endothelium not only serves as a passive barrier between flowing blood and the vascular wall, but also maintains vascular homeostasis using this strategic location. It plays a pivotal role in modulating vascular tone, caliber, and blood flow in response to neural, humoral, and mechanical stimuli by synthesizing and releasing vasoactive substances. This is mainly achieved by constitutively expressing the enzyme endothelial nitric oxide synthase (eNOS) which generates nitric oxide (NO) (Palmer et al., 1988). NO acts on VSMC by activation of guanylate cyclase leading to increased production of cyclic guanosine monophosphate (cGMP) and a reduction in intracellular calcium, resulting in its relaxing

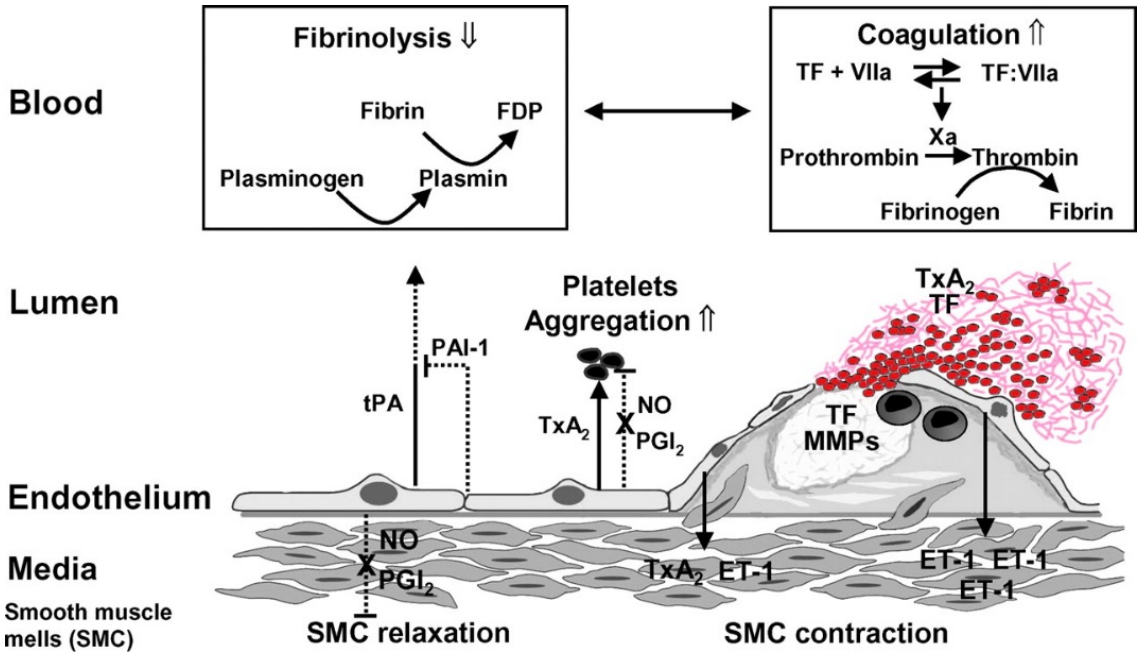

effect.

Figure 1.4. Normal and abnormal endothelial function.

Adapted from Viles-Gonzalez JF, Fuster V and Badimon JJ. *European Heart Journal.* 2004.

The role of the endothelium is not confined to the regulation of vascular tone and vasomotor function but extends to the regulation of inflammation, platelet activation, and thrombosis. NO actively mediates many of these functions exerted by intact endothelium. In addition to its

potent vasodilating effect, NO counteracts leukocyte adhesion to the endothelium (Gauthier et al., 1995; Kubes et al., 1991), vascular smooth muscle proliferation (Cornwell et al., 1994), and platelet aggregation (de Graaf et al., 1992). These biologic actions of NO make it an important component in the endogenous defense against vascular injury, inflammation, and thrombosis.

Disruption of the functional integrity of the vascular endothelium plays an integral role in all stages of atherosclerosis ranging from lesion initiation to plaque rupture. Under the influence of cardiovascular risk factors (e.g., plasma homocysteine level) that disturb vascular homeostasis, the endothelium becomes dysfunctional (Weiss et al., 2002), resulting in enhanced production of cytokines and expression of cellular adhesion molecules (VCAM-1, ICAM-1, PECAM-1, E-selectin and L-selectin ligand etc.) by the endothelium. Adhesion molecules play a crucial role in the interaction of the endothelial surface with circulating leukocytes and mediate the anchoring of leukocytes and their infiltration into the intima of the vessel wall (Ley and Tedder, 1995; Luscinskas et al., 1994; Springer, 1994). Further into the process of atherosclerosis, dysfunctional endothelium sets the stage for both initiation and progression of atherosclerotic lesions by promoting inflammation within the vessel wall (Behrendt and Ganz, 2002). Unstable plaque tends to disrupt at the site of activated endothelial cells (Johnson-Tidey et al., 1994; Poston et al., 1992). Proinflammatory actions of dysfunctional endothelium potentially play an important role in converting stable atheromatous plaques into unstable plaques prone to rupture. Dysfunctional endothelium also leads to increased production of plasminogen activator inhibitor–1, an inhibitor of fibrinolysis, and reduced production of the fibrinolytic component tissue plasminogen activator contributing to a thrombogenic state (Tomiyama et al., 1998).

Statins and angiotensin-converting enzyme (ACE) inhibitors confer large clinical benefit in patients with atherosclerosis. The mechanisms responsible for this substantial benefit appear to extend beyond the cholesterol and blood pressure-lowering effect, respectively, and may involve favorable effects on endothelial function. Clinical studies have shown that cholesterol lowering with statins improves coronary endothelial function in patients with hypercholesterolemia or CAD (Anderson et al., 1995). Improvement in brachial endothelial function with statin therapy has been shown in both healthy middle-aged males and patients with hypercholesterolemia, CAD, and acute coronary syndromes (Cohen et al., 2000). Improvement of endothelial vasomotor function occurs early after initiation of statin therapy and can be observed over a period of weeks in conduit and resistance arteries in both the coronary and forearm circulation (Uehata et al., 1997). Similarly, in patients with atherosclerosis or its risk factors, ACE inhibitors, and especially the ones with high tissue affinity such as quinapril, seem to improve endothelial vasomotor function (Mancini et al., 1996).

1.5. Nucleotides and Purinergic Receptors

Nucleotides are organic molecules that serve as the monomers, or subunits, of nucleic acids like DNA and RNA, which are vital biological materials. Nucleotides are composed of a nitrogenous base, a five-carbon sugar (ribose or deoxyribose), and at least one phosphate group. Thus a nucleoside plus a phosphate group yields a nucleotide. Nucleotides serve as universal currency of energy transaction in the form of the nucleoside triphosphates (ATP, GTP, CTP and UTP), playing a central role in metabolism. In addition, nucleotides participate

in intracellular signaling in the form of cGMP and cAMP, and are incorporated into important cofactors of enzymatic reactions, such as coenzyme A, FAD, FMN, NAD, and NADP+. Other than that, they are also short-term signaling molecules and long-term trophic messengers (Burnstock, 2011).

A nucleotide is referred to as either a purine or a pyrimidine depending on the structure of its nitrogenous base. For example, ATP and GTP are purines, and UTP, TTP and CTP are pyrimidines. The first description of the extracellular signaling by purines was by Drury and Szent-Gyorgyi (Drury and Szent-Gyorgyi, 1929), and purinergic receptors were defined in 1976 (Burnstock, 1976). It was recognized later that pyrimidines can have the same effect on purinergic receptors as purines (Seifert and Schultz, 1989). Today, a systematical classification of these receptors is well-established as shown in Table 1.1 together with their signaling features.

Table 1.1. The families of P2X and P2Y receptors

Receptor	Agonist	Signaling
$P2X_1$-$P2X_7$	ATP	Ligand-gated cation channels
$P2Y_1$	ADP	Gq/PLC/Ca^{2+}+PKC
$P2Y_2$	ATP/UTP	Gq/PLC/Ca^{2+}+PKC
$P2Y_4$	UTP	Gq/PLC/Ca^{2+}+PKC
$P2Y_6$	UDP	Gq/PLC/Ca^{2+}+PKC
$P2Y_{11}$	ATP	Gq/PLC/Ca^{2+}+PKC and Gs/AC/ ↑ cyclic AMP
$P2Y_{12}$	ADP	Gi/AC/ ↓ cyclic AMP; ion channels

$P2Y_{13}$	ADP	Gi/AC/ ↓ cyclic AMP; ion channels
$P2Y_{14}$	UDP-glucose/galactose	Gi/AC/ ↓ cyclic AMP; ion channels

Two major receptor subfamilies have been described, P2X and P2Y. The P2X receptors are ligand-gated channels that gate extracellular cations in response to ATP and comprise seven receptor subtypes ($P2X_1$ to $P2X_7$) (Habermacher et al., 2015). The P2Y receptors are G-protein-coupled receptors that are categorized into a subfamily of receptors that predominantly couple to G_q ($P2Y_{1/2/4/6/11}$) and therefore activate phospholipase C-beta, and into a subfamily of G_i-coupled receptors ($P2Y_{11/12/13/14}$) that inhibit adenylyl cyclase and regulate ion channels. It is noteworthy that $P2Y_{11}$ receptor is coupled to both phospholipase C and adenylyl cyclase activation (Jacobson et al., 2015). Pharmacologically speaking, P2Y receptors can be divided into the adenine-nucleotide-preferring receptors (human and rodent $P2Y_{1/12/13}$ and human $P2Y_{11}$) mainly responding to ATP and ADP the uracil-nucleotide-preferring receptors (human $P2Y_4$ and $P2Y_6$) responding to UTP and UDP, receptors that are less selective (human and rodent $P2Y_2$ and rodent $P2Y_4$), as well as nucleotide-sugar-preferring human $P2Y_{14}$ receptor responding to UDP-glucose and UDP-galactose (Abbracchio et al., 2006).

Purinergic receptors mediate various physiological functions. The regulation of vascular tone in the endothelium of blood vessels is mediated by purinergic signaling. A decreased concentration of oxygen releases ATP from erythrocytes, triggering a propagated calcium wave in the endothelial layer of blood vessels and a subsequent production of nitric oxide that results in vasodilation (Lohman et al., 2012). During the blood clotting process, adenosine diphosphate (ADP) plays a crucial role in the activation and recruitment of platelets and also

ensures the structural integrity of thrombi. These effects are modulated by the $P2Y_1$ and the $P2Y_{12}$ receptors. The $P2RY_1$ receptor is responsible for morphologic change in platelets, increased intracellular calcium levels and transient platelet aggregation, while the $P2Y_{12}$ receptor is in charge of sustaining platelet aggregation through the inhibition of adenylate cyclase and a corresponding decrease in cyclic adenosine monophosphate (cAMP) levels. The activation of both purinergic receptors is necessary to achieve sustained hemostasis (Barn and Steinhubl, 2012). In immune system, nucleotide can act either as an immunosuppressive or an immunostimulatory factor, depending on the cytokine microenviroment and the type of receptor present. In leukocytes such as macrophages, dendritic cells, lymphocytes, eosinophils, and mast cells, purinergic signaling plays a pathophysiological role in calcium mobilization, actin polymerization, release of mediators, cell maturation, cytotoxicity, and apoptosis (Jacob et al., 2013). Large increase in extracellular nucleotides that is associated with apoptosis serve as a find-me signal to promote phagocytic clearance (Elliott et al., 2009). Another crucial stage of purinergic signaling is in the central nervous system where nucleotides are secreted as neurotransmitters in vesicles from synaptic terminals and binds to a plethora of ionotropic and metabotropic receptors. It has an excitatory effect on neurons, and acts as a mediator in neuronal–glial communication (Fields and Burnstock, 2006). The $P2Y_6$ receptor, which is primarily mediated by uridine diphosphate (UDP), plays a significant role in microglial phagoptosis, a type of cell death caused by phagocytosis, while the $P2Y_{12}$ receptor functions as a specialized pattern recognition receptor (Ransohoff and Perry, 2009). $P2X_4$ receptors are involved in the CNS mediation of neuropathic pain (North and Verkhratsky, 2006). On top of that, nucleotides and purinergic signaling influence bile secretion, liver metabolism and regeneration (Oliveira et al., 2013), mucociliary clearance (Lazarowski and Boucher, 2009), bone formation (Orriss et al., 2010) and so forth.

1.6. Extracellular Nucleotide Homeostasis: Release and Degradation

It is pivotal for normal physiology of human body to maintain extracellular nucleotide homeostasis. Usually, the steady state cytosolic concentration of ATP is 3-10 mM to maintain normal metabolic and enzymatic reactions. Steady state extracellular nucleotide varies by tissue and location, but much lower than intracellular one. This gradient favors channeled diffusion. Concentration of UTP and UDP follow the same pattern, only much lower (in micro molar) (Schwiebert and Fitz, 2008). The turnover of extracellular nucleotides are regulated by intricate release and hydrolysis mechanisms.

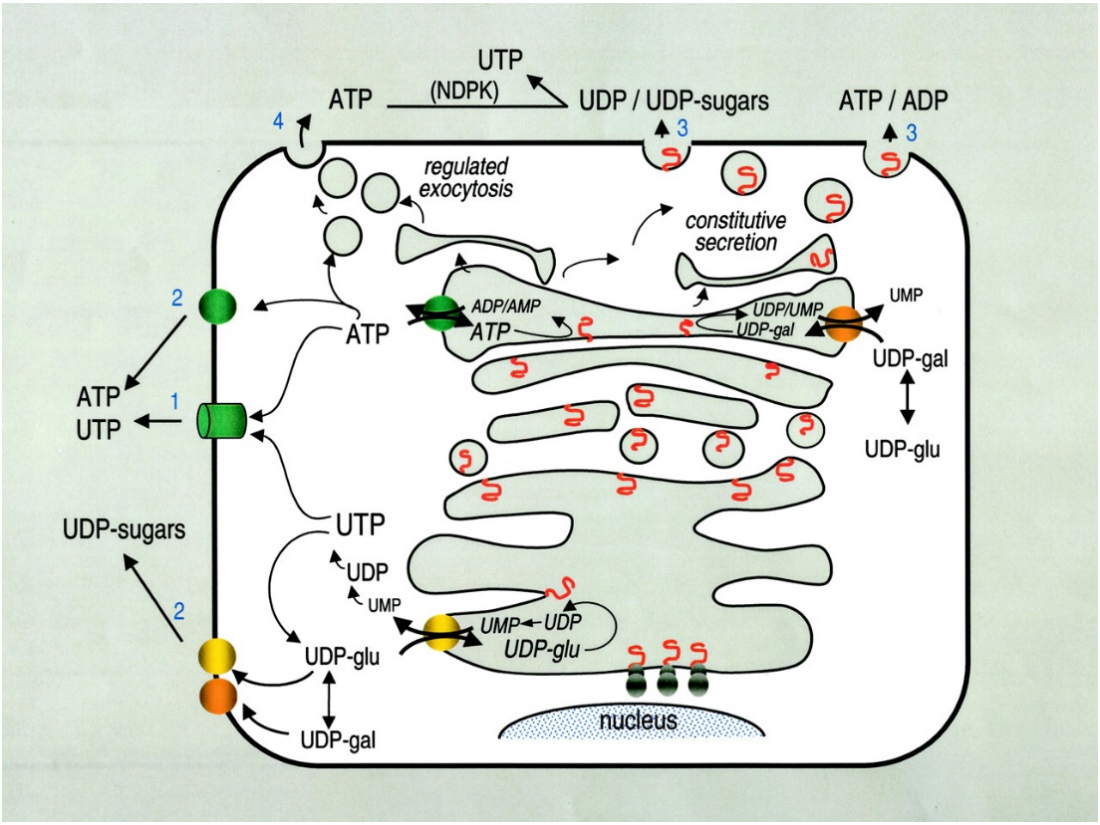

Figure 1.5. Pathways for nucleotide and nucleotide sugar release. 1. Nucleotide transporter, 2. Connecxin hemichannel and innexin/pannexin channel, 3. Constitutive secretion, 4. Regulated exocytosis.

Adapted from Lazarowski et al. *Molecular Pharmacology*. 2003.

Massive leakage of nucleotides might occur upon cell lysis, however this nonspecific mechanism is restricted by or organ injury, traumatic shock or certain inflammatory conditions (Bours et al., 2006). Non-lytic mechanisms of nucleotide efflux represent a distinct and important route of nucleotide appearance in the extracellular milieu. Various excitatory/secretory tissues such as nerve terminals and chromaffin cells (Burnstock, 2007) pancreatic acinar cells (Sorensen and Novak, 2001) and circulating platelets (Gachet, 2006) store ATP and ADP, together with other neurotransmitters and extracellular mediators, in specialized granules (called synaptic vesicles, chromaffin granules or dense core granules) and regulate the release of nucleotide-containing vesicles in a Ca^{2+}-dependent manner via regulated exocytosis. Moreover, nucleotide release occurs from various non-excitatory tissues, including the epithelial (Homolya et al., 2000) and endothelial cells (Bodin and Burnstock, 2001), astrocytes and other glial cells (Lazarowski et al., 2000), fibroblasts (Gerasimovskaya et al., 2002), hepatocytes (Fabre et al., 2006), bone cells, joints and keratinocytes (Burrell et al., 2005), cardiomyocytes (Vassort, 2001), erythrocytes (Sprague et al., 2007), neutrophils (Eltzschig et al., 2006), monocytes/macrophages (Wong et al., 2006) and other hematopoietic cells (Bours et al., 2006). These cells have been shown to release ATP transiently under various mechanical and other stimuli, such as shear stress, hypotonic swelling, hypoxia, stretching, hydrostatic pressure, as well as in response to bradykinin, serotonin and other Ca^{2+}-mobilizing pharmacological agonists. Moreover, the cells release low nanomolar concentrations of ATP at certain basal rates (Lazarowski et al., 2000) and distinctive mechanisms could underlie

constitutive versus stress-stimulated nucleotide release. The diversity of conditions in which the cells release ATP and/or ADP suggests the implication of multiple nucleotide-releasing pathways. The proposed cellular mechanisms might include 1) facilitated diffusion by nucleotide-specific ATP-binding cassette (ABC) transporters, such as the cystic fibrosis transmembrane conductance regulator (CFTR), the multidrug resistance proteins, and the multiple organic anion transporters; 2) electro-diffusional movement through membrane ion channels, including connexin hemichannels, stretch- and voltage-activated channels; and 3) cargo-vesicle trafficking and exocytotic granule secretion (Lazarowski et al., 2003) (Figure 1.5.)

Subsequent to the signal transduction, extracellular nucleotides need to be rapidly inactivated to adenosine. This process involves several different transmembrane enzymes as delineated in Figure 1.6. using ATP as an example: 1) ecto-nucleotide pyrophosphatase/phosphodiesterase (E-NPP) family, 2) ecto-nucleoside triphosphate diphosphohydrolase (E-NTPDase) family, and 3) ecto-5'-nucleotidase (NT5E) (Yegutkin, 2008). Among these hydrolases, CD39 (a member of the E-NTDPase family), and CD73 (a member of the NT5E family) are the major nucleotide metabolizing enzymes especially in immunity and inflammation regulation. D39 and CD73 are important for calibrating the duration, magnitude, and composition of the "purinergic halo" surrounding the multiple types of cells, especially immune cells and cancer cells (Ghiringhelli et al., 2012).

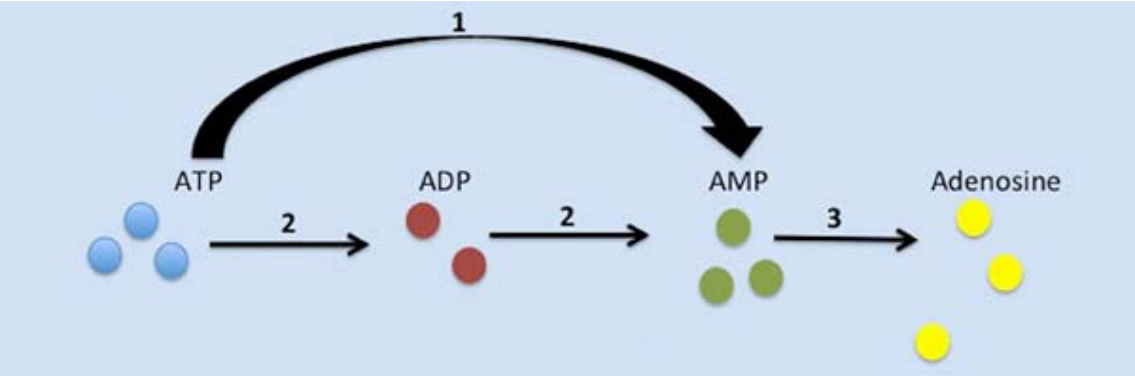

Figure 1.6. Major purine-inactivating activities on the cell surface.

Adapted from Velasquez S and Eugene EA, *Frontiers in Physiology*. 2014

CD39 is an integral membrane protein that phosphohydrolyzes ATP, and less efficiently ADP, in a Ca^{2+}- and Mg^{2+}-dependent fashion, to yield AMP (Heine et al., 2001). Human CD39 is a 510-amino acid protein with seven potential N-linked glycosylation sites, 11 Cys residues, and two transmembrane regions (Luscinskas et al., 1994). Structurally, it is characterized by two transmembrane domains, a small cytoplasmic domain comprising the NH2- and COOH-terminal segments, and a large extracellular hydrophobic domain consisting of five highly conserved domains, known as apyrase conserved regions (ACR) 1–5, which are pivotal for the catabolic activity of the enzyme (Heine et al., 2001). CD39 becomes catalytically active upon its localization on the cell surface, and its glycosylation is crucial for correct protein folding, membrane targeting, and enzyme activity (Smith and Kirley, 1998). CD39 is constitutively expressed in spleen, thymus, lung, and placenta (Enjyoji et al., 1999; Kapojos et al., 2004; Mizumoto et al., 2002; Zimmermann, 1999), and in these organs it is associated primarily with endothelial cells and immune cell populations, such as B cells, natural killer (NK) cells, dendritic cells, Langerhans cells, monocytes, macrophages, mesangial cells, neutrophils, and regulatory T cells (Dwyer et al., 2007). CD39 expression is regulated by several pro-inflammatory cytokines, oxidative stress and hypoxia (Eltzschig et al., 2009)

through the transcription factors Sp1, Stat3, and zinc finger protein growth factor independent-1 transcription factor (Chalmin et al., 2012). In addition, the expression of CD39 is increased in several solid tumors, such as, colorectal cancer, head and neck cancer, pancreatic cancer, as well as in chronic lymphocytic leukemia, suggesting this enzyme is also involved in the development and progression of malignancies (Bastid et al., 2013). Recently, a soluble catalytically active form of CD39 has been shown to circulate in human and murine blood (Yegutkin et al., 2012).

The second step in the metabolism of purine nucleotides is accomplished by CD73, which dephosphorylates extracellular AMP to adenosine. Structurally, CD73 is a dimer of two identical 70 kD subunits, anchored to the plasma membrane via a C-terminal serine residue, Ser 523, linked to glycosylphosphatidyl inositol (GPI), with no membrane-embedded protein segments (Strater, 2006). A soluble form of CD73 can be shed from the membrane through proteolytic cleavage or hydrolysis of the GPI anchor by phosphatidylinositol-specific phospholipase (Heuts et al., 2012). The mature form of CD73 consists of 548 amino acids with an estimated molecular mass of 61 kDa, comprising a 26-amino acid signal peptide at the N-terminus and a C-terminal sequence for the attachment to the pre-formed GPI anchor. The N-terminal domain coordinates the binding of two catalytic divalent metal ions (Co^{2+} and Zn^{2+}) whereas the C-terminal domain provides the binding pocket for AMP (Strater, 2006). Of note, ADP and ATP act as competitive inhibitors of CD73 (Knapp et al., 2012). CD73 is found in a variety of tissues, including colon, brain, kidney, liver, lung, and heart (Thompson et al., 2004); on leukocytes derived from peripheral blood, spleen, lymph nodes, thymus and bone marrow (Thompson et al., 2004); as well as on endothelium (Lennon et al., 1998). There is evidence that the expression and function of CD73 are upregulated under hypoxic conditions (Eltzschig

et al., 2003; Synnestvedt et al., 2002), as well as by the presence of several pro-inflammatory mediators, such as transforming growth factor (TGF)-β, interferons (IFNs), tumor necrosis factor (TNF)-α, interleukin (IL)-1β and prostaglandin E2 (Beavis et al., 2012; Regateiro et al., 2011). An increase in CD73 expression has also been reported in several neoplastic tissues (Beavis et al., 2012), suggesting the involvement of this enzyme in the onset and progression of neoplasia.

Altogether, the effect of these two enzymes drives a shift from an ATP-driven pro-inflammatory environment to an anti-inflammatory milieu induced by adenosine. The CD39/CD73 pathway changes dynamically with the pathophysiological context in which it is embedded. It is becoming increasingly appreciated that altering this catabolic machinery can change the course or dictate the outcome of several pathophysiological events, such as AIDS, autoimmune diseases, infections, atherosclerosis, ischemia-reperfusion injury, and cancer, suggesting these ecto-enzymes are novel therapeutic targets for managing a variety of disorders.

1.7. Purinergic Signaling in Thrombosis

Thrombosis is a major complication of atherosclerosis together with hyperlipidemia and inflammation. Other than the previously mentioned effect of $P2Y_{1/12}$ on platelet clotting, other nucleotide-related mechanisms also exist to adjust the process of thrombosis. Progression of platelet recruitment in association with endothelium activation is enhanced by adenosine nucleotides, which are released from damaged endothelium or other vascular cells, and are secreted in high concentrations by platelets in response to exogenous ADP. This provides an

important positive feedback mechanism. A critical regulatory element in the control of platelet thrombus formation may be the expression of CD39 on endothelium. It has been shown that the antithrombotic effect of the CD39, like heparan sulfate and thrombomodulin, is lost following endothelium activation, both in vitro and in vivo (Robson et al., 1997). Systemic administration of soluble derivatives of CD39 or targeted expression of the native protein to sites of vascular injury may have future therapeutic application (Qawi and Robson, 2000).

On the other hand, purified, unstimulated platelets themselves lack of have minimal CD39 functional activity but release CD39 present on microparticles may be a key modulatory influence of thrombosis. In this regard, monocyte-derived microparticles can bind to activated platelets in the developing thrombus through interaction between platelet P-selectin and microparticle P-selectin glycoprotein ligand 1 (PSGL-1) (Falati et al., 2002; Falati et al., 2003). It is inferred that as the platelet thrombus forms, in parallel, microparticles accumulate in the growing aggregate, which deliver the associated membrane CD39. Hence, CD39, and associated NTPDase activity, is not initially a substantive part of the thrombus but only accumulates after platelet thrombus formation matures. The spatial and temporal expression of NTPDases in the accumulating microparticles may therefore regulate thrombus size by regulating the hydrolysis and hence inactivation of the platelet agonist ADP, ultimately resulting in the observed deaggregation responses (Atkinson et al., 2006).

On platelets, other than $P2Y_1$ and $P2Y_{12}$, $P2X_1$ receptors act to amplify platelet activation and aggregation induced by other platelet agonists. All three of them critically contribute to thrombus stability in small arteries. Besides platelets, studies indicate that these receptors are expressed by neutrophils as well. In a laser-induced injury mouse model of thrombosis, it

appears that neutrophils are required to initiate thrombus formation and coagulation activation on inflamed arteriolar endothelium (Hechler and Gachet, 2015). By using $P2X_1^{-/-}$ mice, researchers recently showed that $P2X_1$ receptors, expressed on platelets and neutrophils, play a key role in thrombus growth and fibrin generation. Intriguingly, in a model of endotoxemia, $P2X_1^{-/-}$ mice exhibited aggravated oxidative tissue damage, along with exacerbated thrombocytopenia and increased activation of coagulation (Oury et al., 2015).

1.8. P2Y2 Signaling

The P2Y2 receptor (Protein Accession Number: P41231) belongs to the family of nucleotide-activated P2Y receptors, featured by seven hydrophobic transmembrane domains connected by three extracellular loops and three intracellular loops. At the extracellular domains, 4 cysteins residues form two disulfide bridges both of which are essential for receptor function. A consensus Arg-Gly-Asp (RGD) integrin-binding domain in its first extracellular loop can bind to $\alpha v\beta_{3/5}$ integrin. In addition, two glycosylation sites are present in the extracellular N-terminus. At the transmembrane regions, basic residues in the upper portions of the sixth and seventh transmembrane α-helices are involved in the interaction with the negatively charged phosphate groups of the nucleotide ligands. The intracellular loops regulate G_q protein binding and its subsequent activation of phospholipase C, that triggers inositol 1,4,5-triphosphate (IP3) and diacylglycerol (DAG) production (Van Kolen and Slegers, 2006), second messengers for calcium release from intracellular stores and protein kinase C activation, respectively (Bagchi et al., 2005; Liao et al., 2007). Moreover, the intracellular C-terminal domain contains two consensus PXXP SH3 domain binding sites, as

well as, potential sites for phosphorylation in the third intracellular loop, which may take part in receptor desensitization and internalization (Guzman-Aranguez and Pintor, 2012).

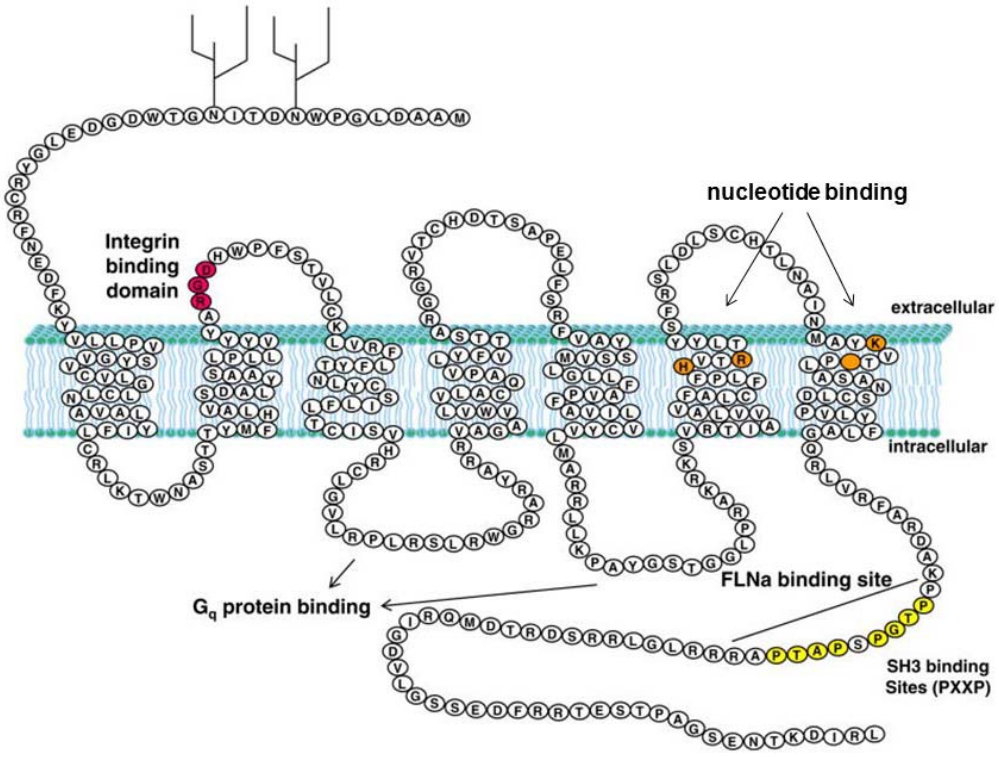

Figure 1.7. $P2Y_2R$ structure and major domains.

Adapted from Weisman GA et al, *Drug Development Research*. 2010

Other than Gq protein, P2Y2R also direct intracellular signaling through two other pathways. P2Y2 binding to $\alpha v\beta_{3/5}$ integrins enables UTP to stimulate G_o and G_{12} proteins leading to the activation the small GTPases Rac and Rho, respectively. Mutation of the RGD sequence to Arg-Gly-Glu (RGE), prevents both integrin binding and UTP-induced activation of G_o, G_{12}, Rac and Rho. Activation of intact P2Y2R induces the phosphorylation of Src and EGFR, responses that are attenuated by a mutant P2Y2R in which the SH3 binding domains for Src in

the intracellular C-terminus of the receptor have been deleted (Liu et al., 2004). Since the activated P2Y2R co-localizes with EGFR in the plasma membrane, these findings suggest that the previously reported ability of the P2Y2R to regulate EGFR phosphorylation (Soltoff et al., 1998) is due to Src-dependent recruitment of the P2Y2R to a signaling complex containing EGFR, thereby inducing EGFR phosphorylation in response to P2Y2R ligands. These studies used kinase inhibitors to demonstrate that P2Y2R-mediated activation of the mitogen-activated protein kinases ERK1/2, is dependent on the kinase activities of Src and EGFR (Peterson et al., 2010). Whereas the activities of ERK1/2 are important for P2Y2R-mediated cell/astrocyte

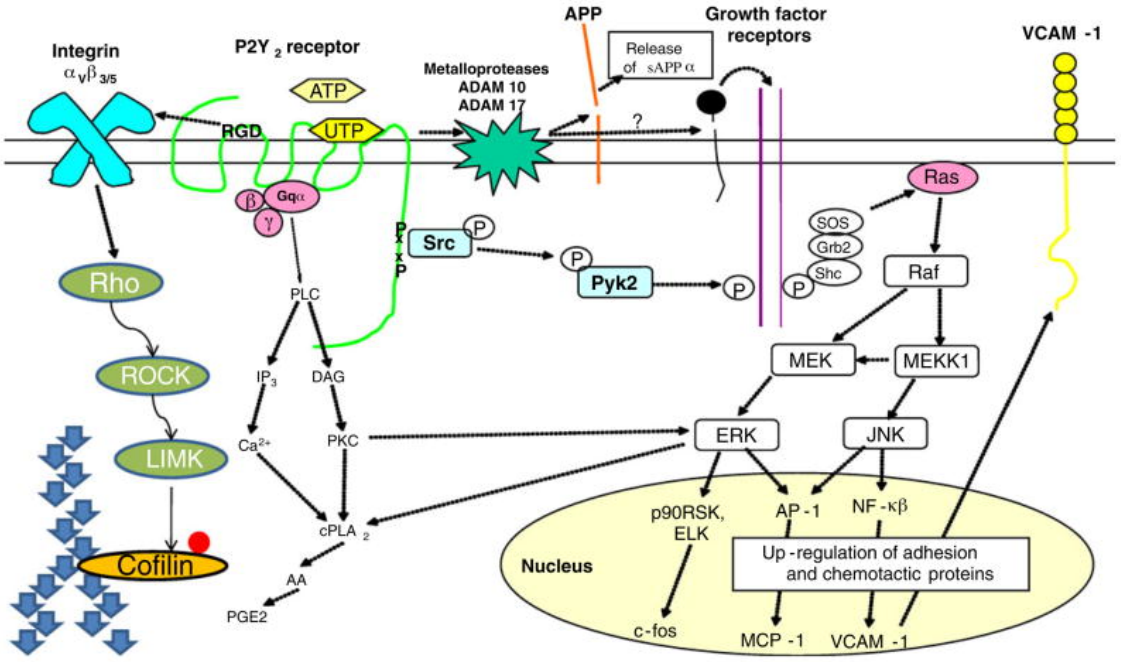

Figure 1.8. Major P2Y2R signaling pathways.

Adapted from Peterson TS et al, *Molecular Neurobiology*. 2010

proliferation (Washburn and Neary, 2006), the activity of another MAP kinase, p38, is important for P2Y2R-mediated upregulation of adhesion molecules, such as vascular cell

adhesion molecule-1 (VCAM-1), which is involved in tight binding of monocytes to endothelial cells (Seye et al., 2003) and lymphocytes to epithelial cells (Baker et al., 2008). In astrocytic cells, the p38 signaling pathway is also required for the P2Y2R to inhibit trauma-induced cell death (Burgos et al., 2007). Other studies indicate that EGFR signaling regulates neuronal survival by promoting cortical but not midbrain astrocyte apoptosis (Wagner et al., 2006), which suggests an endpoint for P2Y2R activation in the CNS. Additionally, it has been shown that the P2Y2R interacts directly with filamin A (FLNa), a crosslinking cytoskeletal maintenance protein (Yu et al., 2008).

1.9. Transcription Regulation of Tissue Factor

As an initial step toward elucidating the regulatory regions involved in control of tissue factor gene expression, a 12.4 kbp human TF gene and its complete DNA sequence was established and organized (Mackman et al., 1989). On top of that, transcriptional regulation of the tissue factor promoter was analyzed in COS-7 cells under different conditions. The region comprising nucleotides -209 to + 121 (relative to the transcription start site) supports high-level transcriptional activity. Two consensus binding sites for the transcriptional activator protein AP-1 were mapped in this region. (Mackman et al., 1990) Later, more transcription factor consensus sequences were discovered: five binding sites for specificity protein 1 (Sp1), three sites for epidermal growth response-1 (Egr-1), and one site for NF-κB. Of these four factors, Sp-1 is in charge of constitutive TF transcription while Egr-1, NF-kB and AP-1 are responsible for induced TF transcription (Li et al., 2009). Interestingly, cis element acting as transcription repressor has also been plotted in the promoter region of tissue factor gene, although its binding proteins have not been well defined .(Holzmuller et al., 1999) With the advance of modern

bioinformatics tools and biotechnology, the role of further upstream sequences continue to be established (Yan et al., 2010).

In monocytes/macrophages and endothelial cells exposed to inflammatory or pro-thrombotic stimulations (e.g. LPS, gram-negative bacteria, TNF-α, cytikines, PMA etc.), induction of tissue factor gene transcription is mainly mediated by functional interaction between Fos-Jun and c-Rel-p65 heterodimers (Mackman, 1996).

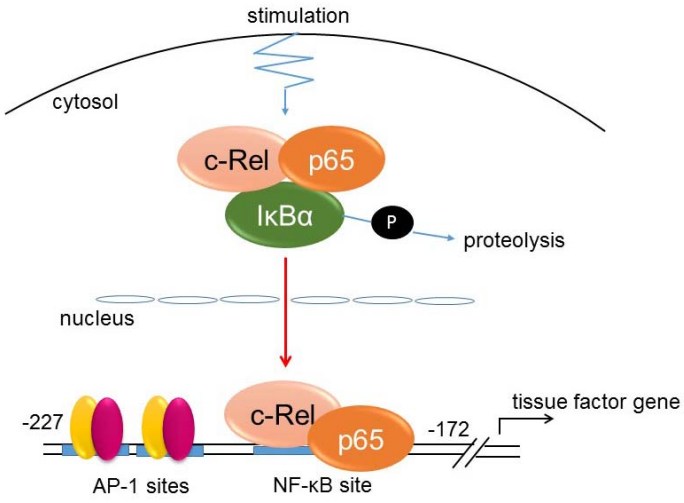

Figure 1.9. Model of the transcriptional activation of tissue factor gene in human monocytic cells and endothelial cells.

Adapted from Mackman N, *FASEB*. 1995

Early growth response protein-1 (Egr-1) also contribute to induced tissue factor expression, other than AP-1 and NF-κB. Egr-1 is reported to be involved in saphenous vein endothelial tissue factor induction caused by CD40 ligand, aside from AP-1 and NF-κB (Bavendiek et al., 2002). While most of these studies are performed on large arteries or vein endothelial cells, the same seems to be true with microvascular endothelium. In human microvascular endothelial

cells, TNF-α is observed to induce tissue factor transcription through NF-κB, leaving its mRNA stability unaffected (O'Reilly et al., 2003). Other than endothelium and monocyte/macrophage, similar regulation patterns are applicable to tissues such as endometrium (Krikun et al., 2000) and epithelial cells (Cui et al., 1994). Multiple potential therapeutics down-regulating tissue factor level impose their effects through these transcription factors. For example, nobiletin represses tissue factor expression through inhibition of NF-κB, AP-1, and Sp1 activation in THP-1 cells (Hirata et al., 2008). Curcumin has the same effect on HUVEC tissue factor against inflammatory stimulators by suppressing the binding of Egr-1 and AP-1 to the DNA and inhibits the activation of c-Rel/p65 (NF-κB) (Pendurthi et al., 1997). Simvastatin inhibits expression of tissue factor in advanced atherosclerotic lesions of apolipoprotein-E deficient mice independently of lipid lowering, but by inhibition of Egr-1 expression and activation (Bea et al., 2003). Transcription factor and related pathways provide promising strategies to control tissue factor level to prevent and treat thrombosis.

1.10. mRNA Stability and Regulation Mechanisms

The level of an mRNA within a cell depends on both its rate of synthesis and rate of decay (Bellofatto and Wilusz, 2011). Two major machineries exist in the field of mRNA stability regulation: microRNA and AU-rich element binding proteins.

A microRNA (miRNA) is a small non-coding RNA molecule (containing about 22 nucleotides) found in plants, animals, and some viruses, which functions in RNA silencing and post-transcriptional regulation of gene expression. As regulators of gene expression, miRNAs can work by essentially two modes. In plants, miRNAs base pair with messenger RNA targets

by precise or nearly precise complementarity, and direct cleavage and destruction of the target mRNA through a mechanism involving the RNA interference (RNAi) machinery. In contrast, most animal miRNAs are imprecisely complementary to their mRNA targets, and they inhibit protein synthesis (translation). (Ambros, 2004)

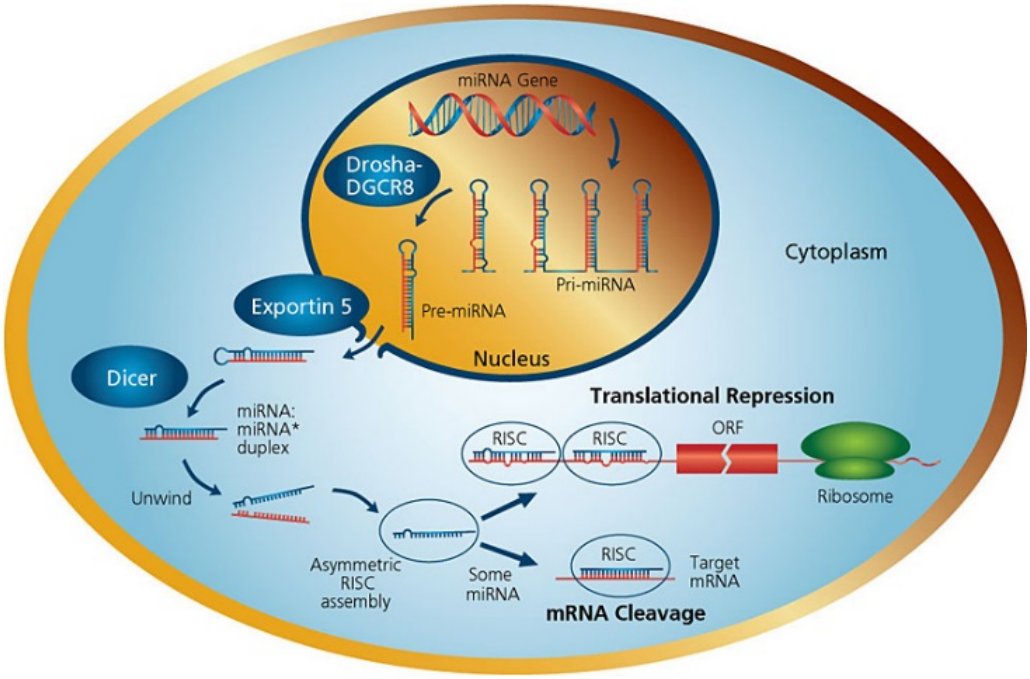

Figure 1.10. Mechanism of microRNA biogenesis and regulation of mRNA stability.

Adapted from Hammond SM et al, *FEBS* Letter. 2005

Impact of several microRNAs on tissue factor expression has been reported. After TNF-α injection, increased tissue factor and decreased miRNA-223 levels were detected in mice aorta. The same trends were observed in HUVEC and immortalized HUVEC cell line. Sequence in tissue factor mRNA 3'-UTR targeted by miRNA-223 was identified by wild-type and mutated design of luciferase assay. This correlation facilitates understanding of thrombogenesis during the process of atherosclerotic plaque rupture. (Li et al., 2014a) Also in cardiovascular system,

microRNA-19b released from endothelium was increased in UA (unstable angina) patients' plasma. In vitro study further showed that miRNA-19b inside HUVEC cells quenches tissue factor expression. These results indicate that miRNA-19b may function as potential anti-thrombotic protector in patients with unstable angina by targeting tissue factor. (Li et al., 2014b) In both colon cancer samples and breast cancer cell lines, tissue factor contributes to their migration and invasion. This effect is quenched by over-expression miRNA-19 (a). (Yu et al., 2013a) Moreover, miRNA-20b was found to downregulate tissue factor expression during human embryonic stem cell (hESC) differentiation into trophoblasts and granulocyte-monocyte (Yu et al., 2013b). Last but not least, miRNA-93/106b directly target tissue factor in MSMC (isolated leiomyoma smooth muscle cells), LSMC (myometrial smooth muscle cells), and SKLM-S1 (leiomyosarcoma cell line), and may play a central role in the genesis of leiomyomas and possibly de novo development of leiomyosarcoma from myometrium (Chuang et al., 2012). These evidences suggest a promising potential treatment for inhibiting thrombogenesis through post-transcriptional regulation of tissue factor.

Beside microRNA targeted sequences, adenylate-uridylate-rich elements (AU-rich elements, AREs) are also mRNA stability regulators found in the 3' untranslated region (UTR), especially of the ones coding for proto-oncogenes, nuclear transcription factors, and cytokines. They represent the most common determinants of RNA stability in mammalian cells. (Chen and Shyu, 1995) Subsequent bioinformatics analyses estimated that 5–8% of the transcriptome contains AREs and these transcripts additionally encode proteins required for apoptosis, immune responses, and intracellular signaling, to name just a few processes (Halees et al., 2008). AREs vary widely in sequence but were originally classified into three broad types: Class I AREs, found in mRNAs such as FOS and MYC, contain 1–3 interspersed copies of the

AUUUA pentamer surrounded by U-rich regions; Class II AREs, found in cytokine mRNAs such as GM-CSF and TNFα, contain multiple overlapping copies (typically 5–8) of the AUUUA motif; Class III AREs, such as the one in JUN mRNA, lack AUUUA pentamers but contain predominantly U-rich sequence (Wilusz et al., 2001). These unique features of AREs suggest that different AUBPs, or more likely, combinations of AUBPs, may differentially regulate the classes of AREs (Wu and Brewer, 2012).

AREs can modulate mRNA stability and/or translation depending on the particular ARE-binding proteins (AUBPs) associated. Not surprisingly, AUBPs can accelerate (e.g., AUF1, TTP, and KSRP), or attenuate (e.g., HuR) ARE mRNA decay. Multi-isoform AUBPs such as AUF1 have been shown to both stabilize and destabilize target mRNAs, consistent with unique isoform functionality caused by methylation, acetylation, phosphorylation and ubiquitination (Shen and Malter, 2015).

The p38 mitogen-activated protein kinase (MAPK) pathway plays an important role in the post-transcriptional regulation of inflammatory genes. This effect is conferred to mRNA via ARE-binding proteins, including HuR, TTP, AUF1, AUF2, FBP1, FBP2 (KSRP), TIA-1, and TIAR. (Dean et al., 2004) Recently, ERK pathway is also shown to regulate mRNA stability through AREs in vascular endothelial growth factor-A (VEGF-A) transcript (Essafi-Benkhadir et al., 2010).

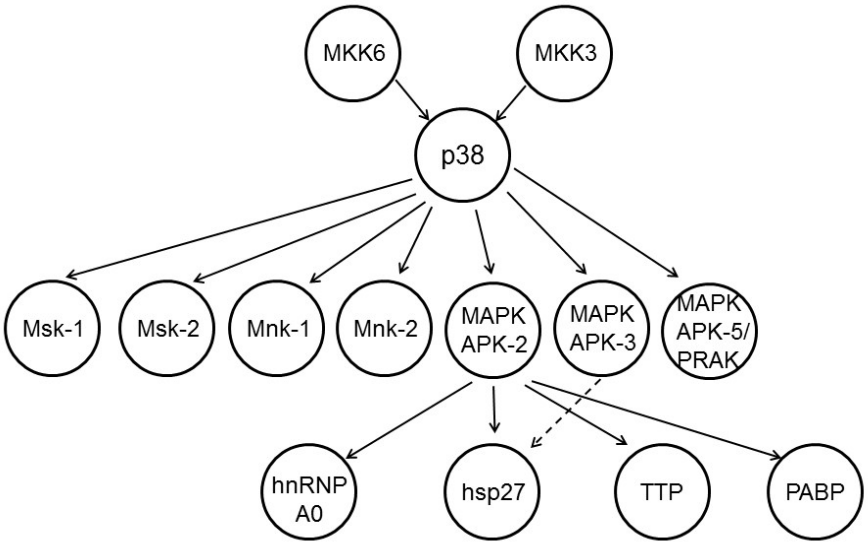

Figure 1.11. p38 Pathways that regulate AREBPs.

Adapted from Dean JLE et al, *Cellular Signaling*. 2004

AREs in tissue factor mRNA were first recognized and characterized by Ahern Shawn et al in 1992 under serum culture (Ahern et al., 1993). Another study demonstrating that Dexamethasone reduced LPS-induced TF gene transcription but increased the stability of tissue factor mRNA dependent on AREs was published over ten years later (Reddy et al., 2004). Yet, it took another ten years to connect two proteins to tissue factor ARE binding, namely PARP-14 and TTP in macrophages (Iqbal et al., 2014).

1.11. Aim of study

Occlusive thrombotic events, especially cardiovascular disease, are the leading cause of morbidity and mortality worldwide. Although anticoagulants and anti-platelets have decreased the risk, they renders lethal adverse effects such as hemorrhage and apnea. Thus, there is a need for better understanding of the procoagulation properties of atherosclerosis and

pathophysiology of atherothrombosis to provide novel treatment option for these conditions. Thrombosis including atherothrombosis are found at various sites throughout the vasculature. Regional differences prime the endothelial phenotype to respond distinctly to such systemic risk factors as hypercholesterolemia, genetics, immune status, gender, and oxidative stress. In human beings, atherothrombosis is mainly studied in coronary artery; although in mice studies, mostly observed in aorta. (VanderLaan et al., 2004) The demand to expand the study on human coronary artery tissue is urgent. Plaque disposition is also found in small blood vessels. Atherogenic dyslipidaemia, characterized by elevated triglycerides and low levels of HDL-C, is very common in patients with type 2 diabetes mellitus and metabolic syndrome and is associated with both macrovascular and microvascular complications. (Simic et al., 2013) Microcirculation disorder is also the corner stone of impaired homeostasis in sepsis. The total endothelial surface area is approximately 4000 to 7000 m^2 with most of the elements being within the microcirculation, and compose the largest 'organ' in the human body (Lundy and Trzeciak, 2009).

TF is a membrane-bound transmembrane glycoprotein that is normally not exposed to the blood circulation. It facilitates both intrinsic and extrinsic pathways of coagulation and is a crucial protein in thrombotic diseases. In a normal blood vessel, TF is present mostly in tunica adventitia (fibroblasts), moderately in tunica media (smooth muscle cells), but virtually undetectable in endothelium (Wilcox et al., 1989). However, a diversity of stimuli can induce TF expression in endothelium. Some are endogenous molecules, such as TNF-α, interlukin-1β, CD40 ligand (Steffel et al., 2006), or UTP/ATP (Ding et al., 2011); others are exogenous factors, including endotoxin (Colucci et al., 1983) and caffeine(Gebhard et al., 2012). These inducers share some similar signal transduction pathways regulating TF induction in different

cells. Among them, the MAP kinases p38, p42/44 (ERK1/2), and c-Jun terminal NH2-kinase (JNK), and protein kinase C are commonly discussed as the positive regulatory pathways. In contrast, the PI3K/AKT pathway is shown to negatively regulate TF expression through an unknown mechanism (Steffel et al., 2006). In this regard, our initial study already showed that endothelial P2Y2R activates ERK1/2, JNK, and p38 MAPK pathways without affecting the PI3K/AKT negative pathway (Ding et al., 2011). On the transcription level, TF was shown to under concerted regulation of NF-κB, AP-1, and Sp-1 in porcine aortic endothelial cells by binding to sequences in a ~300 bp region from the transcription starting site (Moll et al., 1995). Egr-1 is also involved in TF transcription in mononuclear cells and affects process of diseases such as pulmonary fibrosis (Aljada et al., 2002; Yan et al., 1998). However, the transcriptional molecular mechanism in response to G protein-coupled receptor activation, i.e. P2Y2R, remains largely unknown.

Nucleotides matter more than being the universal currency of energy transaction and the building-blocks of genes. They are also short-term signaling molecules and long-term trophic factors through P2X or P2Y receptors (Burnstock, 2011). Among the eight G protein coupled P2Y nucleotide receptors, the ADP-preferring P2Y12 receptor on platelets is targeted by Plavix to prevent thrombosis in cardiovascular diseases including percutaneous coronary intervention and atherosclerosis (Jarvis and Simpson, 2000; Verheugt, 2013). In addition, non-platelet P2Y1, P2Y2, and P2Y6 receptors are documented to mediate inflammatory response and plaque formation in animal models of atherosclerosis or restenosis (Guns et al., 2010; Hechler et al., 2008; Seye et al., 2007). A potential role of P2Y2 receptor (P2Y2R) in thrombosis is barely recognized, but it is already targeted in clinical drug development to treat cystic fibrosis (Kellerman et al., 2008), and dry eye disease (Lau et al., 2014). We recently

reported that stimulation of human coronary artery endothelial cells (HCAEC) by ATP/UTP leads to dramatic up-regulation of tissue factor (TF) expression and activity through the P2Y2R (Wilcox et al., 1989). Although we have defined the post-P2Y2R signaling mechanism in control of TF expression, the exact transcriptional or post-transcriptional mechanisms remained to be determined.

Our overall hypothesis is that P2Y2 receptor (P2Y2R), the sibling of P2Y12 receptor, is a promising target for therapeutic control of thrombosis, especially in inflammation-induced vascular thrombogenesis. We proposed that P2Y2R mediate HCAEC TF expression on transcriptional and post-transcriptional levels. To fill in the gaps between existing studies, we further hypothesized that TF induction and relationship to extracellular nucleotide follows different patterns across tissues related to thrombosis. To test the above hypothesis, three specific research aims were addressed:

Aim 1: To determine TF induction and relationship to purinergic stimulation in HCAEC, HUVEC, HMVECad, THP-1 and human primary monocytes.

Aim 2: To explore the transcriptional regulation of TF gene mediated by P2Y2R in HCAEC.

Aim 3: To assess the post-transcriptional influence caused by P2Y2R activation in HCAEC.

Chapter 2. Material and Methods

2.1. Materials

The commercial sources of the chemicals and recombinant proteins used in this study are listed in Table 2.1 and Table 2.2. Lipopolysaccharide (LPS) of two serotypes (*E. coli* O111: B4 and *E. coli* O55: B5) were used. When not specified, *E. coli* O111: B4 was used in the experiment. *E. coli* O111: B4 from two manufacturers were purchased. When not specified, the one from Sigma-Aldrich was used in the experiment.

Table 2.1. Chemicals

Items	Catalog Number	Company
Actinomycin D	1229	Tocris
SB203580	1202	Tocris
SP600125	1496	Tocris
U0126	9903	Cell Signaling Technology
Y-27632 dihydrochloride	1254	Tocris
PP 2	1407	Tocris
Uridine 5'-triphosphate (UTP) tris salt	U6875	Sigma-Aldrich
2-thio-UTP tetrasodium salt	3280	Tocris
UTPγS trisodium salt	3279	Tocris
Adenosine 5'-triphosphate (ATP) disodium salt hydrate	A1852	Sigma-Aldrich

Uridine 5'-diphosphate (UDP) disodium salt hydrate	94330	Sigma-Aldrich
Adenosine 5'-diphosphate (ADP) sodium salt	A2754	Sigma-Aldrich
Adenosine 5'-monophosphate (AMP) disodium salt	01930	Sigma-Aldrich
2'-Deoxyadenosine 5'-Triphosphate (dATP)	GE27-1850-04	GE Healthcare
β-Nicotinamide adenine dinucleotide hydrate (NAD)	N7004	Sigma-Aldrich
Adenosine	9251	Sigma-Aldrich
Phorbol12-myristate-13-acetate (PMA)	1201	Tocris
PF3644022	4279	Tocris

Table 2.2. Recombinant proteins and LPS

Items	Catalog Number	Company
EcoRV	1042A	Takara
Apyrase	A6535	Sigma-Aldrich
recombinant human TNF- α	210-TA	R&D Systems
LPS (*E. coli* O111: B4)	L 4391	Sigma-Aldrich
LPS (*E. coli* O111: B4)	437627	Calbiochem
LPS (*E. coli* O55: B5)	L6529	Sigma-Aldrich

2.2. Cell Culture

2.2.1. Human coronary artery endothelial cells

Human coronary artery endothelial cells (HCAEC) were purchased form Lonza Group Ltd, cultured in EBM-2 medium supplemented with VEGF, FGF, EGF, IGF, ascorbic acid, GA 1000 (Lonza Group Ltd), and 5% FBS (v/v) at 37 °C in Forma Series ii Water Jacketed incubator (Thermo) in a humidified atmosphere with 5% CO2. HCAECs between the third and eighth passages were used for experiments. The cells were harvested by trypsinization and washed in EBM-2 complete medium. For most procedures, one milliliter of the suspension containing $3x10^5$ endothelial cells was then seeded per well in six-well flat-bottom tissue culture plates (Greiner Bio One) followed by 24 h incubation and starvation overnight. Where inhibitors were used, cells were pretreated with inhibitors for 1 h before stimulation.

2.2.2. THP-1 cells: Culture and Differentiation

The human myelomonocytic cell line THP-1 was purchased from American Type Culture Collection (ATCC). This cell line is derived from the blood of a one-year-old boy with acute monocytic leukemia (Tsuchiya et al., 1980). These cells can be continuously cultured in suspension and be further differentiated into macrophage-like cells. THP-1 cells were cultured in RPMI-1640 (HyClone, Thermo) supplemented with 10% (v/v) heat-inactivated fetal bovine serum (FBS) (HyClone, Thermo), 100U/ml penicillin, and 100 µg/ml streptomycin (Lonza) at 37 °C in Forma Series ii Water Jacketed incubator (Thermo) in a humidified atmosphere with 5% CO2. The THP-1 cells were maintained in 75 cm^2 flask by replacing 2/3 to 3/4 of the medium when splitting. Alternatively, cells were collected and centrifuged at ~1100 rpm for 5 min and subsequently re-suspended in a concentration of ~ $2\text{-}4x10^5$ cells/ml. For the induction of cell differentiation, THP-1 cells were seeded at $5x10^5$ cells/well in six-well plates in RPMI-1640 supplemented with 5% FBS with 40 nM PMA for 48 h.

2.2.3. Human Umbilical Vein Endothelial Cells

Human umbilical vein endothelial cells (HUVECs) cell line was obtained from ScienCell Research Laboratories. HUVECs were maintained in Dulbecco's Modified Eagle's Medium (DMEM, GIBCO) supplemented with 20% (v/v) fetal bovine serum (FBS, GIBCO), 100 U/ml penicillin G, and 100 U/ml streptomycin in a humidified 37ºC, 5% CO2 incubator. HUVECs between the third and eighth passages were used for experiments. Detachment and seeding procedures were the same as HCAEC.

2.2.4. Human Microvascular Endothelial Cells

Human microvascular endothelial cells from adult dermis (HMVECad) were purchased from Gibco, cultured and passaged in Medium 131 supplemented with Microvascular Growth Supplement (MVGS) in the presence of antibiotics and antimycotics. HMVECad were cultured in 75 cm^2 flasks which were coated with 3 ml Attachment Factor (AF, a sterile solution containing 0.1% gelatin) (Gibco) each for 2 h at room temperature before use. Passaging and seeding procedures are the same as HCAEC.

2.2.5. Isolation and Culture of Human Primary Blood Monocytes

Human peripheral blood mononuclear cells (PBMCs) were separated from buffy coat (Biological Specialty Corp) by density-gradient centrifugation on Histopaque-1077 (Sigma). Briefly, 5ml buffy coat was diluted with two volumes of PBS. Then the diluted buffy coat was

carefully layered on top of the same volume of Histopaque-1077. After 2000 rpm centrifuge for 30 min at room temperature, human PBMCs can be visible at PBS/ Histopaque-1077 interface. PBMCs were carefully collected and washed with PBS twice. Then untouched human primary monocytes were purified by negative selection using a Dynabeads kit (Invitrogen), yielding an average 98% purity. Freshly isolated monocytes were cultured in RPMI 1640 supplemented with 10% heat-inactivated FBS and antibiotics, and used in experiments after being stabilized for at least 2 h. In some experiments, the purified monocytes were allowed to differentiate into macrophages with the presence of recombinant human GM-CSF (50 ng/ml) plus LPS (100 ng/ml) or IFN-γ (100 ng/ml) plus LPS (1 μg/ml) for 2~3 days.

2.2.6. Long-term Storage

For long-time storage, confluent cells were collected and centrifuged at ~1100 rpm for 5 min. The pellets were re-suspended in complete growth medium supplemented with 10% (v/v) DMSO (EMD Milipore) at a concentration of ~$3x10^6$ in 2 ml cryovials (Greiner Bio One). The vials were transferred into an isopropanol freezing container (VWR) to reach 1 °C/min cooling rate required for successful cryopreservation of cells, then the container was kept in -80 °C overnight. The following day, the frozen vials were transferred to a liquid nitrogen (-196 °C) tank (taylor-wharton). To thaw the frozen cells, rapidly immerse the lower half of the cryovials into a 37 °C water bath and gently swirl the vials till the medium starts to thaw. Then dilute the cells suspension with pre-warmed growth medium and centrifuge at ~1100 rpm for 5 min. After the centrifugation, re-suspend the cells in complete growth medium into the appropriate culture vessel at the appropriate culture environment.

2.3. PCR Analysis

2.3.1. Isolation and Measurement of RNA and DNA

Cells were grown in six-well plates until confluence. The total RNA and DNA were extracted from HCAECs according to manufacturer's protocol for the RNeasy and DNeasy kits, respectively (Qiagen). For yield determination, the DNA concentration was measured by UV spectrophotometry with NanoDrop 2000 (Thermo Scientific). The absorption maximum of nucleic acids is 260 nm while amino acids or proteins respectively absorb best at 280 nm. Thus the quotient of the absorption measured at these two wave length determines the degree of purity. A ratio of 1.8 or higher indicated sufficient DNA/RNA purity for other procedures.

2.3.2. cDNA Synthesis

For the synthesis of the first strand of cDNA, 1μg of total RNA after DNase (Ambion) treatment was reverse-transcribed using Taqman reverse transcription reagents (Applied Biosystems) using the recipe in Table 2.3..

Table 2.3. Reaction composition for cDNA synthesis

Component	Volume/reaction
10xTaq RT buffer	5μL
25mM $MgCl_2$	11μL
10mM dNTP	10μL

oligo dT	2.5µL
Rnase inhibitor	1µL
Reverse Transcriptase or RNase free H2O	1.25µL
RNA	variable
RNase free H2O	variable
Total Volume	50µL

The mixture of all the components was incubated at 25 °C for 10 min; 48 °C for 30 min; 95 °C for 5 min and then held at 4 °C.

2.3.3. RT-PCR Analysis

The cDNA samples were then amplified by PCR using HotStarTaq DNA Polymerase (Qiagen) using the recipe in Table 2.4..

Table 2.4. Reaction composition using HotStarTaq DNA polymerase

Component	Volume/reaction
10xPCR buffer	5µL
10mM dNTP	1µL
5x Q-solution	10µL
HotStarTaq DNA polymerase	0.5µL
Rnase inhibitor	1µL
Reverse transcriptase or RNase free H_2O	1.25µL

Forward primer	0.5µL
Reverse primer	0.5µL
Rnase/Dnase free H_2O	27.5µL
cDNA template	5µL
Total Volume	50µL

The PCR amplification was performed using an iCycler iQ5 detection system (Bio-Rad) with jump start for 2 min at 95 °C, followed by 40 thermal cycles of denaturation for 1 min at 95 °C, annealing for 1 min at 56 °C, and extension at 72 °C for 1 min with a final extension at 72 °C for 10 min. The resulting PCR products were resolved on a 1% agarose (amresco) gel with 0.01% ethidium bromide (sigma) in electrophoresis gel system (minicell primo, Thermo), and the bands were visualized with universal hood imaging system (Bio-Rad) under ultraviolet light as we previously described (Ding et al., 2011; Ma et al., 2013).

2.3.4. Real-time PCR Analysis

Real time RT-PCR was carried out using an iCycler iQ5 detection system (Bio-Rad) with SYBR Green reagents (Applied Biosystems), as we previously described (Ding et al., 2011; Ma et al., 2013). The PCR mixture (20 µL) contained 0.5 µM concentration of each primer, 4 µl of water, 10µL of SYBR Green mixture, and 5µL of cDNA template from previous step. The samples were placed in 96-well plates that were sealed with optical clear cap (Fisher) with the following reaction condition: initial PCR activation step (5 min at 95 °C), and cycling steps (denaturation for 1 min at 95 °C, annealing for 1 min at 60 °C, extension for 2 min at 72 °C; 40

cycles). Internal controls, GAPDH or β-actin were amplified in separate wells. For data analysis, we used the comparative cycle threshold method (ΔΔCt method) for relative quantitation of gene expression. Basically, the cycle threshold (Ct) for the target amplicons and internal controls were determined. The fold change in the target gene relative to the endogenous control gene is determined by:

Fold Change = $2^{-\Delta(\Delta Ct)}$

where ΔCt = Ct (target genes)—Ct (internal controls)

and Δ(ΔCt) = ΔCt (stimulated) – ΔCt (control)

Thus, all values for experimental samples were expressed as differences (n-fold) between the sample mRNA and the calculator mRNA. The sequences of primers are listed in the Table 2.5..

Table 2.5. Primers used for PCR assay

Gene	Forward Primer	Reverse Primer
hTF hnRNA	5'- CCCCTGGGTTGCTATGAGG-3'	5'- CCTGGCTGTGGTGTTCTGTGC-3'
hTF mRNA	5'-ACGCTCCTGCTCGGCTGGGT-3'	5'-CGTCTGCTTCACATCCTTCA -3'
h β-actin	5'-ATTGCCGACAGGATGCAGAA-3'	5'-GCTGATCCACATCTGCTGGAA-3'
h GAPDH	5'-TCAACAGCGACACCCACTCC-3'	5'-TGAGGTCCACCACCCTGTTG-3'

2.4. Western Blotting

2.4.1. Solutions

The commercial sources of the buffers and chemicals used in this study for Western blotting are listed in Table 2.6.

Table 2.6. Buffers used for Western blot

Items	Catalog Number	Company
10x Tris Glycine Buffer	75894	USB Affymetrix
10x Tris/Glycine/SDS Buffer	161-0732	Bio-Rad
20x Tris-Buffered Saline and Tween 20	77500	USB Affymetrix
Western Lightning® Plus-ECL	NEL105001EA	PerkinElmer
Blotto (non-fat dry milk)	sc-2324	Santa Cruz Biotechnology
Albumin, Bovine Fraction V	9048-46-8	Research Products International Corp.

Milli-Q purified water was used to dilute the buffers. Electrophoresis buffer was diluted from 10x Tris/Glycine/SDS Buffer and the dilution contains 25mM Tris, 192mM Glycine and 0.1% (w/v) SDS at PH 8.3. Transfer buffer was diluted from 10x Tris Glycine buffer and 20% (v/v) methanol with a final concentration of 25 mM Tris, 192 mM Glycine at PH 8.3. Tris-Buffered Saline and Tween 20 (TBS-T) buffer was made from 10x TBS-T buffer and containing 500 mM Tris, 60 mM KCl, 2.8 mM NaCl, and 1.0% Tween-20. Blocking buffer was made with 5% non-fat dry milk in TBS-T buffer. Primary antibody was diluted in 5% bovine serum albumin (BSA) in TBST buffer.

2.4.2. Sampling

Cells were cultured in six well plates and serum-deprived for 10 h before treatments at indicated concentration and duration. For adherent cells, the supernatant was discarded and cells were lysed in 250μL ice-cold Laemmli sample buffer (Sigma-Aldrich) and scratched with rubber policeman. For floating cells, the supernatant was centrifuged and cell pallets were resuspended in 250μL Laemmli sample buffer (Sigma-Aldrich). All lysates were collected on ice followed by being heated in boiling water for 5 min.

2.4.3. Blotting

Precision plus protein dual color standard (Bio-Rad) was used as a reference to identify the approximate molecular weight. Samples were loaded and separated on 12% Mini-PROTEAN® TGX™ Precast Gel (Bio-Rad) in a SDS-PAGE gel chamber (Bio-Rad) in electrophoresis buffer for 45 min with the voltage of 110 V. After running the gel, assemble the stack in the order of two layers of absorbent paper, which was thoroughly soaked in transfer buffer; the SDS-PAGE gel; a wet polyvinylidene difluoride (PVDF) membrane (Thermo); two layers of absorbent paper, which was thoroughly soaked in transfer buffer. Gels were blotted using a semi-dry blotting apparatus (Bio-Rad) for 35 min with the voltage of 20 V. After transfer, the stack was carefully disassembled. The membrane was blocked for 1 h (room temperature, shaking) in Western blot blocking solution. The membrane was probed with the primary antibody overnight in 5% BSA in TBS-T buffer. The primary antibodies used for Western in this study are listed in Table 2.7.. Next day, the blots were washed in TBS-T buffer for four times 10 min each time. A horseradish-conjugated secondary antibody (Cell Signaling)

was incubated for 1 h at room temperature (5 % dry milk in TBS-T buffer). Unbound antibodies were washed in TBS-T buffer four times for 10 min each time. The bound antibody was detected by incubating the blots in Western Lightning® Plus-ECL (PerkinElmer). The image was captured on a sensitive photographic film (research products international corp.), placed against the membrane, and visualized by medical film processor (Konica Minolta medical & graphic Inc.).

Table 2.7. The primary antibodies used for Western blot

Items	Catalog Number	Clone	Company
anti-human TF mAb	612161	10H10	Calbiochem
p-p38 MAPK	4511	D3F9	Cell Signaling
Evi-1	2593	C50E12	Cell Signaling
p-c-Jun	9165	60A8	Cell Signaling
p-Fra-1	5841	D22B1	Cell Signaling
p-c-Fos	5348	D82C12	Cell Signaling
p-ATF-2	5112	11G2	Cell Signaling
p-MK-2	3007	27B7	Cell Signaling
p-hsp27	9709	D1H2F6	Cell Signaling
β-actin	3700	8H10D10	Cell Signaling
GAPDH	2118	14C10	Cell Signaling
α-tubulin	2125	11H10	Cell Signaling
β-tubulin	2128	9F3	Cell Signaling

2.4.4. Imaging Analysis

The images on the films were then scanned into the computer for presentation and analysis. The intensity of signals was acquired in the linear range of the digital images using specific densitometric software, Quantity One. Images were calibrated against the background and given in relative density units.

2.4.5. Stripping and Re-probing

Equal protein loading was verified by stripping off the original antibodies and re-probed with the primary antibodies. Blots were rinsed with TBS-T buffer and incubated for 15 min at room temperature in restore PLUS Western blot stripping buffer (Thermo). After which, the membrane was extensively rinsed with TBS-T buffer three time for 1 min each time, and blocked for 30 min in 5% non-fat dry milk in TBS-T buffer. Subsequently, the blots were re-probed with desired primary antibodies as described previously (Ding et al., 2011; Ma et al., 2013).

2.5. Immunofluorescence Assay

HCAECs were seeded in 8-chamber glass slides (Nalge Nunc International) at $3x10^5$ /well, followed by 24 h incubation and starvation overnight before treatment. After treatment, the medium was aspirated and cells were fixed in cold methanol for 10 min. The fixed cells were washed with PBS buffer (Calbiochem) three times and blocked with 3% horse serum (Sigma-aldrich) for 1 h at room temperature. Then the cells were incubated with rabbit

monoclonal antibodies to p-c-Jun, p-Fra-1 and p-ATF-2 (1:50) (Cell Signaling Technology) overnight at 4^{o}C followed by incubation with FITC-conjugated anti-rabbit IgG (1:200) (KPL) for 90 min at room temperature in darkness. For negative controls, cells were incubated with non-immune rabbit IgG in place of the specific primary antibody or only the FITC-conjugated secondary antibody. Cells were then washed with PBS three times and incubated with Alexa Flour 555 Phalloidin (Cell Signaling Technology) for 1 h. Finally, mounting medium containing DAPI was added to seal the slides. Images with fluorescent signals in random fields were acquired and captured using an AMG EVOS digital inverted multi-functional microscope (AMG). (Ding et al., 2011; Ma et al., 2013).

2.6. Luciferase Activity Assay

2.6.1. Luciferase Reporter Construction

pGL4.12[luc2CP] Vector from Pomega was used as our transcription activity reporting vector. A map of its backbone is shown in Figure. 2.1. The pGL4.12[luc2CP] vector (~4.4 kb) encodes the luciferase reporter gene luc2CP (Photinus pyralis) which is expressed into a 61kDa protein. Its multiple cloning region contains a sequence recognized and cut by EcoRV restriction endonuclease, resulting in a blunt end in the middle of the sequence. Purchased vector was cleaved into linear dsDNA in the mixture shown in Table 2.8. with EcoRV before ligation. It also has a BamHI site at location 2199 bp.

Table 2.8. Reaction composition using EcoRV restrictive endonuclease

Component	Volume/reaction
EcoRV	1μL
10X H Buffer	2μL
Vector	1μL
Sterilized distilled water	up to 20μL
Total Volume	20μL

Promoter constructs encompassing the region from -1427 to +207 bp (~1.6kb), and -4078 to +207 bp (~4.3kb), relative to the transcription starting site of the human TF gene were amplified from human genomic DNA (prepared from HCAECs) by PCR as described in 2.3.3. using specifically designed forward and reverse primers containing the EcoRV restriction enzyme site. Forward primer for 1.6kb promoter fragment: 5'-GCTAGCCTCGA GGATATCCTACCTTCAATCCCAGAG-3'; forward primer for 4.3kb promoter fragment: 5'-GCTAGCCTCGAGGATATCGGTGGACATTCAAGCATT-3'; shared reverse primer: 5'-

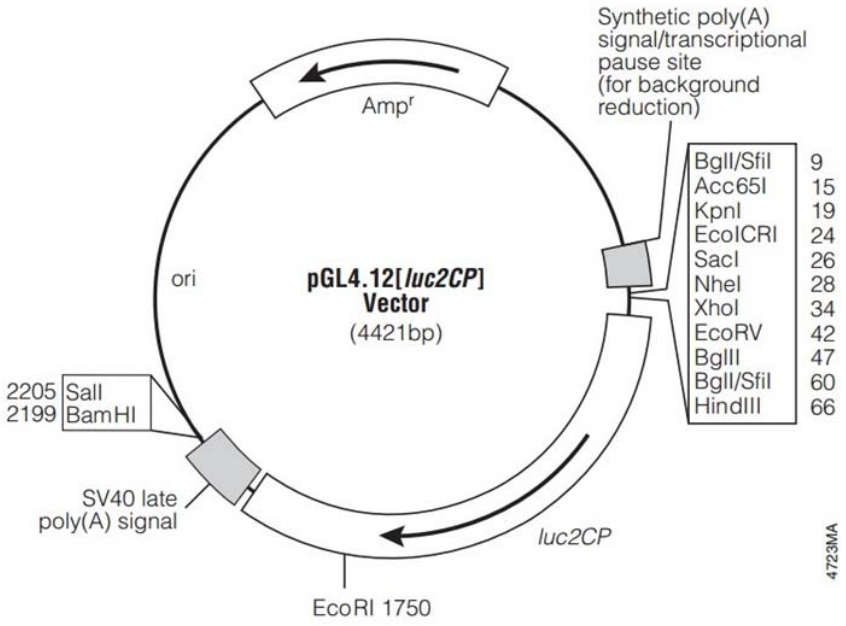

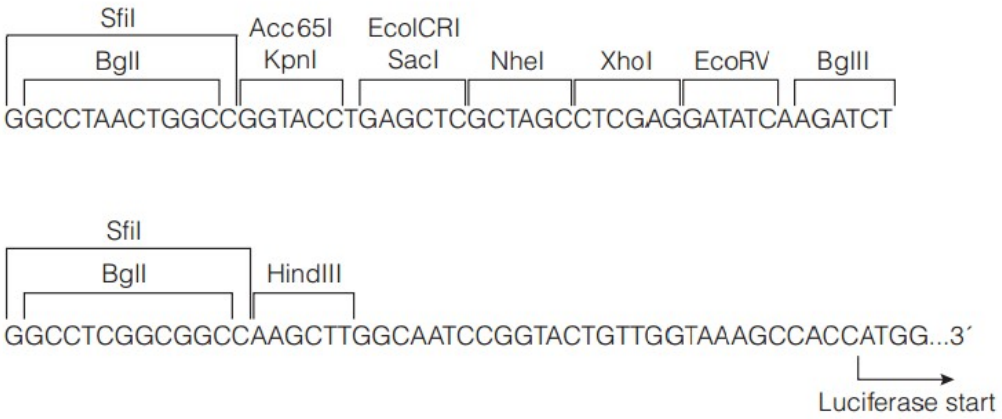

Figure 2.1. pGL4.12[luc2CP] vector backbone and multiple cloning region

Adapted from Browning J et al. *Promega Notes*. 2003

AGGCCAGATCTTGATATCTCCATGTCTACCAGTTGGCG-3'. The promoter region was cloned into pGL4.12 vector (Promega) with In-Fusion HD EcoDry Cloning Kit (Clonetech). Deleted, truncated or mutated constructs on the 1.6kb promoter fragment were built with same method but different primers. Deletion forward primer: 5'-CTCTTAGGGAAAAGGCTAGA GCCTGCATAAAAAGAG-3'; deletion reverse primer: 5'-CCTTTTCCCTAAGAGATCTT CAGCTCCACCTGGGAT-3'. Truncation forward primer: 5'-GCTAGCCTCGAGGATATC GGCTAGAGCCTGCATAAAAAG-3'; truncation reverse primer is same as wild-type reverse primer. Mutation forward primer: 5'-GGAAAAGTCAGACGGCTAGAGCCTGCATAAAA AGAG-3'; mutation reverse primer: 5'-CCGTATGACTTTTCCCTAAGAGATCTTCAGCT CCAC-3'. Extension time was elongated according to the length of fragments in need. The resulting PCR products were resolved on a 1% agarose (amresco) gel with 0.01% ethidium bromide (sigma) in electrophoresis gel system (minicell primo, Thermo), and the bands were visualized with ultraviolet translluminator (UVP). Visible bands in ideal sizes were cut from gel. Corresponding PCR products were recovered from gel chunks with QIAquick Gel

Extraction Kit (Qiagen). These insert fragments were mixed with linearized vector at ratio of 2:1 and ligated with In-Fusion HD EcoDry Cloning Kit (Clonetech) at 15 min at 37°C, followed by 15 min at 50°C. Thus, the ligated vector is ready to be used to transform electrocompetent E.coli.

Electrocompetent E.coli HST08 strain was purchased from Clontech. Ligation product and E.coli were mixed and heat shocked at 42^{o}C for 45 sec in SOC medium (Clontech). Transformed E.coli was spread on an LB agar plate with ampicillin, incubated at 37^{o}C overnight. Monoclonal colonies grown on plates were inoculated into 5 ml of LB culturing medium (with ampicillin) each and cultured in a 37^{o}C incubator for 15 h. Monoclonal E.coli were collected and lysed and plasmids inside were purified with QIAprep Spin Miniprep Kit (Qiagen) according to the manufacturer's manual. To verify inserted fragments, plasmids were sequenced by Eurofins MWG Operon with primers. Forward sequencing primer: 5'-TAACTGGCCGGTACCTGA-3'; reverse sequencing primer: 5'-CCATGGTGGCTTTACCA ACA-3'.

2.6.2. Reporter Vector Transient Transfection

HCAECs were seeded in 48-well plates with white wall and clear bottom designed for luminescence detection (Griener Bio One), were used after 24 h at 75% confluency. Xfect Transfection Reagent (Clonetech) was used to deliver vectors into target cells following the manufacturer's instruction. For each well 5μg of luciferase reporter plasmid containing different forms of tissue factor promoter and 1μg pSV-b-galactosidase reference plasmid

(pSV-β-gal) were co-transfected at the same time. 36 h post transfection cells were starved overnight in serum-depleted culturing medium before UTP treatment.

2.6.3. Reporter Activity Analysis

Cells were lysed on plates for 15 min with 500µl lysis buffer (Luciferase Assay System, Promega). The lysates were split in two aliquots which were used for determination of -galactosidase activity or luciferase activity. A 250 µl aliquot was centrifuged at 13000 rpm for 5 min and the supernatant was used to measure luciferase activity with Luciferase Assay System (Promega) and β-galactosidase activity with Galacto-Light chemiluminescent reporter assay (Tropix, Bedford, MA, USA) in a Lumat LB 9501 luminometer (Berthold,Wildbad, Germany).

2.7. Electrophoretic Mobility Shift Assay

DNA probe fragments were ordered from IDT and labeled with biotin at 3' end with the DNA 3' End Biotinylation Kit (Pierce). Nuclear proteins were isolated from HCAEC with NE-PER Nuclear and Cytoplasmic Extraction Reagents (Pierce). Each binding reactions contained 10 µg of nuclear extract proteins. To distinguish specific from nonspecific protein-DNA complex formation, incubations were also performed in the presence of 200-fold excess unlabeled probes. After incubation, the reaction mixtures were electrophoresed on a pre-casted 6% TBE polyacrylamide gel (Lonza). The reactions were transferred to a nylon membrane and detected with LightShift Chemiluminescent EMSA Kit (Pierce). The sequence of human TF promoter -1363 AP-1 site is as follows: 5'-GGAAAATGACTCAGGCTAGA-3'.

2.8. Chromatin Immunoprecipitation Assay

The chromatin immunoprecipitation (ChIP) assay was performed using the Agarose ChIP Kit (Pierce) according to the manufacturer's instructions. HCAECs were treated with or without UTP stimulation, after which cells were cross-linked in formaldehyde. MNase was used to digest the chromatin. Approximately 10% of the resulting sample was kept to serve as an input genomic DNA control, and the rest was incubated with candidate antibody overnight with rotation, followed by 1 h incubation with protein A-agarose beads for ChIP. The precipitated chromatin-protein complexes were washed and eluted, and the cross-links were reversed. The genomic DNA fragments were amplified by real-time quantitative PCR. For the sequence containing the new AP-1 site, the primer sequences were: forward 5'-CTACCTTCAATCCCAGAG-3', reverse 5'-CCTTGTAGACTTTCC TTCC-3'.

2.9. Co-immunoprecipitation

HCAECs were starved overnight and treated with or without UTP for 30 min, lysed and sonicated on ice. Cell lysate was pre-cleared, and then incubated with 1 µg rabbit anti-c-Jun antibody (Santa Cruz) overnight at 4^{o}C. Protein A agarose beads (Cell Signaling Technology) were added to the lysate-antibody mixture and incubated for another 2 h. The beads were then washed five times with cell lysis buffer and re-suspended with 3xSDS sample buffer. Samples were heated to 95oC, loaded on SDS-PAGE gel and analyzed by standard Western Blotting.

2.10. Silencing of AP-1 Subunits by siRNA

To knock down the three AP-1 subunits c-Jun, Fra-1 and ATF-2, HCAEC were transfected with the four sequence pool (ON-TARGET plus Human SMARTpool L-003268-00-0005, L-004341-00-0005, L-009871-00-0005, Dharmacon) using DharmaFECT 4 Transfection reagent following the manufacturer's protocol. Briefly, HCAEC were seeded in 6-well plates at 80-90% confluence; the medium was replaced with complete EBM-2 without antibiotics before transfection. DharmaFECT 4 and siRNA products were incubated separately in EBM-2 at room temperature for 5 min. Mixtures were combined, incubated another 20 min, and added to cells at a final concentration of 2 µl/ml DharmaFECT 4 and 25 nM siRNAs. Cells in control group were treated with DharmaFECT 4 plus a scramble control siRNA. For UTP stimulation of the cells, siRNA and transfection reagent were removed 24 h post-transfection, and complete culture medium was added. After overnight starvation, cells were stimulated by UTP for 30 min or not. Western blotting was employed to verify knock-down efficiency 24hr post-transfection. Real-time quantitative RT-PCR was used to detect TF pre-mRNA level after knock-down of the individual AP-1 subunits.

2.11. Animal Handling

All animal procedures were reviewed and approved by the Auburn University Institutional Animal Care and Use Committee. 10 weeks old $P2Y2R^{-/-}$ and wild type C57bl/6 mice were purchased from Jackson Laboratories. All animals were housed on a 12 hour light: 12 hour dark cycle and provided standard laboratory chow and water *ad libitum*. Male mice 2-3 months old between 25-35g were ether-anesthetized and injected by the tail vein. Weight LPS dosage

tale vein injection. LPS from E. coli (serotype O111:B4) was injected at a single dosage of 30μg/g body weight. Mice survived at 24 hours were euthanized by CO2 inhalation. The circulation system was perfused with 4% paraformaldehyde in PBS (Thermo Scientific) through the heart to obtain the best possible preservation of the blood vessels. Hearts and aortas were isolated from euthanized and perfused mice, fixed in 4% paraformaldehyde in PBS overnight, dehydrated in 30% sucrose, then cryoembedded in VWR Clear Frozen Section Compound (Cat. No. 95057-838). 10 micrometer sections were cut and loaded onto poly-L-lysine (Electron Microscopy Sciences) coated slides.

2.12. Immunohistochemistry Analysis

Mouse heart and aortic sections were thawed at room temperature and rehydrated in PBS for 15 min. Sections were blocked with 5% horse serum at room temperature for 1 h. The rat monoclonal anti-mouse coagulation factor III/tissue factor antibody and hamster monoclonal anti-mouse CD31 antibody, or isotype control antibodies, were added to the sections at 10 μg/ml and incubated at 4^{o}C overnight in a humid chamber. Sections were rinsed thoroughly in PBS for 3 times and incubated with goat NL637-conjugated anti-rat IgG (R&D Systems) and rabbit FITC-conjugated anti-hamster IgG (Thermo Scientific) at 2 μg/ml for 1 h at room temperature. Sections were then rinsed thoroughly in PBS for 3 times, and cover slipped with Vectashield Mounting Medium containing DAPI (Vector laboratories), as previously reported (Ding et al., 2011; Ma et al., 2013). All images were acquired and captured on EVOS. The TF-positive and CD31-positive areas were determined in 4 sections from each mouse, using 80 μm intervals between the sections; the results were confirmed in three P2Y2R-null and control mice.

2.13. microRNA Expression Profiling

The Human Genome RT^2 miRNA PCR Array System (Qiagen), which profiles the expression of 708 human microRNAs, was used. Total RNA including small RNAs, was prepared from HCAECs with or without 1 h UTP 100μM treatment with miRNeasy Kit (Qiagen). 1 μg total RNA from each group was reverse transcribed with RT^2 miRNA First Strand Kit (Qiagen). cDNA was mixed with 2x RT^2 SYBR Green PCR Master Mixt and loaded on the array plates for real time-PCR analysis. Data analysis was performed using the manufacturer's integrated web-based software package for the PCR Array System using ΔΔCt based fold-change calculations.

2.14. microRNA RT-PCR

Primer for hsa-mir-181a-2 as described by Chen et al (Chen et al., 2005) using the method called stem-loop RT-PCR. Total RNA from HCAEC were prepared as described in **2.13.**. Reverse transcription (RT) recipe and procedure were the same as described in **2.3.3.**. Real-time PCR were performed in the same way as described in **2.3.4.**.Sequence for stem-loop RT is 5'-GTCGT ATCCAGTGCAGGGTCCGAGGTATTCGCACTGGATACGACGGTACG-3'. Real-time PCR primers for has-mir-181a-2 are: forward primer: 5'-GCGGCGGACC ACTGACCGTAGAC-3'; reverse primer: 5'-GCGGCGGACCACTGACCGTTGAC-3'. RNU6C was used as housekeeping gene. Reverse transcription (RT) of RNU6C was performed the same as described in **2.13.** with RT^2 miRNA First Strand Kit (Qiagen). Real-time PCR

primers for RNU6C are: forward primer: 5'-GTTAAACTCACTGGCACCCA-3'; reverse primer: 5'-GATGAGTTGCCATGCTAATAC TG-3'.

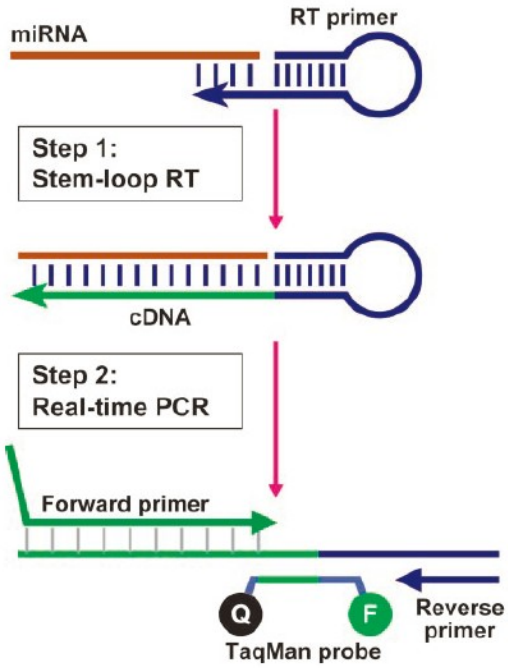

Figure 2.2. Scheme of microRNA stem-loop RT-PCR.

Adapted from Chen C et al. *Nucleic Acids Research*. 2005; Vol. 33, No. 20

2.15. Data Analysis

Data are expressed as the mean ± S.E.M.. The means of two groups were compared using Student's t test (unpaired, two tailed), and one-way analysis of variance was used for comparison of more than 2 groups with $p < 0.05$ considered to be statistically significant. Unless otherwise indicated, all experiments were repeated at least three times. Statistical analysis was performed with Graphpad Prism 5.0.

Chapter 3. Results

3.1. Heterogeneity of TF Expression in Response to P2Y2R Activation in Different Tissues

According to our earlier publication (Ding et al., 2011), UTP/ATP upregulate TF protein level via P2Y2R activation. TNF-α (10ng/ml) was used as positive control due to its typical inflammatory and thrombogenic character. To investigate whether there exists a relationship between the two different types of inducers, we co-treated HCAEC with UTP and TNF-α at various concentrations. Figure 5.1.A shows that, in our new batch of HCAEC from a different donor, UTP itself induced moderate increase of TF protein level after 4 h exposure. TNF-α, on the other hand, showed strong induction as positive control at 10ng/ml, but had negligible effect at 0.1ng/ml and mediocre effect at 1ng/ml. When applied together with 100μM UTP, TF induction by TNF-α far exceeded the one caused by itself. This is especially obvious for the TNF-α 1ng/ml group, where the collective result exceled positive control (TNF-α 10ng/ml). These results suggest that UTP has synergistic effect upon TNF-α induction of TF. LPS is another well-known inducer of TF especially in monocytes (Meszaros et al., 1994), had little effect on HCAEC (Figure 5.1.1A).

Moreover, we hypothesis that TNF-α also incurs nucleotide release from endothelial cells since it programs them into apoptosis direction, which involves releasing of nucleotide-containing vesicles and cytolysis (Wiley et al., 1995). If this hypothesis is true, depleting extracellular nucleotide will ablate partially the TF-inducing effect of TNF-α. To test this hypothesis, we

employed apyrase, a soluble counterpart of human endonucleotidase CD39 extracted from potato, to degrade any nucleotide, including UTP and ATP, released from HCAEC during TNF-α treatment. As shown in Figure 5.1. B, while apyrase itself had no effect on HCAEC TF expression at both low and high concentration (2U/ml and 10U/ml), it significantly quenched TF protein level caused by TNF-α.

Instead of HCAEC, many in vitro studies on cardiovascular diseases are done on HUVEC. Here we treated HUVEC with LPS from three different sources with or without apyrase pre-treatment, but found no significant induction of TF protein, although transient TF mRNA level increased has been reported (Parry and Mackman, 1995). UTP itself had negligible effect (Figure 5.1.C).

Then we expanded our study to aorta P2Y2R activation in animal models. LPS challenge has been commonly used on mice to create models for inflammation, endotoxemia and sepsis studies (Proctor et al., 1994). As shown in Figure 5.2. A, LPS significantly induced TF expression in mouse heart coronary artery in wild-type mice. However, in wild-type mouse aorta, LPS did not exert the same effect (Figure 5.2. B&C). Surprisingly, high aorta endothelial TF expression and blood clotting were observed in P2Y2R knock-out mice (Figure 5.2. B&C). These results indicate that endothelial TF expression regulated by purinergic stimulation follow different mechanisms and patterns in coronary artery aorta.

Microvascular thrombosis is a common phenomenon in endotoximia and sepsis. We then used HMVECad to study microvascular endothelium in response to purinergic stimulation. After treating HMVECad with different nucleotide/nucleoside compounds, no significant induction

of TF protein was observed compared to positive control of TNF-α (Figure 5.3.A& B UTP). We moved on to test TF expression under more typical inducers LPS and TNF-α and their interaction with nucleotide degrading apyrase. To our surprise, apyrase itself has induction effect on TF protein level and also boosted the induction caused by LPS and TNF-α. These results indicate that HMVECad itself is not sensitive to purinergic stimulation. TF expression regulated by apyrase might be mediated through other receptors or pathways.

Monocytes and macrophages are another family of cells actively involved in atherothrombosis and express induced TF. We used two sublines of THP-1 monocytic cells (differentiation-prone and differentiation-resistant) to study the effect of purinergic stimulation on TF expression by itself or in collaborating with inflammatory factors. Figure 5.4.A demonstrates that two disparage THP-1 sublines displayed completely different response to these stimulators. Generally speaking, differentiation-prone subline (upper panel) is more likely to express TF protein under purinergic and inflammatory stimulation compared to differentiation-resistant subline (lower panel) with is more proliferation active. In Figure 5.4.B&C, it is clearly shown that apyrase itself does not have any effect on TF expression, but partially abolished induced TF caused by LPS and UTP. As positive control TNF-α and 15% FBS (fetal bovine serum) both manifested strong induction of TF (Figure 5.4.A upper panel TNF-α & Figure 5.4.B) while the effect of differentiation inducer PMA was not appreciable (Figure 5.4.C). These result support the hypothesis that LPS may induce nucleotide release from differentiation-prone THP-1 monocytic cells and this effect further amplify TF induction and thrombogenicity.

From THP-1 monocytic cells, we extrapolate our study to primary monocytes isolated from human peripheral blood. Firstly, neither UTP nor ATP has detectable induction on TF expression, while apyrase pre-treatment seemed to have a slight induction when applied prior to those two nucleotides (Figure 5.5.A). There was no apparent additive caused by UTP/ATP on LPS induction of TF protein either (Figure 5.5.A). Another closer trial revealed that apyrase did visibly promoted LPS induction of TF (Figure 5.5.B), especially with O111: B4 serotype, while it had no induction effect alone. TNF-α did not show any TF induction in human primary monocytes either. In summary, these cells displayed response profile different from THP-1 cell line.

3.2. P2Y2R Activation Promotes TF Gene Transcription

Since our previous study demonstrated that P2Y2R is the only UTP-sensitive nucleotide receptor expressed in HCAEC (Ding et al., 2011), UTP was routinely used to activate the P2Y2R throughout this study. Two pairs of primers were designed to selectively amplify non-spliced TF pre-mRNA (also termed hnRNA) and mature TF mRNA, respectively. The pair for mature mRNA span from exon 1 to exon 3 with 2 introns in the middle. The amplicon length is 233 bp for the TF mature mRNA after splicing (Figure 5.6.A). The pair of primers for pre-mRNA is located in the same intron (intron 2) which will be spliced away before forming the mature mRNA. This pair of primers would produce a 244 bp amplicon from the non-spliced pre-mRNA pool (Figure 5.6.A). Figure 5.6.B shows that activation of HCAEC by TNF-α increased the TF expression levels of pre-mRNA and mature mRNA, which peaked at 30 min and 1 hr, respectively. A similar pattern of time dependent induction of both TF pre-mRNA and mature mRNA by UTP stimulation of the P2Y2R was observed (Figure 5.6.C & D). These data

indicate that TF pre-mRNA and mature mRNA are changed similarly overtime by TNF-α and UTP stimulation, and that HCAEC is a good cell model for studying TF transcriptional mechanisms.

3.3. Identification of New Transcription Factor Binding Sites

Figure 5.7.A portraits the classic proximal human TF gene promoter is 227 bp in length upstream from transcription starting site. There are binding sites for four transcription factors in this region: AP-1, NF-κB, Egr-1, and Sp1. Sp1 is required for constitutive TF gene transcription while the other three are responsible for inducible TF gene transcription (Li et al., 2009). Egr-1 usually comes into effect very slowly because it needs to be synthesized de novo (Guha et al., 2001), suggesting that it may not be a significant factor in our system, since our previous study showed that de novo protein synthesis is not required for P2Y2R-mediated TF induction (Ding et al., 2011). In addition, our prior study also excluded the involvement of the NF-κB pathway (Ding et al., 2011), leaving AP-1 as an attractive candidate. Two established proximal AP-1 binding sites are located at -124 bp (TGAATCA) and -111bp (TGAGTCA). Only one of these two is 100% in accordance with the IUPAC string consensus (TGAG/CTCA). One nucleotide difference from consensus compromises its contribution to promoter activity although they are almost next to each other in position (Oeth et al., 1997). This lead us to search for perfect consensus match into upper stream of TF promoter with TRANSFAC (http://www.biobase-international.com/product/ transcription-factor-binding-sites), and found another 100% consensus AP-1 binding site at -1363 bp (Figure 5.7.B green). Interestingly, a binding site for transcription factor Evi-1 was also found at -3819 bp (Figure 5.7.B blue). Orthologous sequences were found in other species

and aligned in parallel for Evi-1 site (Figure 5.7.C) and new AP-1 site (Figure 5.7.D) to represent their conservativeness, an important constraint in transcription factor binding site prediction (Matys et al., 2003).

3.4. Evi-1 Site and New Distal AP-1 Site Have Different Impact on TF Promoter Activity

To determine how these transcription factor binding sites we located affect TF promoter activity, we constructed luciferase vector with TF promoter region covering these sites. To cover the Evi-1 site, a total length of ~4.3 kb sequence was cloned and inserted into vector pGL4.12. To cover the new distal AP-1 site, a total length of ~1.6 kb sequence was cloned and inserted into vector pGL4.12. Successful constructions were verified after digestion with restrictive endonuclease (Figure 5.8) and sequencing. Verified constructs were amplified, purified and used for transfection and luciferase assay in HCAEC. A plasmid containing β-galactosidase driven by the SV40 promoter was co-transfected to normalize the transfection efficiency. 36 h after transfection, cells were starved overnight, then treated with indicated reagents for different durations.

To study the role of Evi-1 site, we compared promoter activity induced by TNF-α, UTP and 2-thio-UTP (a hydrolysis-resistant analog of UTP) in vectors containing 4.3 kb insert, 1.6 kb insert, or empty vector. Compared to empty vector, both 1.6 kb insert and 4.3 kb insert gave high rise in transcription activity (Figure 5.9.) at ~1 h into stimulation. Relative extent of induced promoter activity is TNF-α>UTP>2-thio-UTP. However, under all three stimuli, no significant difference was observed between 1.6 kb insert and 4.3 kb insert. These result

indicate that most TF promoter activity is from within the 1.6 kb insert. Not much activity lies beyond this region. The Evi-1 binding site we found failed to alter transcription efficiency considerately.

To investigate the new distal AP-1 binding site, HCAECs were transfected with the luciferase construct promoter region up to -1427 bp (1.6 kb insert) containing the new AP-1 site or its deleted/truncated/mutated forms. 36 h after transfection, cells were starved overnight, then pre-treated with or without 30μM p38 inhibitor SB203580 or JNK inhibitor SP600125for 1 h, then treated with 100 μM UTP for 1.5 h. Then luciferase and β-galactosidase activities were determined. Figure 5.10.A shows the verification of success mutation of the new distal AP-1 site. Figure 5.10.B shows that UTP induced ~8 fold of increase in luciferase activity over non-stimulated cells. Deletion, truncation and mutation of this new AP-1 site all significantly decreased the promoter activity. Both p38 inhibitor and JNK inhibitor attenuated promoter activity to the same extent as truncation. These data indicate that the new AP-1 site at -1363 bp has significant impact on TF gene transcription. MAPK pathways p38 and JNK are highly likely to affect TF transcription through AP-1 in HCAEC.

3.5. Evi-1 May Function in Other Fashions in Atherothrombosis Related Cells

To determine whether Evi-1 has other function in atherothrombosis related tissues and cells, endothelium and monocytes, although it has little impact on TF transcription raised by TNF-α and extracellular nucleotide in HCAEC. Evi-1 has three isotypes: the MDS1/Evi-1 fusion protein ~ 200 kD in size, the prototype Evi-1 itself ~145kD in size, and truncated Evi-1 ~105 kD in size. The presence and abundance of each isotype varies from tissue to tissue and

depending on physiological conditions. (Fears et al., 1996; Morishita et al., 1990) In Figure 5.11.A, Evi-1 level was down-regulated by TNF-α, which usually induce TF expression in HCAEC. In Figure 5.11.B, in THP-1 monocytic cell line, Evi-1 level was changed in the process of differentiation which is an important component of atherosclerosis development. Amount of all three isotypes of Evi-1 gradually increased through differentiation progress up till 24 h and dropped dramatically at 48 h. We also investigated how UTP and monocyte differentiator PMA alter Evi-1 level. Both had slight increasing effect in Evi-1 levels in THP-1 monocytic cell (Figure 5.11.C left panel), but no effect in human primary monocytes (Figure 5.11.C right panel). These data point to a possibility that Evi-1 might negatively regulate TF transcription by TNF-α in HCAEC, and that it is involved in monocyte differentiation and purinergic response.

3.6. More Evidence on the New Distal AP-1 Binding Site Regulating TF Gene Transcription

An EMSA was conducted with biotin-labeled AP-1 probe equivalent to the region -1369 bp to -1350 bp in the human TF promoter to confirm our luciferase activity assay in session 3.4 and Figure 5.10.B. We found that nuclear extract from HCAEC has higher occupancy over this TF AP-1 site after UTP stimulation of the cells for 30 min. In addition, excessive un-labeled probes competed against labeled ones and eliminated the signal, indicating the specificity of the protein-DNA complex. Moreover, TNF-α stimulation for 30 min caused the same change as UTP did, which suggests that the same site may be also taken up in TNF-α-induced TF induction (Figure 5.12.A). Quantitative data indicate that both UTP and TNF-α treatment increased probe occupancy about 4 folds (Figure 5.12.B).

3.7. P2Y2R Activation Has Differential Effects on AP-1 Subunits

AP-1 components bind to DNA promoter in a dimerized form (Glover and Harrison, 1995). The two subunits come from members of the Jun protein family (c-Jun, JunB and JunD), Fos protein family (c-Fos, FosB, Fra-1 and Fra-2) and some members of the ATF subfamily (ATFa, ATF-2 and ATF-3). (Glover and Harrison, 1995) To determine the roles of different subunits, we first assessed the effect of P2Y2R activation on their phosphorylation status. Figure 5.13.A, B, C, E, F and G show that UTP or its analog 2-thio-UTP caused rapid phosphorylation of c-Jun, Fra-1 and ATF-2 in a dose- and time-dependent manner. However, UTP failed to induce phosphorylation of c-Fos, one of the most classic AP-1 subunits, timely (Figure 5.13.D). JunB and JunD, on the other hand, were not detectable (data not shown). It has been known that Jun protein is mainly in charge of the binding affinity while the others rely on dimerizing with a Jun protein to influence the promoter activity (Hess et al., 2004). We furthered our study on subunits with a co-immunoprecipitation experiment to confirm that the phosphorylated Fra-1 and ATF-2 are c-Jun-bound so that they can recognize and attach to their targeting sites. Cell extracts from HCAECs treated with or without UTP were incubated with 1 μg rabbit anti-c-Jun antibody, precipitated with protein A agarose beads and detected with antibodies specific for Fra-1, ATF-2 and c-Jun (as loading control). Figure 5.11.H shows that UTP treatment dramatically increased the amount of Fra-1 and ATF-2 bound to c-Jun, indicating their higher DNA-binding potential after forming a dimer with c-Jun.

For AP-1 subunits to be fully functional, they have to reside in nucleus. The abundance of them in the nucleus correlates with their activity on target (Schreck et al., 2011).To define the

location of phosphorylated c-Jun, Fra-1 and ATF-2, immunofluorescent images were compared between groups with or without UTP stimulation for 30 min. In control groups without stimulation, very little FITC signal was detected for any of the three phosphorylated subunits. In UTP stimulated groups, however, intense green light from FITC indicates high level of phosphorylated c-Jun, Fra-1 and ATF-2. Overlaying with DAPI and Phalloidin image shows that majority of the phosphorylated subunits accumulated in HCAEC nucleus, instead of cytoplasm/cell skeleton (Figure 5.14.). Of note, no positive staining was observed once p-c-Jun, p-Fra-1 and p-ATF-2 antibodies were replaced by its IgG control antibody or when only FITC-conjugated secondary antibody was used (Figure 5.14.D).

3.8. The New Distal AP-1 Site is Responsible for Endogenous c-Jun, Fra-1 and ATF-2 Binding to TF Promoter.

The new AP-1 site is responsible for endogenous c-Jun, Fra-1 and ATF-2 binding to TF promoter. To confirm the binding specificity of the AP-1 components to the new AP-1 binding site, we further performed ChIP and EMSA studies using specific c-Jun, Fra-1 and ATF-2 antibodies and cell lysates with or without P2Y2R activation. With primers amplifying a PCR product spanning from -1427 bp to -1217 bp of TF promoter, which includes the AP-1 site, a 210 bp DNA fragment was amplified from anti-c-Jun, anti-Fra-1 and anti-ATF-2 chromatin precipitates by real-time PCR (Figure 5.15.A-C). All three precipitates from UTP-treated HCAECs resulted in dramatic increment in DNA amplification with expected size and sequence. In addition to ChIP assay, EMSA supershift assays were performed with labeled wild-type AP-1 site probe. Different AP-1 protein antibodies and control IgG were added to the nuclear extracts before electrophoresis to detect further decreases in electrophoretic mobility.

The addition of c-Jun, Fra-1 and ATF-2 antibodies to the EMSA reaction mixture resulted in the inhibition of specific complex formation (Figure 5.15.D-F), indicating that all three subunits are the proteins binding to this site in HCAECs after P2Y2R activation. Higher amount (2μg) of antibodies caused more inhibition compared to lower amount (1μg) of the same antibody. Control IgG (2μg) did not change the binding of the labeled probe with the AP-1 components. These data demonstrate that P2Y2R activation induces specific binding of c-Jun, Fra-1 and ATF-2 to the -1363 bp new AP-1 site of the TF gene in HCAECs.

3.9. Knockdown of c-Jun, Fra-1 or ATF-2 Has Differential Roles in TF Transcription Following P2Y2R Activation.

To determine the roles of the three AP-1 subunits in control of TF transcription, we knocked down c-Jun, Fra-1 and ATF-2 respectively by a siRNA approach. Western blotting assay indicated a complete elimination of ATF-2 and a significant decrease of c-Jun and Fra-1 on their total protein levels in HCAECs (Figure 5.16.A-C). The siRNA-transfected HCAECs were exposed to UTP for 30 min or not before TF pre-mRNA was quantified by real-time PCR. Transfection with different siRNA pools did not change the basal levels of TF pre-mRNA without UTP treatment. Upon UTP treatment, though, TF pre-mRNA markedly decreased in HCAECs in lack of c-Jun and ATF-2. Surprisingly, however, TF transcription level was significantly increased in cells with Fra-1 knockdown as compared with control scrambled siRNA-transfected ones (Figure 5.16.D). Collectively, these data suggest that Fra-1 affects TF transcription negatively in response to P2Y2R activation in HCAECs, while the other two AP-1 subunits involved, c-Jun and ATF-2 are positive regulators.

3.10. The Effect of Different Post-P2Y2R Signaling Pathways on AP-1 Subunits and TF Gene Transcription

We then further explored which post-P2Y2R signaling pathways are responsible for regulating the three AP-1 subunits and net TF transcription. As shown in Figure 5.17.A, treatment of the cells with SP60012, a well-established JNK inhibitor, abolished c-Jun phosphorylation completely after P2Y2R activation. Similarly, phosphorylation of ATF-2 was changed in exactly the same way as c-Jun did after JNK inhibition (Figure 5.17.A). However, Fra-1 phosphorylation is resistant to JNK pathway inhibition (Figure 5.17.A). Afterward, we used the classic ERK1/2 inhibitor U0126 to study the effect of ERK1/2 on Fra-1 and ATF-2. As shown in Figure 5.17.B, U0126 dose-dependently inhibited UTP-induced Fra-1 phosphorylation, whereas phosphorylation level of ATF-2 was insensitive. Given that Rho kinase is the upstream regulator of JNK as we reported previously (Ding et al., 2011), we then hypothesized that Rho may induce c-Jun and ATF-2 activation through JNK. To test this hypothesis, we examined the effect of Rho kinase inhibitor Y27632 on c-Jun and ATF-2 phosphorylation. Pre-incubation of HCAECs with Y27632 at 3 μM inhibited UTP-induced c-Jun and ATF-2 phosphorylation (Figure 5.17.C). Similarly, we verified whether the other kinase activated by UTP treatment, Src (Ding et al., 2011), can act on ERK1/2 and its downstream Fra-1, because there is a well-established connection between Src and ERK1/2 (Arany et al., 2004). Figure 5.18.D shows that increasing dosage of Src inhibitor PP2 gradually quenched phosphorylation of Fra-1. These data clearly indicate that the P2Y2R utilizes different signaling pathways to control the activity of the three AP-1 components.

Finally, we validated the impact of the above pathways on TF transcription. Since Src and ERK1/2 are in control of Fra-1, they are expected to have the same effect on TF transcription as Fra-1 does. Likewise, Rho and JNK should possess the opposite effect as compared with Src/ERK1/2. In line with our assumption, ERK1/2 inhibitor U0126 and Src inhibitor PP2 mimicked the effect of Fra-1 knock-down and boosted TF transcription. On the other hand, JNK inhibitor SP60012 and Rho inhibitor Y27632 act in the same as c-Jun and ATF-2 knock-down and caused a loss in TF transcription (Figure 5.17.E).

3.11. P2Y2R Activation Increases TF mRNA Stability in HCAEC

To determine whether P2Y2R activation up-regulate TF mRNA level by increasing its stability, we used actinomycin D as a transcription inhibitor, to rule out the effect of transcription and give a more accurate view on post-transcriptional mechanism itself. We designed the following experiment to test the effectiveness of actinomycin D. Without actinomycin D, TF pre-mRNA level soared under UTP stimulation. With a 10μg/ml co-treatment of actinomycin D, the transcription was completely blocked within half an hour, similar to the group with no UTP at all. (Figure 5.18.A) This regiment was employed to treat HCAEC in following studies on TF mRNA stability.

When two groups of HCAEC were both treated with 10μg/ml actinomycin D, one was stimulated with 100μM UTP, the other one was not. TF mRNA levels at different time points were measured by real-time PCR. Fold changes undergone logarithmic transformation were plotted against corresponding time point into decay curves (Figure 5.18.B). Calculation showed that TF mRNA half-life was prolonged by two folds from 5.6 h to 14.2 h with the

addition of UTP. These results persuades us that P2Y2R activation up-regulate TF steady-state mRNA level by not only promoting transcription, but also increasing TF mRNA stability.

3.12. p38/MK-2 mRNA Stabilizing Pathway Activation Following Purinergic Stimulation in HCAEC

Not the whole TF mRNA transcript is translated into peptide. TF coding sequence starts with AUG and ends with UAA. The part after UAA till the end of the transcript is 3'-untranslated region (3'-UTR). In TF mRNA 3'-UTR, all three classes of ARE described in session **1.10**. were found as schemed in Figure 5.19.A. Since we already reported that p38 pathway is indispensable for P2Y2R signaling (Ding et al., 2011), it is reasonable to stretch the study on p38 to mRNA stability regulation mediated by p38/MK-2. Therefore, we investigated how P2Y2R activation affect MK-2 phosphorylation. Figure 5.19.B shows that UTP stimulation upregulates MK-2 phosphorylation in time- and dose-dependent manner. Increment in UTP concentration resulted in higher efficacy on MK-2 activation at 5 min. Induction of MK-2 phosphorylation by UTP is transient and fast, starting within 5 min and fading by 1 h. These data suggest that p38/MK-2 pathway might be involved in TF mRNA stabilization controlled by P2Y2R activation in HCAEC.

Further, we employed two inhibitors, p38 inhibitor SB 203580 and MK-2 inhibitor PF3644022 to study this pathway in mRNA stabilization. Phosphorylation of Hsp27 was used as an indicator of mRNA stabilization potential of p38/MK-2 pathway. It is the direct substrate of both p38 and MK-2 and a component in ARE binding complex. Phosphorylated hsp27 is on the stabilization side of AREBP/mRNA stability balance instead of the destabilization side.

Western blot image depicts that (Figure 5.20.A) SB203580 partially attenuated hsp27 phosphorylation and completely blocked MK-2 phosphorylation. On the other hand, the effect of PF compound on hsp27 was not very obvious but still visible. On the base of these results, we went on to detect TF mRNA stability change under treatment of these pharmacology tools. All transcription activity was suppressed in HCAEC with actinomycin D as described in **3.10.**, while treated with UTP with or without inhibitors. As shown in Figure 5.20.B, after 1.5 h treatment, group with only transcription inhibitor had only 54.7% TF mRNA left compared to the one stabilized by UTP, corroborating the mRNA stabilization effect of P2Y2R activation. By inhibiting p38 at the same time, less TF mRNA survived decay compared to UTP only group (50.5%), indicating that the mRNA stabilization effect was compromised. By inhibiting MK-2 kinase, 62.4% of TF mRNA was saved compared to UTP only treatment. These results indicate that p38/MK-2 pathway activation has crutial contribution to TF mRNA stability after UTP stimulation.

3.13. Candidate microRNAs Regulated by P2Y2R Activation in HCAEC

To acquire initial insights into the potential microRNAs regulated by HCAEC P2Y2R, we analyzed the expression profile of 708 miRNAs with or without UTP treatment using commercially available microarrays. Of the 708 miRNAs, 24 were upregulated by at least one fold and 20 were downregulated by more than 50% (Figure 5.21.). Since miRNA is a negative regulator of mRNA stability, higher stability of a certain mRNA means less amount of the miRNA targeting it. Thus, we are more concerned about the 20 miRNAs downregulated. By searching TF mRNA 3'-UTR for perspective targeting seed for the 20 downregulated miRNAs with free online tool miRanda (http://www.microrna.org/), we found a quality match for

hsa-miRNA-181a. Figure 5.22.A shows an alignment between microRNA-181a sequence and matching seed in TF 3'-UTR from different species including human. To validate this discovery, we performed stem-loop RT and real-time PCR to quantify miRNA-181a levels with or without 1 h UTP treatment in HCAEC. After P2Y2R activation, miRNA-181a level dropped to 23.5% of control on average. These result suggest that P2Y2R signaling can regulate multiple gene expression through microRNAs. miRNA-181a might one of them that contributes to TF mRNA stability regulation.

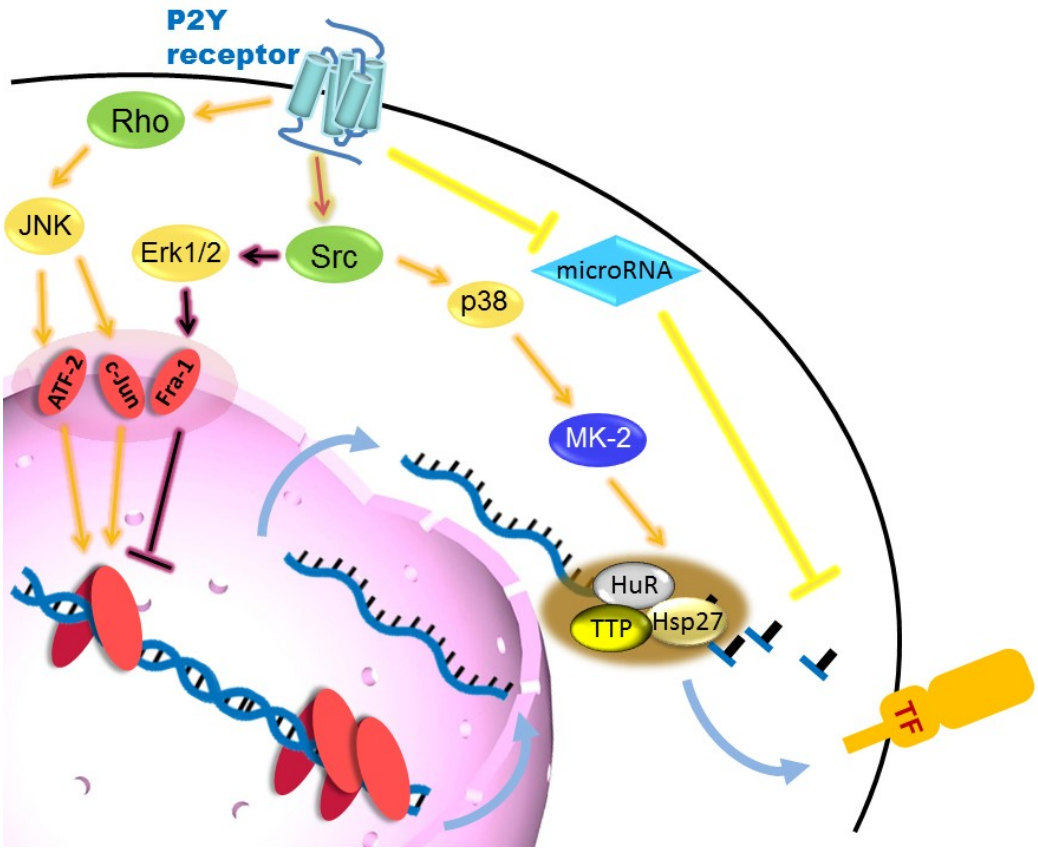

Figure 4.1. Summary of the study.

At the core of our present study, we show for the first time that activation of P2Y2R in HCAEC promotes TF transcription and stabilizes TF mRNA. A new distal AP-1 binding site contributes to promoted TF transcription. We also show that in addition to c-Jun, ATF-2 is a new positive regulator of TF transcription in response to P2Y2R signaling to the JNK pathway. Furthermore, we have identified Fra-1 as a first negative regulator fine-tuning the overall transcription activity of TF gene promoter, which is controlled by P2Y2R signaling to the

ERK1/2 pathway. On the other hand, this is the first time that connections are built between P2Y2R and mRNA stability regulation via AU-rich element binding proteins and microRNAs. We identify p38/MK-2 and miRNA-181a as promising mediators. Furthermore, although scrutinized in platelets in lieu of thrombogenicity (Leon et al., 2003), by demonstrating variant response to purinergic changes, we emphasize the importance of studying purinergic receptor and their functions in non-platelet cells, such as endothelial cells from both large and small vessels, and monocytes/macrophages.

Aside from cell apoptosis and necrosis, nucleotide release also occurs under other conditions in different cells, including platelets, monocytes/macrophages, and vascular endothelial cells (Yegutkin, 2008). These cells release nucleotides including ATP and UTP under various mechanical and other stimuli, such as shear stress, hypotonic swelling, hypoxia, as well as in response to thrombin and other Ca2+-mobilizing receptor agonists (Yegutkin, 2008). Released extracellular nucleotides have been established as important mediators of vascular inflammation (Deaglio and Robson, 2011), thrombosis (Robson et al., 2005), and atherosclerosis (Di Virgilio and Solini, 2002) by acting on various platelet, endothelial and leukocyte P2X and P2Y receptors. P2Y2R, one of the eight G protein-coupled P2Y nucleotide receptors (P2Y1, 2, 4, 6, 11-14), has been shown to induce VCAM-1 expression in HCAEC (Seye et al., 2003) and ICAM-1 expression in vascular smooth muscle cells (Seye et al., 2012), suggesting its potential role in control of leukocyte interaction with the vascular walls.

Initially we showed that the P2Y2R is upregulated in response to coronary artery stenting (Shen et al., 2004), and recently we also reported that activation of the human coronary artery P2Y2R induces a dramatic upregulation of TF, the initiator of coagulation cascade (Ding et al.,

2011). This original finding has been extended to mouse macrophages by other group showing a role of P2X7 receptor in LPS-induced TF upregulation (Lee et al., 2012). Together, these findings suggest that non-platelet nucleotide receptors, i.e. P2Y2R, may have a role in the initiation and/or progression of thrombogensis. However, the exact molecular mechanisms underlying P2X or P2Y receptor- controlled TF expression remained largely unknown. In the current study, we found that activation of P2Y2R in HCAEC increased not only the mature TF mRNA level, but also the TF pre-mRNA level, consistent with our previous study that blocking cellular transcription by actinomycin D suppressed UTP-induced TF mRNA accumulation (Ding et al., 2011), indicating a transcriptional mechanism responsible for P2Y2R-mediated TF upregulation in HCAEC, although additional mechanisms at post-transcriptional level can't be excluded.

Studies on TF transcription have been limited to a short promoter region up to -227 bp from the transcription start site (Li et al., 2009). Binding sites for four types of transcription factors are located in this area. Of these four factors, Sp-1 is in charge of constitutive TF transcription while Egr-1, NF-kB and AP-1 are responsible for induced TF transcription (Li et al., 2009). It is well-known that Egr-1 usually acts very slowly because it needs to be synthesized de novo, suggesting that it may not play a significant role in our testing system, since our previous report showed that de novo protein synthesis is not required for P2Y2R-mediated TF upregulation. Also, in our prior study, no change in IkBa and p65 phosphorylation was observed in response to P2Y2R activation in HCAEC, excluding the involvement of the NF-kB pathway (Ding et al., 2011). Although the classical AP-1 sites are worth to be studied, we were more intrigued by our original finding through bioinformatics search on a much wider region of the TF promoter. Our in silicon search identified a new distal AP-1 binding site which matches 100% to the AP-1

consensus sequence and also is well conserved across multiple species. In addition, we found that this new site is located at -1363 bp in human TF promoter, and that the deletion, truncation or mutation of which all significantly diminished UTP-induced TF transcription, suggesting that this new distal AP-1 site plays a significant role in regulating TF gene transcription in response to membrane receptor activation in HCAEC. This notion is strongly supported by our EMSA study showing that both UTP and TNF-α treatments all significantly increased AP-1 probe occupancy.

To date, very few studies systemically reflect how nucleotide receptor activation acts on transcription factors and their target genes. P2Y2R is reported to mediate sustained phosphorylation of transcription factor CREB on sensory neurons (Molliver et al., 2002). Signaling through P2X7 receptor is reported to activate AP-1 (c-Jun/c-Fos) in human T cells (Budagian et al., 2003), while others found that P2X7 receptor activates FosB/AP-1 complex in monocytic and osteoblastic cells (Gavala et al., 2010). In the present study, we found that three AP-1 subunits and their binding affinity were under control of P2Y2R in HCAECs, namely c-Jun, Fra-1 and ATF-2. Unexpectedly, we ruled out c-Fos although it is the most classic partner of c-Jun and has been reported in TF induction (Oeth et al., 1997; Parry and Mackman, 1995). Both JUN and ATF members can form homodimers by themselves and have different preferences for DNA binding sites (van Dam and Castellazzi, 2001). JUN and FOS subunits favor TRE haptamer (TGAC/GTCA) while ATF members prefer CRE octamer (TGACGTCA). It has been reported that when Jun dimerizes with ATF, the complex has higher affinity to CRE (Benbrook and Jones, 1990). Herein we demonstrated that transcription factor complexes contacting ATF-2 could also recognize and bind to AP-1 consensus site as evidenced by our ChIP and EMSA studies showing that ATF-2-specific monoclonal antibody

not only precipitated a TF promoter fragment containing the new distal AP-1 site, but also significantly decreased AP-1 probe binding capacity. In addition, we found that siRNA knockdown of ATF-2 also significantly suppressed UTP-induced TF gene transcription. This c-Jun/ATF-2 combination is new to both TF gene transcription and nucleotide receptor signaling.

Transcription activity of different AP-1 subunits has been uncanny on different genes under various conditions. Taking c-Jun for example, although a positive regulator mostly, it was reported to suppress transcription of cPLA2a gene (Bickford et al., 2013). Existing reports on Fra-1 is even more controversial (Belguise et al., 2005; Rajasekaran et al., 2012). Negative effect of Fra-1 was reported in chemotherapy resistance and tumor progression (Obenauf et al., 2015). Although TF transcription was up-regulated immensely under phosphorylation of all three subunits, our current loss-of-function study yielded more truth of their differential impact. To the best of our knowledge, the present study is the first to identify Fra-1 as a negative regulator in control of TF transcription while c-Jun and ATF-2 are strong positive ones in line with most studies. This is supported by our unexpected finding that knockdown of Fra-1 boosted TF gene transcription in response to P2Y2R activation in HCAEC. In addition, we found that c-Jun is slightly more effective than ATF-2 in TF transcription up-regulation. The overall effect of them three covered up the fact that Fra-1 is in the opposite direction as compared with c-Jun and ATF-2. These results indicate that at least in HCAEC, the TF gene is under fine-tuning by P2Y2R signaling.

Our previous report has documented that P2Y2R is the predominant P2Y nucleotide receptor subtype expressed in HCAEC, and that activation of this receptor stimulates all the three MAP

kinase pathways including ERK1/2, JNK and p38 (Ding et al., 2011). In addition, we found that inhibition of JNK or p38, but not ERK1/2, all attenuated UTP-induced TF protein expression (Ding et al., 2011), suggesting that both JNK and p38 play an essential positive role in TF protein upregulation. However, whether such a MAP kinase signaling mechanism also applies to P2Y2R-controlled TF gene transcription was unknown. In the present study, we found that inhibition of JNK suppressed UTP-induced phosphorylation of c-Jun and ATF-2, but not of Fra-1, indicating that JNK is an upstream kinase in control of the two positive regulators c-Jun and ATF-2, but not the negative regulator Fra-1. Since our prior study also demonstrated that P2Y2R activates JNK through the Rho kinase pathway (Ding et al., 2011), we reasoned that blocking Rho kinase should also inhibit c-Jun and ATF-2. Indeed, this notion is supported by our observation that UTP-induced c-Jun and ATF-2 phosphorylation was inhibited by Y27632, a well-known selective Rho kinase inhibitor. On the other hand, although both ERK5 and ERK1/2 have been shown to activate Fra-1 in different cells (Terasawa et al., 2003), we did not find any evidence that P2Y2R activates ERK5 (data not shown). Instead, our findings indicate a new P2Y2R/Src/ERK1/2/Fra-1 pathway that negatively regulates TF gene transcription. Several lines of evidence support this view: 1) we found that UTP-induced Fra-1 phosphorylation was inhibited by U0126, a highly selective ERK1/2 kinase inhibitor which did not have any effect on ATF-2 and c-Jun phosphorylation; 2) we also found that UTP-induced Fra-1 phosphorylation was dose-dependently inhibited by PP2, a selective Src kinase inhibitor, which is consistent with our previous report showing that Src is required for P2Y2R signaling in HCAEC (Ding et al., 2011); and 3) importantly, blocking either ERK1/2 or Src kinase all boosted TF pre-mRNA transcription in response to P2Y2R activation.

The ecotropic viral integration site-1 (Evi-1) gene was first recognized as a common locus of retroviral integration in myeloid tumors in mice. In humans, Evi-1 has a crucial role in embryonic hematopoietic stem cell development and differentiation. In adults, Evi-1 gene rearrangement and activation is frequently related to acute myeloid leukemia (AML). (Goyama et al., 2008) In further AML, THP-1 cells were reported to express Evi-1 mRNA which was regulated by arsenic therapeutics. (Zhou et al., 2014) Taken together, the change in Evi-1 protein in THP-1 during differentiation we observed may have clinical significance and therapeutic value.

Our study on P2Y2R activation and mRNA stability regulation is remarkably initiative. As more and more microRNAs are documented in publication and related to myriad diseases, several databases are established to map microRNA groups/clusters-disease associations (Chen et al., 2015; Ruepp et al., 2010). In the future, we will annotate the miRNAs significantly altered by HCAEC P2Y2R through these databases, so that we can make connections between diseases and HCAEC P2Y2R activation. Once this is done, this study can shed more light on new treatment possibilities.

The level of an mRNA within a cell depends on both its rate of synthesis and rate of decay. Our study points to a chance that: the regulation of transcription and mRNA decay can communicate with each other. Transcription factors and DNA promoters may directly influence the relative stability of transcripts that they produce (Bellofatto and Wilusz, 2011). This would enhance efficiency in the usage of enzymes and substrates involved in the regulation of gene expression in the cell. Moreover, coordination of the two processes would

enable more precise regulation of the kinetics of RNA accumulation in response to a variety of cellular signals.

With the help of soluble nucleotidase apyrase, we are able to study the impact of purinergic stimulation under the background of other inflammatory conditions without adding exogenous nucleotide. Our data show opposite effects of apyrase. In HCAEC and THP-1 monocytic cells, it works against TF induction caused by nucleotide and inflammatory stimulations. However, in mouse aorta, HMVECad, and human primary monocytes, apyrase enhance TF induction under the same treatments. These results stress the importance of profiling P2Y receptor expression pattern across multiple tissues and cell types to better understanding the relationship between extracellular nucleotide and diseases tissue-specifically. For example, THP-1 cells do not only carry P2Y2R, but also P2Y6R which is activated by UDP (Jin et al., 1998). Apyrase can hydrolyze UTP into UDP and activate P2Y6R to regulate expression of genes, possibly TF. Noticeable, apyrase has contradicting effect on THP-1 and human primary monocytes. This might hint that purinergic signaling is involved in carcinogenesis.

In summary, our most outstanding achievements in these studies are: identification of a new active distal AP-1 binding site in the TF gene promoter, which plays an essential role in P2Y2R-mediated TF gene transcription in human coronary artery EC; revealing a new positive regulatory pathway for TF gene transcription, namely P2Y2R-Rho-JNK-c-Jun/ATF-2, and discovering a first repressor Fra-1 for the TF gene, which is controlled by P2Y2R signaling via Src and ERK1/2. These findings indicate that the TF gene is under complex two-way fine-tuning by membrane receptor signaling. Overall, our findings highlight that coronary artery endothelial P2Y2R is an intriguing intersection of extracellular nucleotide signaling,

vascular inflammation, and thrombogenesis. Future study should focus on the in vivo significance of the P2Y2R-TF axis and whether P2Y2R antagonist or Fra-1-selective chemical activator would be effective new pharmacotherapy options for prevention and/or treatment of TF-related thrombotic and inflammatory diseases.

Chapter 5. Figures and Legends

Figure 5.1. Effect of purinergic stimulation on induced TF expression in HCAEC and HUVEC.

(A) TF expression levels in HCAECs were determined by Western blotting after the cells were stimulated with or without UTP (100μM), LPS (1μg/ml) or TNF-α at indicated concentrations (ng/ml) for 4 h. When two stimulations were used as co-treatment, they were added at the same time. Equal loading was verified by re-probing with anti-β-actin antibody after stripping the original membranes.

(B) TF expression levels in HCAECs were determined by Western blotting after the cells were stimulated with or without 10ng/ml TNF-α for 4 h. Cells were pre-treated with or without apyrase at indicated concentrations for 30 min. Equal loading was verified by re-probing with anti-β-actin antibody after stripping the original membranes.

(C) TF expression levels in HUVECs were determined by Western blotting after the cells were stimulated with or without UTP (100μM) or LPS (1μg/ml) for 4 h. Cells were pre-treated with or without 2U/ml apyrase for 30 min. Equal loading was verified by re-probing with anti-β-actin antibody after stripping the original membranes.

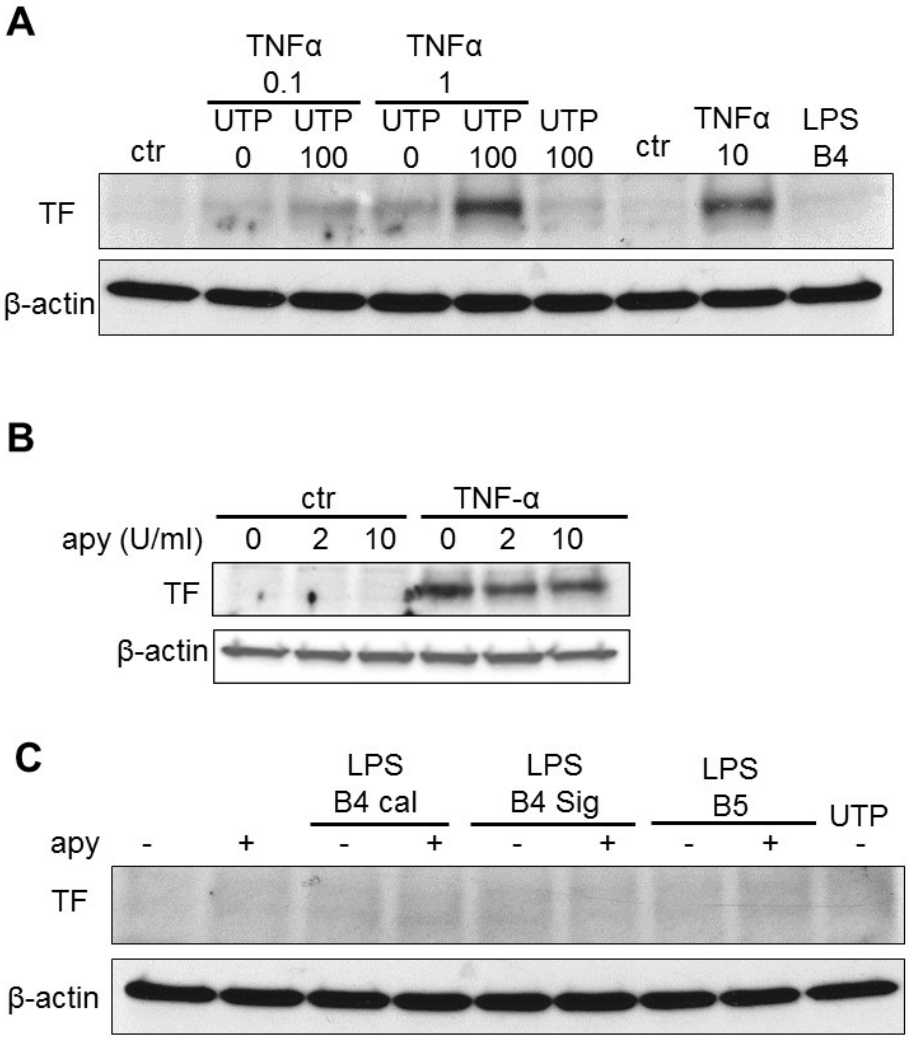
A
TNFα 0.1
TNFα 1
UTP 0
UTP 100
UTP 0
UTP 100
UTP 100
ctr
ctr
TNFα 10
LPS B4
TF
β-actin
B
ctr
TNF-α
apy (U/ml)
0 2 10 0 2 10
TF
β-actin
C
LPS B4 cal
LPS B4 Sig
LPS B5
UTP
apy - + - + - + - + -
TF
β-actin

Figure 5.2. Effect of LPS and P2Y2R on TF expression in mouse coronary artery and aorta.

(A) Immunohistochemistry detection of TF (red), endothelial marker CD31 (green) in coronary arteries of wild-type mice challenged with or without LPS and their co-localization. Nuclei were visualized by DAPI staining (blue). White arrows indicate location of endothelium. Representative images from three mice in each group were shown (original magnification: 20 X).

(B) Immunohistochemistry detection of TF (red) in aortas of wild-type or $P2Y2R^{-/-}$ mice challenged with LPS and their co-localization with elastin. Nuclei were visualized by DAPI staining (blue). Representative images from three mice in each group were shown (original magnification: 10 X).

(C) Immunohistochemistry detection of TF (red) in aortas of wild-type or $P2Y2R^{-/-}$ mice challenged with LPS and their co-localization with elastin. Nuclei were visualized by DAPI staining (blue). Representative images from three mice in each group were shown (original magnification: 20 X).

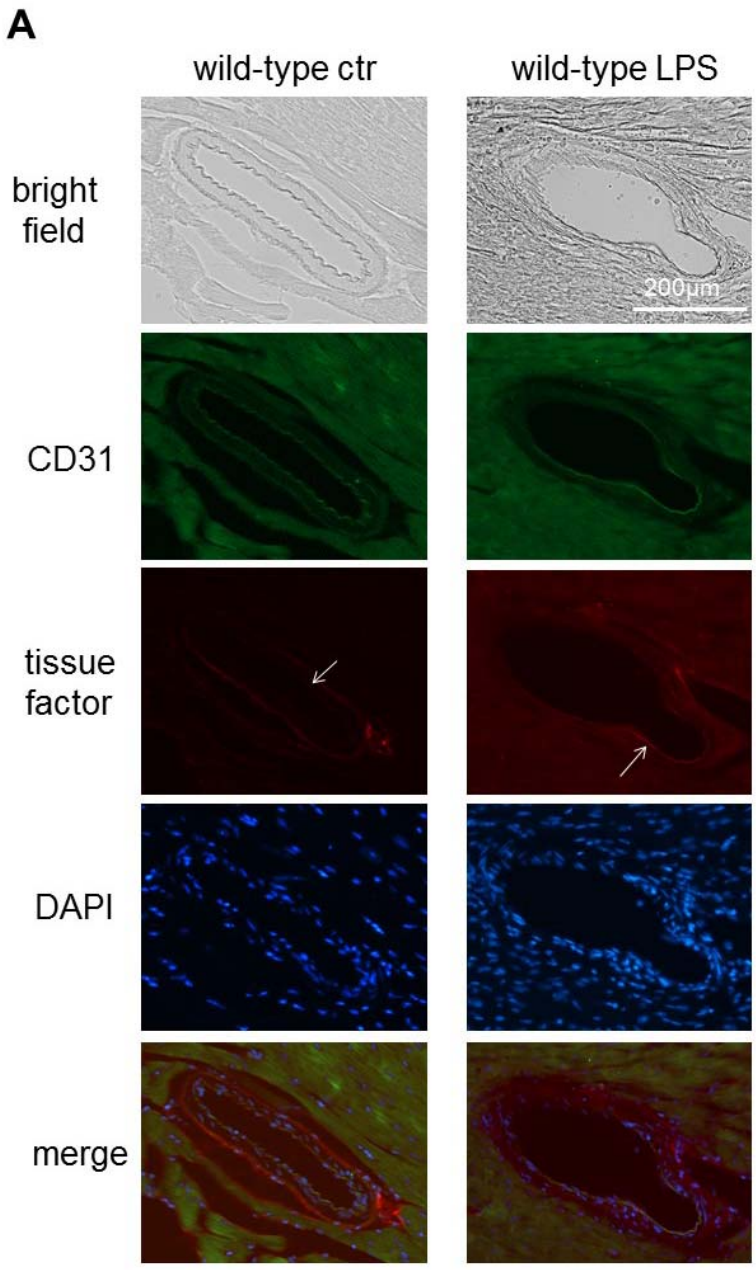
A
wild-type ctr
wild-type LPS
bright field
CD31
tissue factor
DAPI
merge
200µm

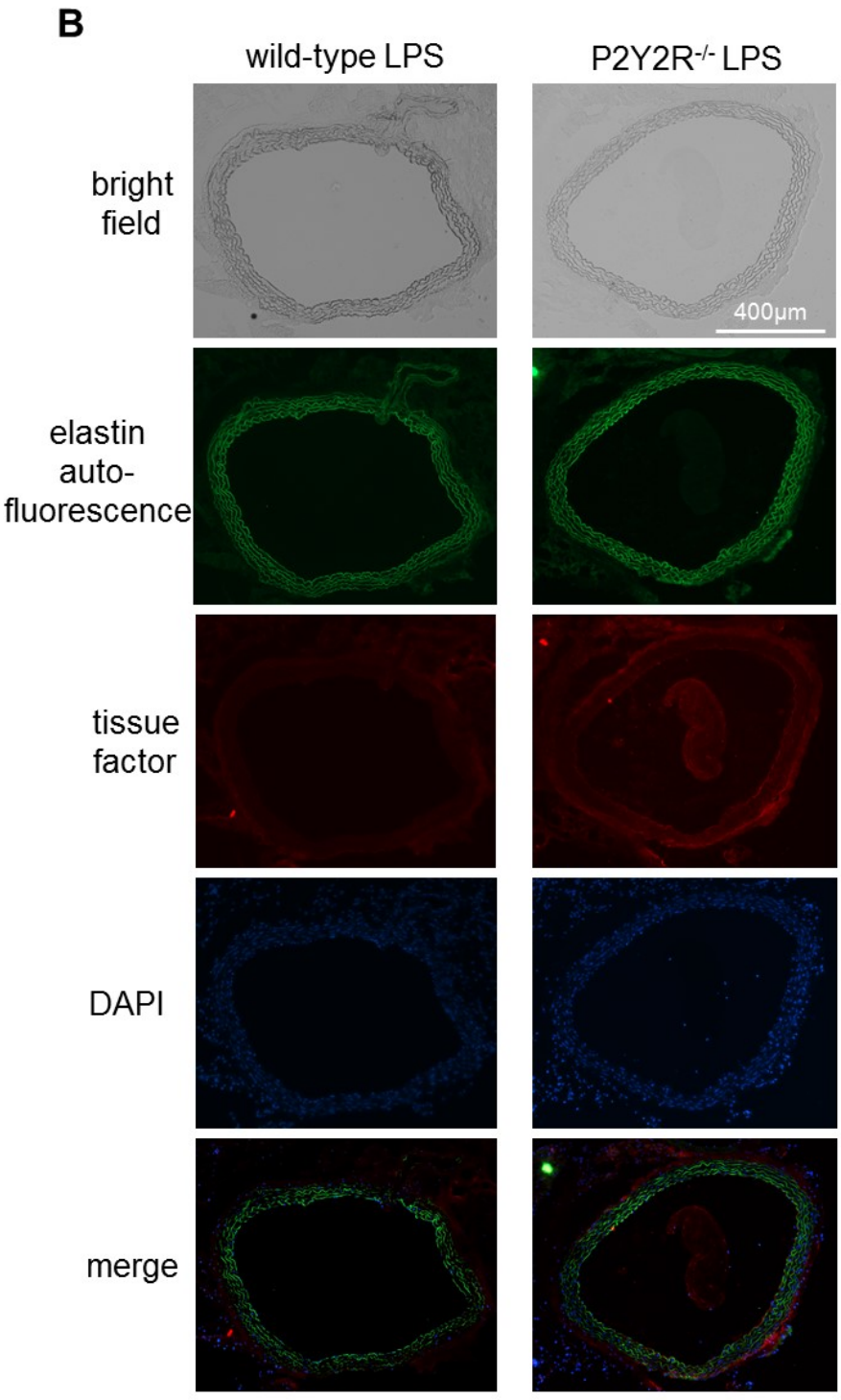
B
wild-type LPS
P2Y2R-/- LPS
bright field
400µm
elastin auto-fluorescence
tissue factor
DAPI
merge

C

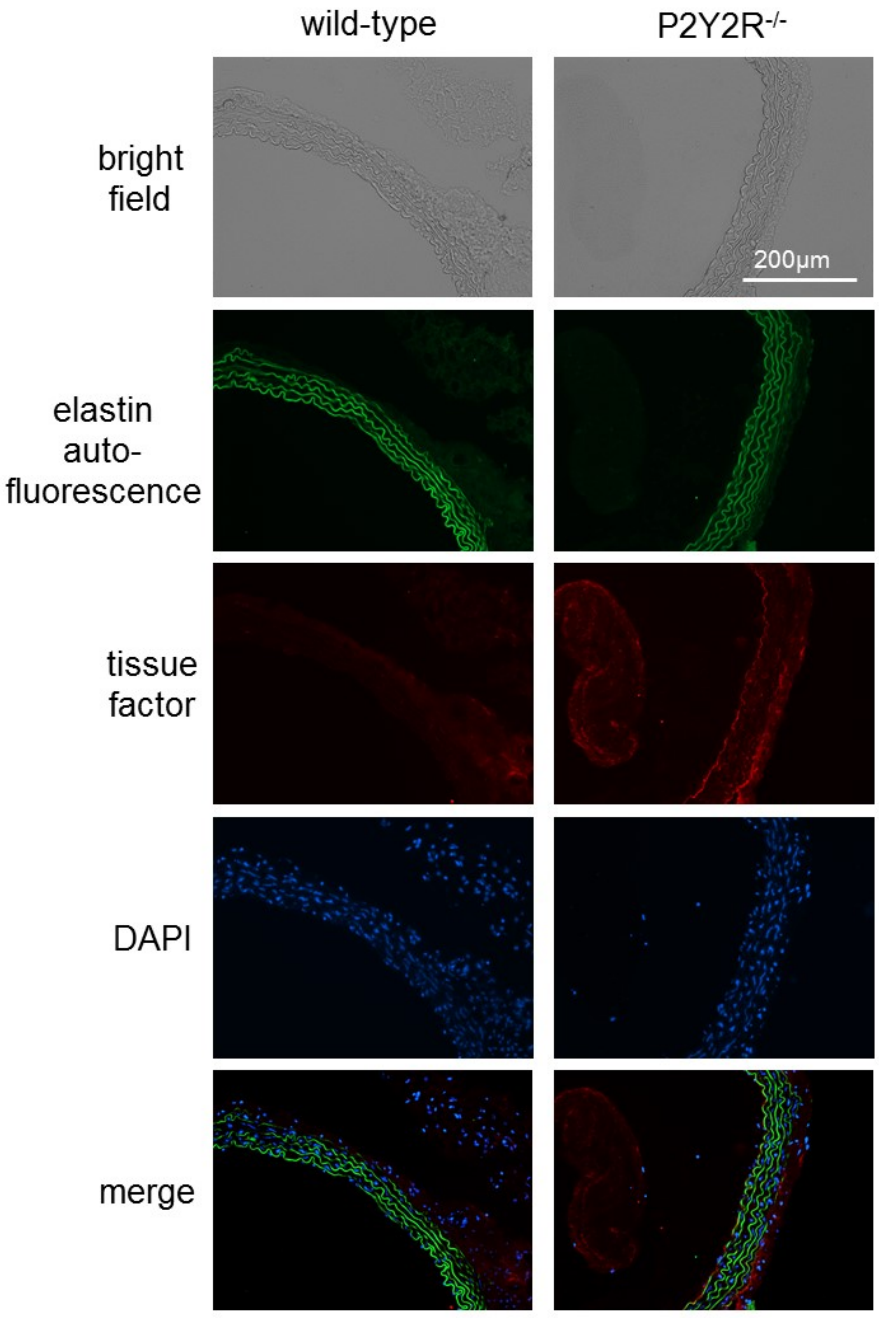
wild-type
P2Y2R-/-
bright field
200µm
elastin auto-fluorescence
tissue factor
DAPI
merge

Figure 5.3. Effect of purinergic stimulation on induced TF expression in HMVECad.

(A) TF expression levels in HMVECad were determined by Western blotting after the cells were stimulated with various nucleotide/nucleoside (100μM) for 4 h. TNF-α (10ng/ml) was used as positive control. Equal loading was verified by re-probing with anti-β-actin antibody after stripping the original membranes.

(B) TF expression levels in HMVECad were determined by Western blotting after the cells were stimulated with or without 1μg/ml LPS, 100μM UTP or 10ng/ml TNF-α for 4 h. Cells were pre-treated with or without 2U/ml apyrase for 30 min. Equal loading was verified by re-probing with anti-β-actin antibody after stripping the original membranes.

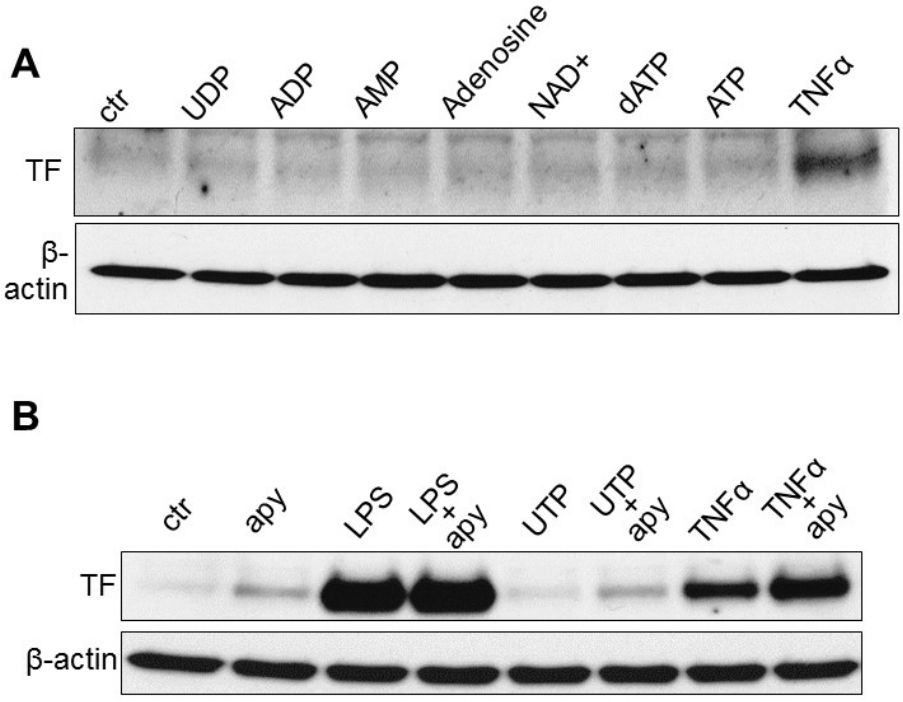
A
ctr
UDP
ADP
AMP
Adenosine
NAD+
dATP
ATP
TNFα
TF
β-
actin
B
ctr
apy
LPS
LPS
+
apy
UTP
UTP
+
apy
TNFα
TNFα
+
apy
TF
β-actin

Figure 5.4. Effect of purinergic stimulation on induced TF expression in THP-1 monocytic cell line.

(A) TF expression levels in THP-1 monocytic cell line were determined by Western blotting after the cells were stimulated with 1μg/ml LPS, 100μM UTP, or 10ng/ml TNF-α for 4 h. Cells were pre-treated with or without 2U/ml apyrase for 30 min. Equal loading was verified by re-probing with anti-GAPDH antibody after stripping the original membranes. Two sublines of THP-1 cells were used. Upper panel: differentiation-prone; lower panel: differentiation-resistant.

(B) TF expression levels in THP-1 monocytic cell line were determined by Western blotting after the cells were stimulated with 1μg/ml LPS, 100μM UTP, or 15% PBS for 4 h. Cells were pre-treated with or without 2U/ml apyrase for 30 min. Equal loading was verified by re-probing with anti-GAPDH antibody after stripping the original membranes. Differentiation-prone THP-1 were used.

(C) TF expression levels in THP-1 monocytic cell line were determined by Western blotting after the cells were stimulated with 1μg/ml LPS, 100μM UTP, or 100nM PMA for 4 h. Cells were pre-treated with or without 2U/ml apyrase for 30 min. Equal loading was verified by re-probing with anti-GAPDH antibody after stripping the original membranes. Differentiation-prone THP-1 were used.

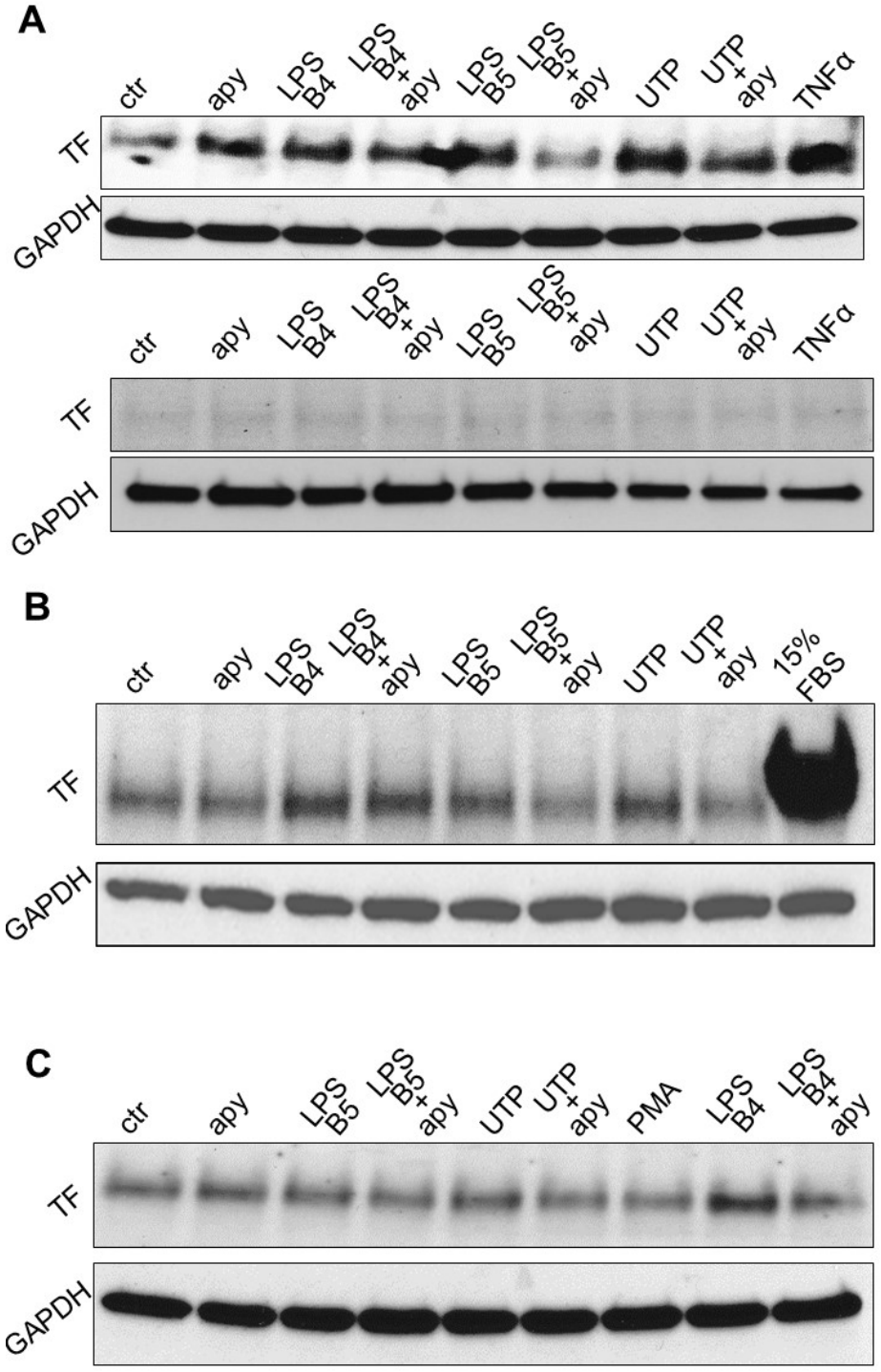
A
ctr
apy
LPS B4
LPS B4 + apy
LPS B5
LPS B5 + apy
UTP
UTP + apy
TNFα
TF
GAPDH
B
15% FBS
C
PMA

Figure 5.5. Effect of purinergic stimulation on induced TF expression in human primary blood monocytes.

(A) TF expression levels in human primary blood monocytes were determined by Western blotting after the cells were co-treated with or without LPS (1μg/ml) and UTP/ATP at indicated concentrations at the same time for 4 h. Cells were pre-treated with or without 2U/ml apyrase for 30 min. Equal loading was verified by re-probing with anti-GAPDH antibody after stripping the original membranes.

(B) TF expression levels in human primary blood monocytes were determined by Western blotting after the cells were stimulated with 1μg/ml LPS, 100μM UTP, or 10ng/ml TNF-α for 4 h. Cells were pre-treated with or without 2U/ml apyrase for 30 min. Equal loading was verified by re-probing with anti-GAPDH antibody after stripping the original membranes.

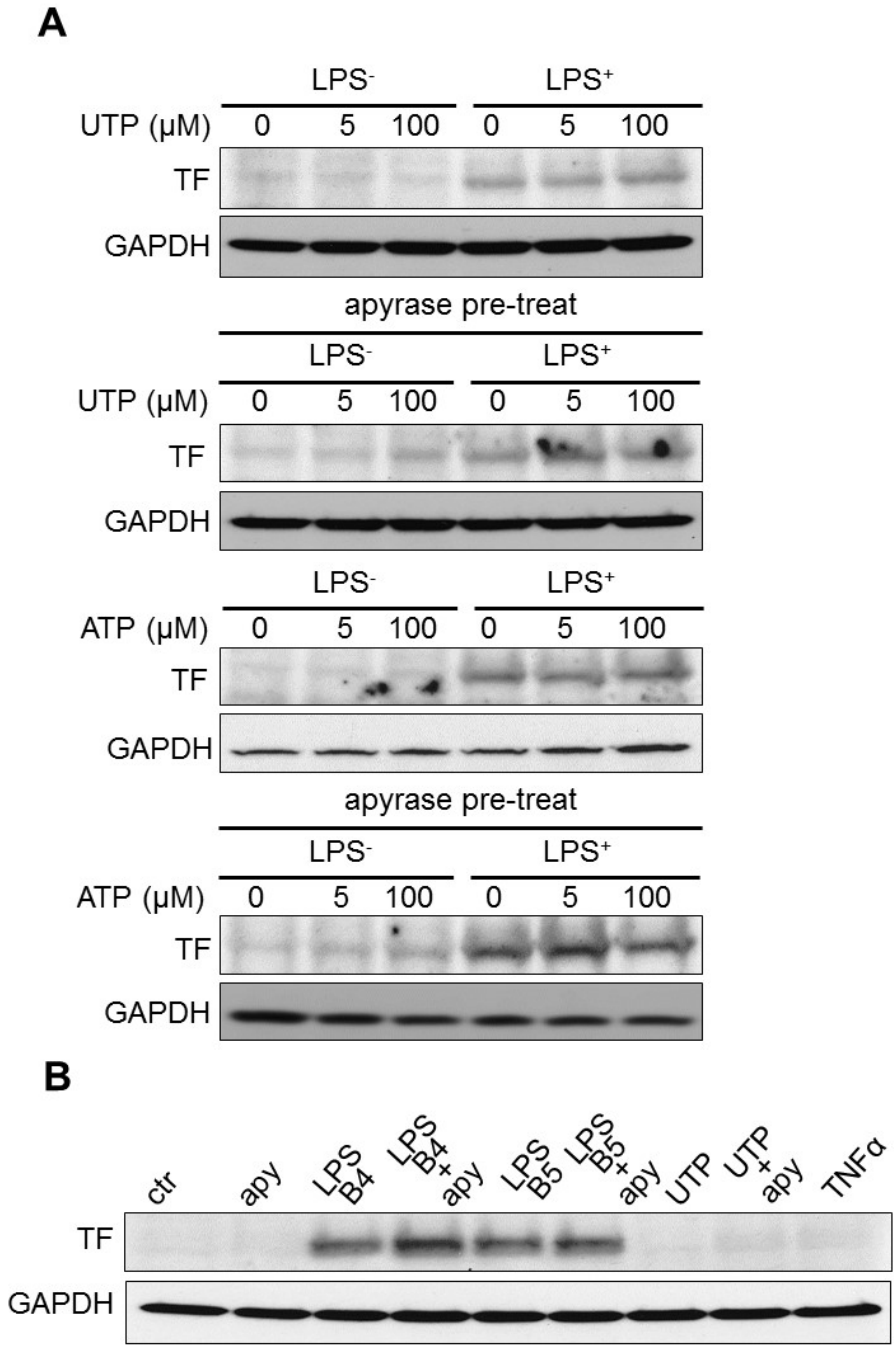
A
LPS-
LPS+
UTP (μM)
0
5
100
0
5
100
TF
GAPDH
apyrase pre-treat
LPS-
LPS+
UTP (μM)
0
5
100
0
5
100
TF
GAPDH
LPS-
LPS+
ATP (μM)
0
5
100
0
5
100
TF
GAPDH
apyrase pre-treat
LPS-
LPS+
ATP (μM)
0
5
100
0
5
100
TF
GAPDH
B
ctr
apy
LPS B4
LPS B4 + apy
LPS B5
LPS B5 + apy
UTP
UTP + apy
TNFα
TF
GAPDH

Figure 5.6. P2Y2R activation promotes TF gene transcription in HCAEC.

(A) Two pairs of primers were designed to quantify human TF mature mRNA and pre-mRNA (hnRNA) by RT-PCR respectively. A structural scheme of TF gene is depicted and relative positions of primers are marked.

(B) Representative RT-PCR gel images showing mRNA and pre-mRNA levels of TF in HCAEC treated with TNF-α (10ng/ml) for indicated duration. Genomic DNA was used as positive control. GAPDH was used as housekeeping gene to indicate equal loading. (n = 3)

(C) Representative RT-PCR gel images showing mRNA and pre-mRNA levels of TF in HCAEC treated with UTP (100 μM) for indicated duration. Genomic DNA was used as positive control. GAPDH was used as housekeeping gene to indicate equal loading. (n = 3)

(D) Quantitative data on time course change of TF mRNA and pre-mRNA in response to UTP (100 μM) treatment were determined by real-time RT-PCR. For clarity, error bars and markers for statistical analysis were omitted (n=3).

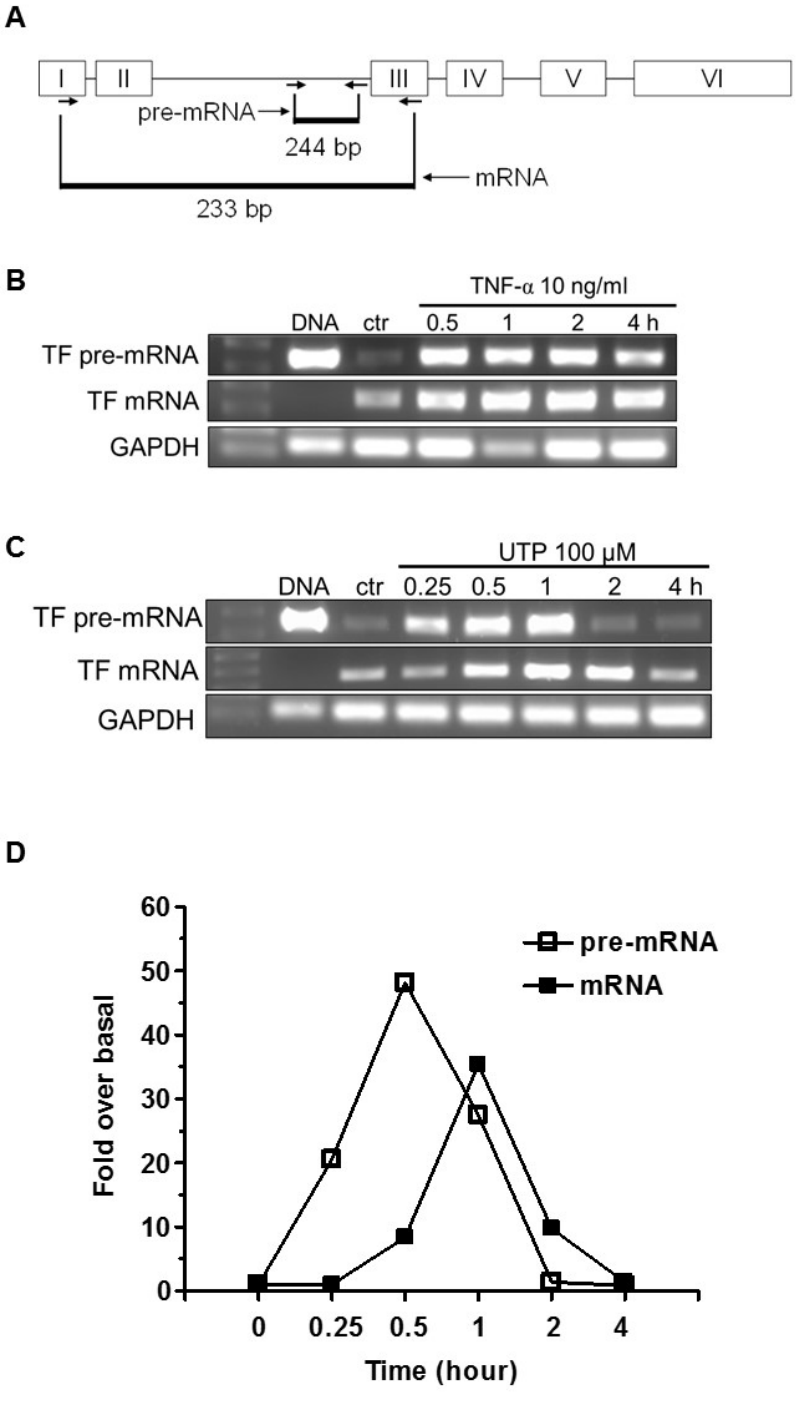
A
I
II
III
IV
V
VI
pre-mRNA
244 bp
mRNA
233 bp
B
TNF-α 10 ng/ml
DNA
ctr
0.5
1
2
4 h
TF pre-mRNA
TF mRNA
GAPDH
C
UTP 100 μM
DNA
ctr
0.25
0.5
1
2
4 h
TF pre-mRNA
TF mRNA
GAPDH
D
pre-mRNA
mRNA
Fold over basal
60
50
40
30
20
10
0
0
0.25
0.5
1
2
4
Time (hour)

Figure 5.7. Identification of new Evi-1 and AP-1 binding sites in TF promoter.

(A) The classic proximal human TF gene promoter is 227 bp in length upstream from transcription starting site. Binding sites for four transcription factors are found in this region.

(B) An Evi-1 binding site was found at -3819 bp (blue). A new AP-1 binding site was found at -1363 bp (green). Transcription starts from ‘gga’ in bold and underlined.

(C) The Evi-1 binding site at -3819 bp is well conserved across multiple species.

(D) The new distal AP-1 binding site at -1363 bp is well conserved across multiple species.

A

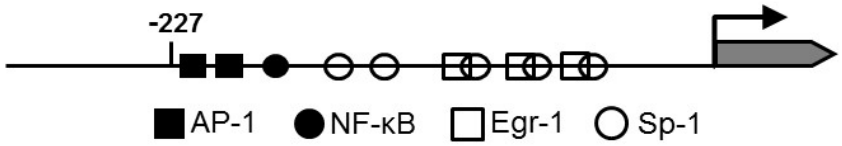

B

…(-3879)actaaaataatacccacaattcatatttattattta
tctattttgtcaccattgtatgta(-3819)**gataataaaataa**
tatttactgttcatcaaaatgaaagttgaaaggtagtttgataa
gctttacgtttataaaaatagatgtctgctgaaaataccaatcc
cagtctaagacttgaattggaaggttttt……(-1419)aatcc
cagagagcaaagaatcacatcccaggtggagctgaagatctctt
agggaaaa(-1363)**tgactca**ggctagagcctgcataaaaaga
ggattgcatggcttagttttgcaaacataaatttgtgggtttc
agagctggcagagagctcaaagaggaaatcatcaagggcaactt
tctgcttcgaggaagg……(-279)cttccaaggcgccctccct
ttcctgccatagacctgcaacccaccta(-227)agctgcacgt
cggagtcgcgggcctgggtgaatccgggggccttgggggacccg
ggcaactagacccgcctgcgtcctccagggcagctccgcgctcg
gtggcgcggttgaatcactggggtgagtcatcccttgcagggtc
ccggagtttcctaccgggaggaggcggggcaggggtgtggactc
gccgggggccgcccaccgcgacggcaagtgacccgggccggggg
cgg(0)**gga**

C

Consensus	GA(C/T)AAGA(T/C)AAGATAA
Human	GAGA T AATA AAATAA
Mouse	GGA C AGGT T AAGATT
Rat	GGG C AGGT T AAGATT

D

Consensus		TGACTCA	
Human	TTAGGGAAAA	TGACTCA	GGCTAGAGCC
Mouse	TGAATTTTAT	TGATTCA	AATGTGTCAA
Rat	CTAATCGACT	TTACTCA	AGGAAAGTAA
Rabbit	TTAGGGAAAA	TGACTCA	GGCCAGAGGG
Pig	CAAGTGTTTC	TGGCTCA	GGCTTAGCAC
Cow	GCTTTCGGGA	TGACTCA	AGCACATTGC

Figure 5.8. Verification of luciferase vector construct.

(A) Verification of luciferase vector. Band 1: linearized pGL4.12 empty vector. Size on gel in accordance with its bp number (4.421 kb). Band 2: circular pGL4.12 empty vector which moves faster than linear one and shows up at a lower size on gel.

(B) Verification of luciferase vector with TF promoter containing new -1363 bp AP-1 binding site. Plasmids from seven colonies were purified, digested with EcoRV and ran on 0.75% agarose gel. Band 3: Linear pGL4.12. Band 4: 1.6 kb insert of TF promoter containing new -1363 bp AP-1 binding site. Lane 2, 3, 5, and 7 indicate successful ligations.

(C) Verification of luciferase vector with TF promoter containing -3819 bp Evi-1 binding site. Plasmids from five colonies were purified, digested with EcoRV and BamHI (lane 3, 5, 7, 9, 11) , or not (lane 2, 4, 6, 8, 10), and ran on 0.75% agarose gel. Band 5: circular luciferase vector with 4.3 kb insert of TF promoter containing -3819 bp Evi-1 binding site. Band 6: 4.3 kb insert of TF promoter containing -3819 bp Evi-1 binding site. Band 7&8: fragment generated from empty pGL4.12 luciferase vector. Lane 2&3 and 10&11 indicate successful ligations.

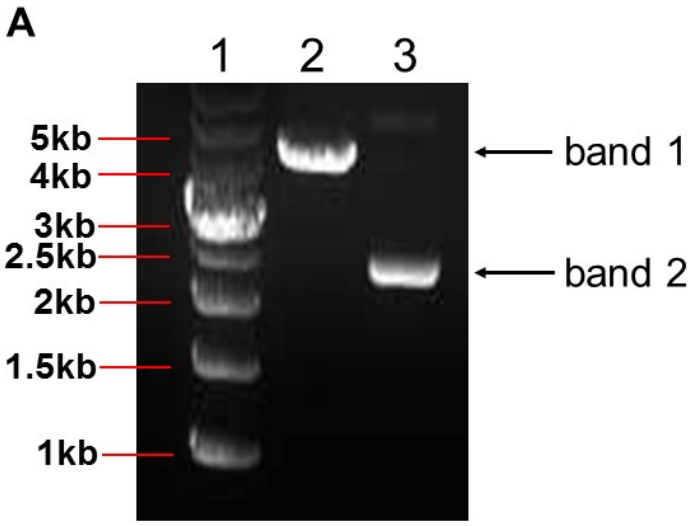
A
1
2
3
5kb
4kb
3kb
2.5kb
2kb
1.5kb
1kb
band 1
band 2

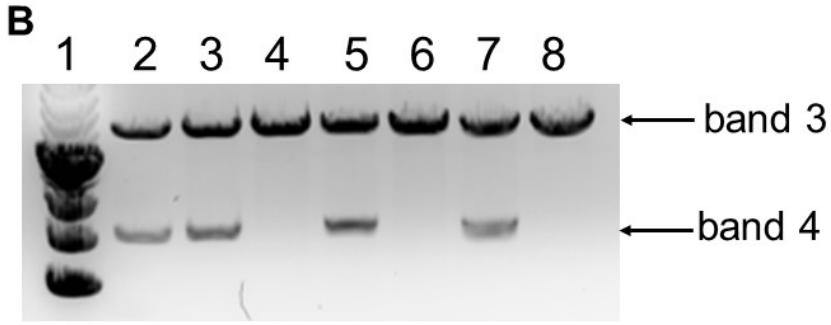
B
1
2
3
4
5
6
7
8
band 3
band 4

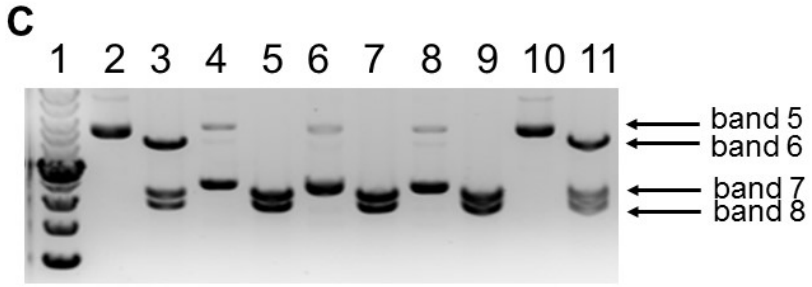
C
1
2
3
4
5
6
7
8
9
10
11
band 5
band 6
band 7
band 8

Figure 5.9. Role of -3819 bp Evi-1 binding site in TF promoter activity.

(A) HCAECs were transfected with different luciferase plasmid constructs and stimulated with TNF-α (10ng/ml), after which levels of luciferase activity relative to non-stimulated control were corrected for transfection efficiency. For clarity, error bars and markers for statistical analysis were omitted (n=3).

(B) HCAECs were transfected with different luciferase plasmid constructs and stimulated with UTP (100μM), after which levels of luciferase activity relative to non-stimulated control were corrected for transfection efficiency. For clarity, error bars and markers for statistical analysis were omitted (n=3).

(C) HCAECs were transfected with different luciferase plasmid constructs and stimulated with 2-thio-UTP (100μM), after which levels of luciferase activity relative to non-stimulated control were corrected for transfection efficiency. For clarity, error bars and markers for statistical analysis were omitted (n=3).

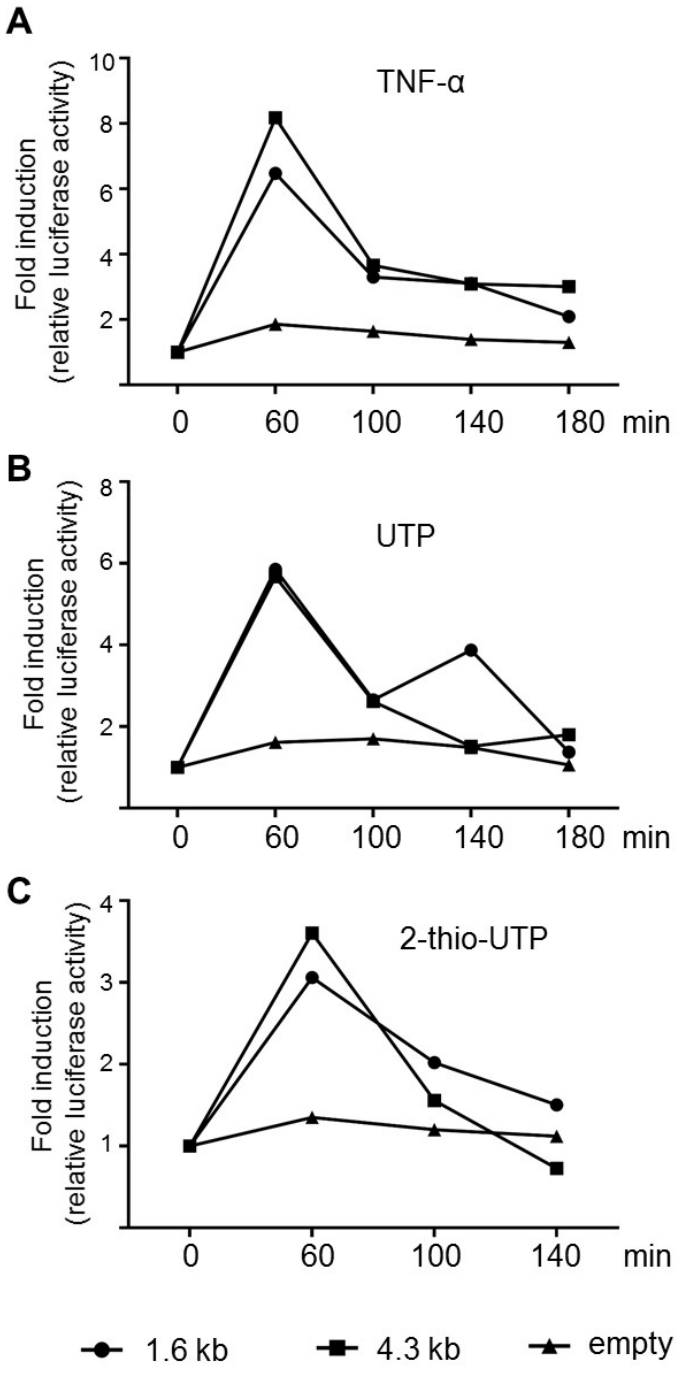
A
TNF-α
Fold induction
(relative luciferase activity)
10
8
6
4
2
0
60
100
140
180
min
B
UTP
Fold induction
(relative luciferase activity)
8
6
4
2
0
60
100
140
180
min
C
2-thio-UTP
Fold induction
(relative luciferase activity)
4
3
2
1
0
60
100
140
min
1.6 kb
4.3 kb
empty

Figure 5.10. Critical role of a new distal AP-1 binding site in TF promoter.

(A) Schematic description of successful mutation of the new distal AP-1 binding site in human TF gene promoter.

(B) HCAEC were transfected with different luciferase plasmid constructs and pre-treated with or without inhibitor SB203580 or SP600125 before stimulated with UTP (100 μM) for 1 h, after which levels of luciferase activity relative to non-stimulated control were corrected for transfection efficiency and summarized data were shown on the right. (n=5, *, $p<0.05$).

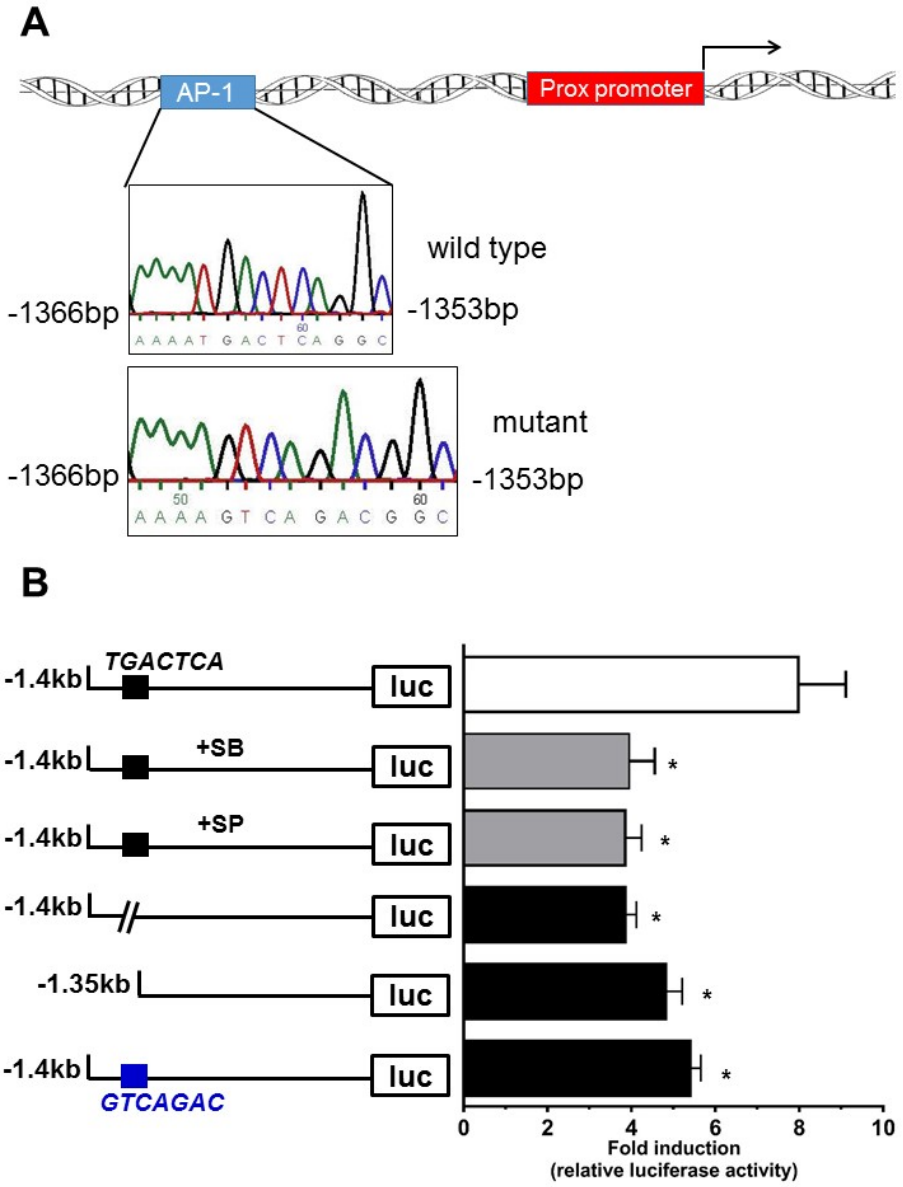
A
AP-1
Prox promoter
wild type
-1366bp
-1353bp
A A A A T G A C T C A G G C
mutant
-1366bp
-1353bp
50
60
A A A A G T C A G A C G G C
B
-1.4kb
TGACTCA
luc
+SB
+SP
-1.35kb
GTCAGAC
0
2
4
6
8
10
Fold induction
(relative luciferase activity)

Figure 5.11. Changes in Evi-1 level caused by purinergic and inflammatory stimulations.

(A) Evi-1 expression levels in HCAECs were determined by Western blotting after the cells were stimulated with or without UTP (100μM), LPS (1μg/ml) or TNF-α (10ng/ml) for 4 h. Equal loading was verified by re-probing with anti-GAPDH antibody after stripping the original membranes.

(B) Western blotting result showing Evi-1 expression levels in THP-1 monocytic cell line during differentiation induced by 5% FBS and 40nM PMA at indicated time points up to 48 h. Equal loading was verified by re-probing with anti-GAPDH antibody after stripping the original membranes.

(C) Evi-1 expression levels in THP-1 monocytic cell line (left panel) and human primary blood monocytes (right panel) were determined by Western blotting after the cells were stimulated with or without UTP (100μM), or PMA (100nM) for 4 hr. Equal loading was verified by re-probing with anti-GAPDH antibody after stripping the original membranes.

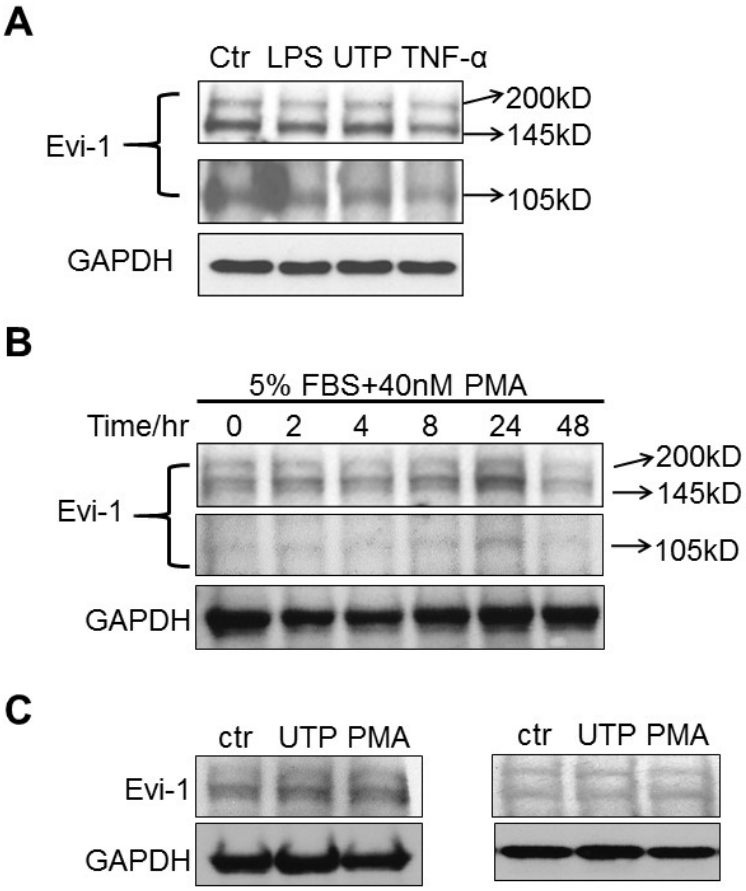
A
Ctr LPS UTP TNF-α
Evi-1
200kD
145kD
105kD
GAPDH
B
5% FBS+40nM PMA
Time/hr 0 2 4 8 24 48
Evi-1
200kD
145kD
105kD
GAPDH
C
ctr UTP PMA
ctr UTP PMA
Evi-1
GAPDH

Figure 5.12. Evidence of nuclear protein binding to the new distal AP-1 site and its regulation by P2Y2R.

(A) HCAEC nuclear protein was isolated after treatment of the cells with UTP (lane 4, 5, 6) or TNF-α (lane 7, 8, 9) or vehicle (lane 1, 2, 3) for 30 min, incubated with unlabeled and/or biotin-labeled probes, fractionated by electrophoresis and visualized by ECL detection after the membrane was incubated with horse-radish peroxidase-conjugated streptavidin.

(B) Summarized data for band density of (A) were quantified with Quantity One. (n=4, *, $p<0.05$).

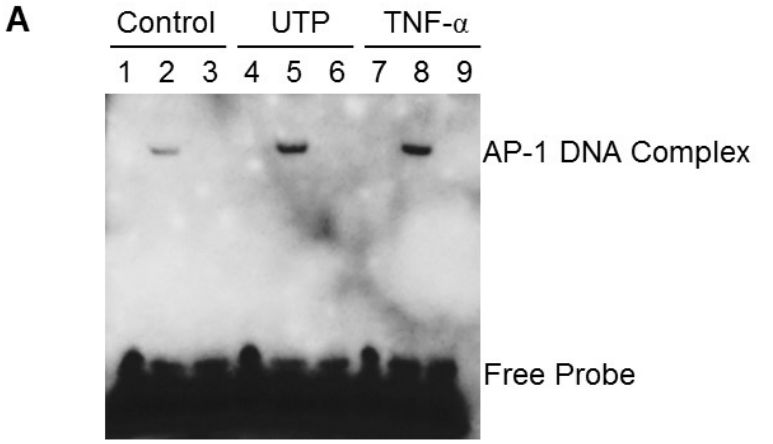

Lane 1, 4, 7: free probe only
Lane 2, 5, 8: probe + nuclear protein
Lane 3, 6, 9: probe + nuclear protein + unlabelled probe

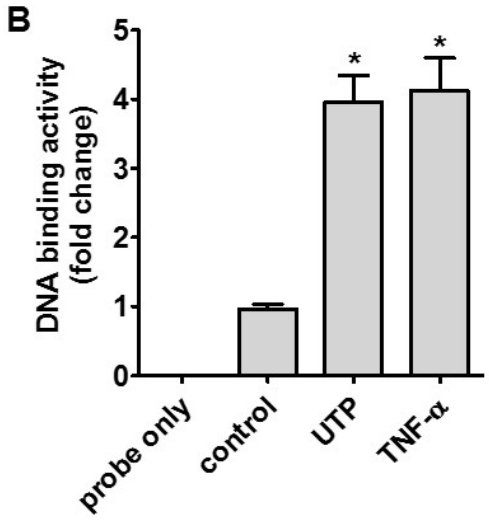

Figure 5.13. Differential effect of P2Y2R stimulation on AP-1 subunit activation.

HCAEC were treated with UTP or its less degradable analog 2-thio-UTP and phosphorylation levels of c-Jun, c-Fos, Fra-1 and ATF-2 were detected by Western blotting. Concentration-dependent change of phosphorylation levels after stimulation of the cells for 15 min (A, B and G). Time-dependent change of phosphorylation levels after stimulation of the cells with100 μM UTP or 2-thio-UTP (C, D, E and F). Amount of Fra-1 and ATF-2 bound with c-Jun in HCAEC treated with or without UTP for 30 min was detected with Co-IP and Western blotting (H). IgG used as negative control. Data were representative of at least three independent experiments.

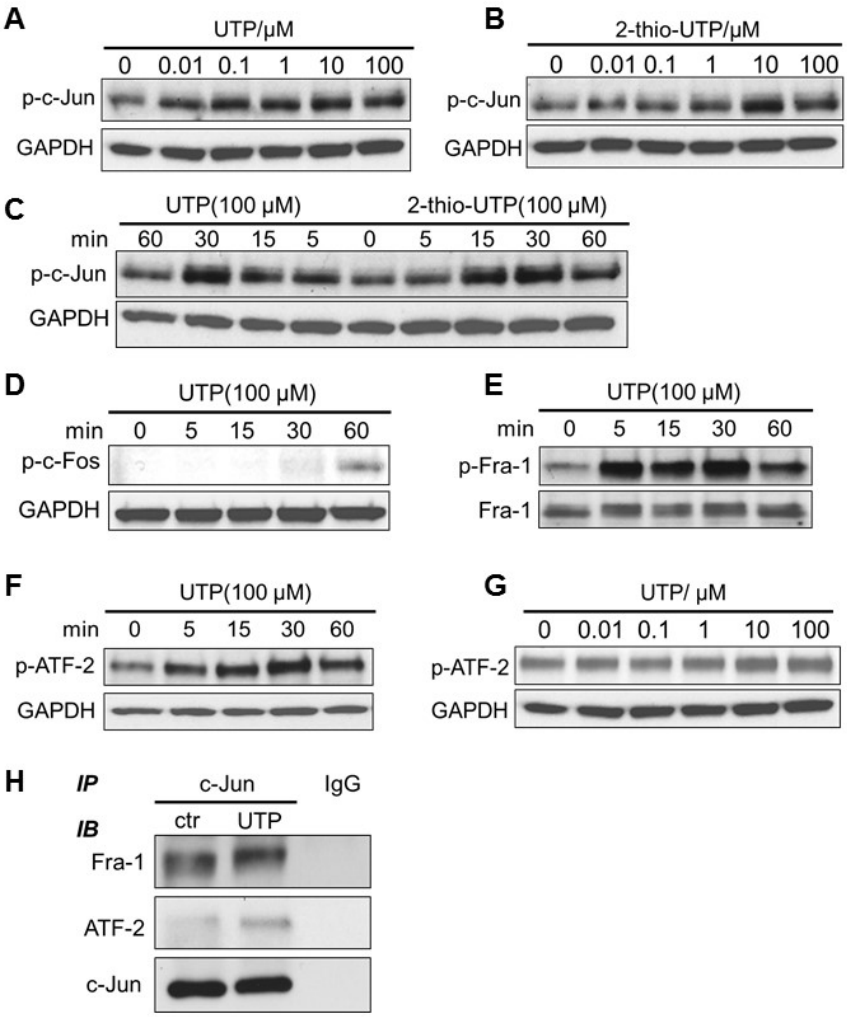
A
UTP/μM
0 0.01 0.1 1 10 100
p-c-Jun
GAPDH
B
2-thio-UTP/μM
0 0.01 0.1 1 10 100
p-c-Jun
GAPDH
C
UTP(100 μM)
2-thio-UTP(100 μM)
min 60 30 15 5 0 5 15 30 60
p-c-Jun
GAPDH
D
UTP(100 μM)
min 0 5 15 30 60
p-c-Fos
GAPDH
E
UTP(100 μM)
min 0 5 15 30 60
p-Fra-1
Fra-1
F
UTP(100 μM)
min 0 5 15 30 60
p-ATF-2
GAPDH
G
UTP/ μM
0 0.01 0.1 1 10 100
p-ATF-2
GAPDH
H
IP
c-Jun
IgG
IB
ctr
UTP
Fra-1
ATF-2
c-Jun

Figure 5.14. Nuclear accumulation of activated AP-1 subunits after P2Y2R stimulation in HCAEC.

Locations of p-c-Jun (A), p-Fra-1 (B) and p-ATF-2 (C) were indicated by FITC staining (green). HCAEC were stimulated with vehicle (control) or 100 μM UTP for 30 min before fixed for standard immunofluorescence assays. Cell nuclei were counterstained with DAPI (blue). Cytoskeleton was stained with phalloidin (red). Isotype-matched primary antibody (IgG) and FITC-conjugated secondary antibody were used for negative controls (D). Data were representative of at least three independent experiments.

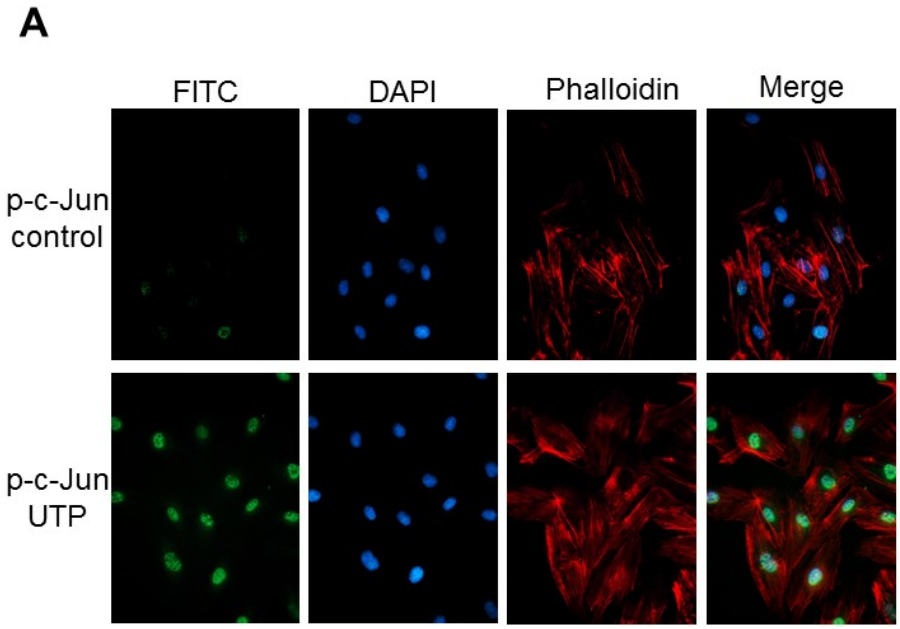
A
FITC
DAPI
Phalloidin
Merge
p-c-Jun control
p-c-Jun UTP

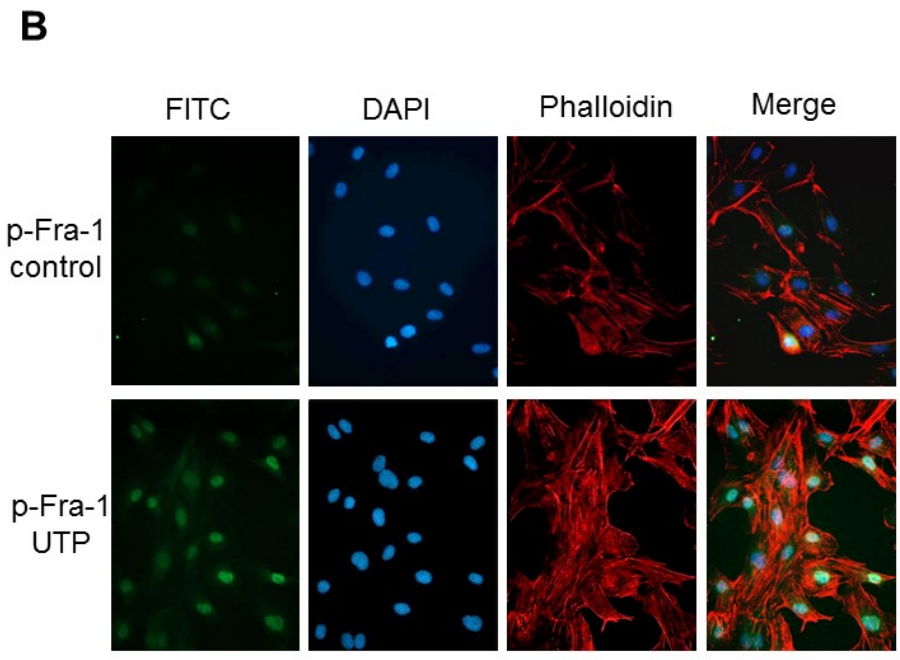
B
FITC
DAPI
Phalloidin
Merge
p-Fra-1 control
p-Fra-1 UTP

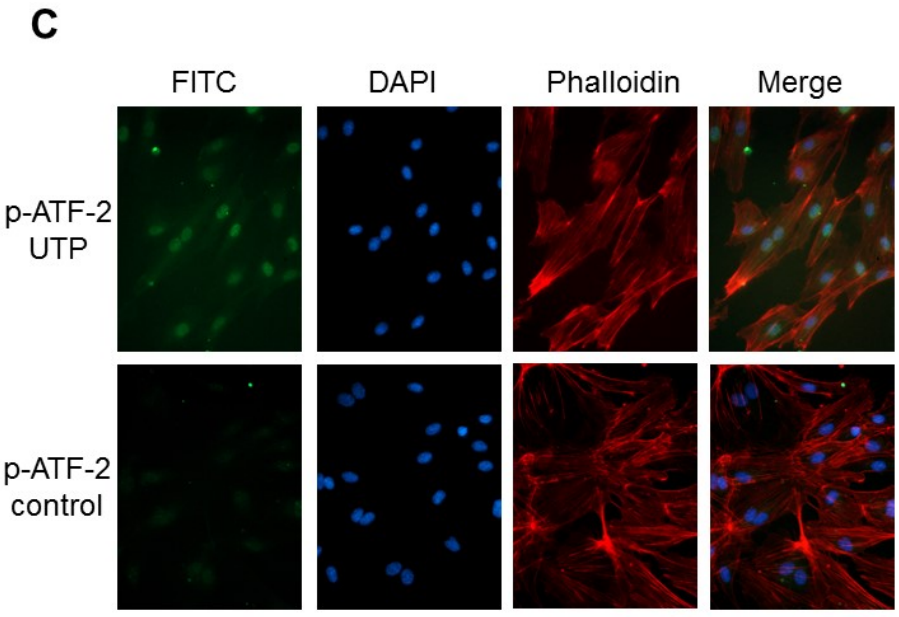
C
FITC
DAPI
Phalloidin
Merge
p-ATF-2
UTP
p-ATF-2
control

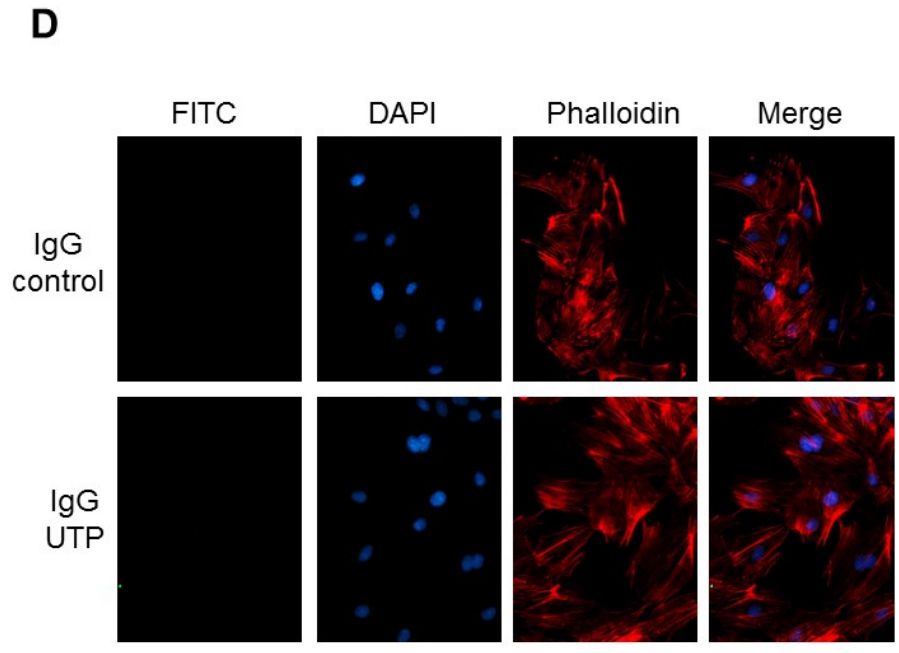
D
FITC
DAPI
Phalloidin
Merge
IgG
control
IgG
UTP

Figure 5.15. Identification of AP-1 components binding to the new distal AP-1 element within the TF promoter.

Chromatin immunoprecipitation (ChIP) assay and electrophoretic mobility shift assay (EMSA) demonstrate specific binding of c-Jun, Fra-1 and ATF-2 to the new AP-1 site in response to P2Y2R activation in HCAEC. (A to C) ChIP assay of the new AP-1 site in TF promoter with anti-c-Jun, Fra-1 and ATF-2 antibodies using HCAEC chromatin. Histograms were acquired from four independent real-time PCR experiments followed by electrophoresis gel imaging of amplified PCR products. (D to F) Confirmation of the roles of c-Jun, Fra-1 and ATF-2 binding to the new AP-1 site with EMSA experiments. 1 μg and 2 μg antibody were used in binding reactions, or 2 μg IgG was used as negative controls. Location of arrows indicate band of interest. Data were representative of three independent experiments.

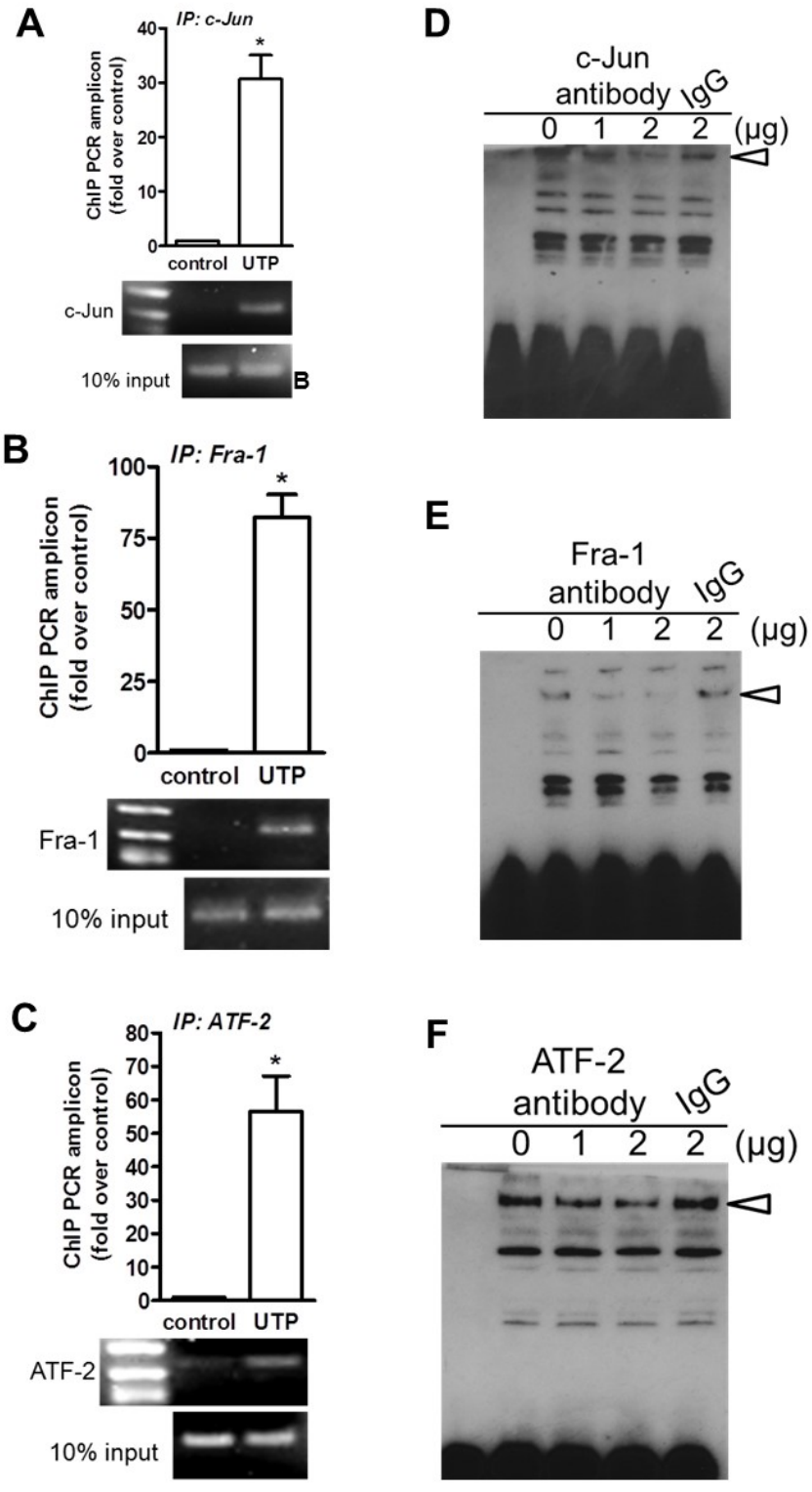
A
IP: c-Jun
ChIP PCR amplicon (fold over control)
40
30
20
10
0
*
control
UTP
c-Jun
10% input
B
B
IP: Fra-1
ChIP PCR amplicon (fold over control)
100
75
50
25
0
*
control
UTP
Fra-1
10% input
C
IP: ATF-2
ChIP PCR amplicon (fold over control)
80
70
60
50
40
30
20
10
0
*
control
UTP
ATF-2
10% input
D
c-Jun antibody
IgG
0 1 2 2 (µg)
E
Fra-1 antibody
IgG
0 1 2 2 (µg)
F
ATF-2 antibody
IgG
0 1 2 2 (µg)

Figure 5.16. Differential roles of AP-1 subunits in P2Y2R-mediated TF gene transcription.

(A-C) c-Jun, Fra-1 and ATF-2 protein levels were determined by western blotting after HCAECs were transfected with their respective siRNA for 48 h. UTP-induced TF pre-mRNA was evaluated after c-Jun, Fra-1 or ATF-2 was knocked down by siRNA in HCAEC. *, $p<0.05$ versus UTP-stimulated cells transfected with scrambled siRNA (D). n=5.

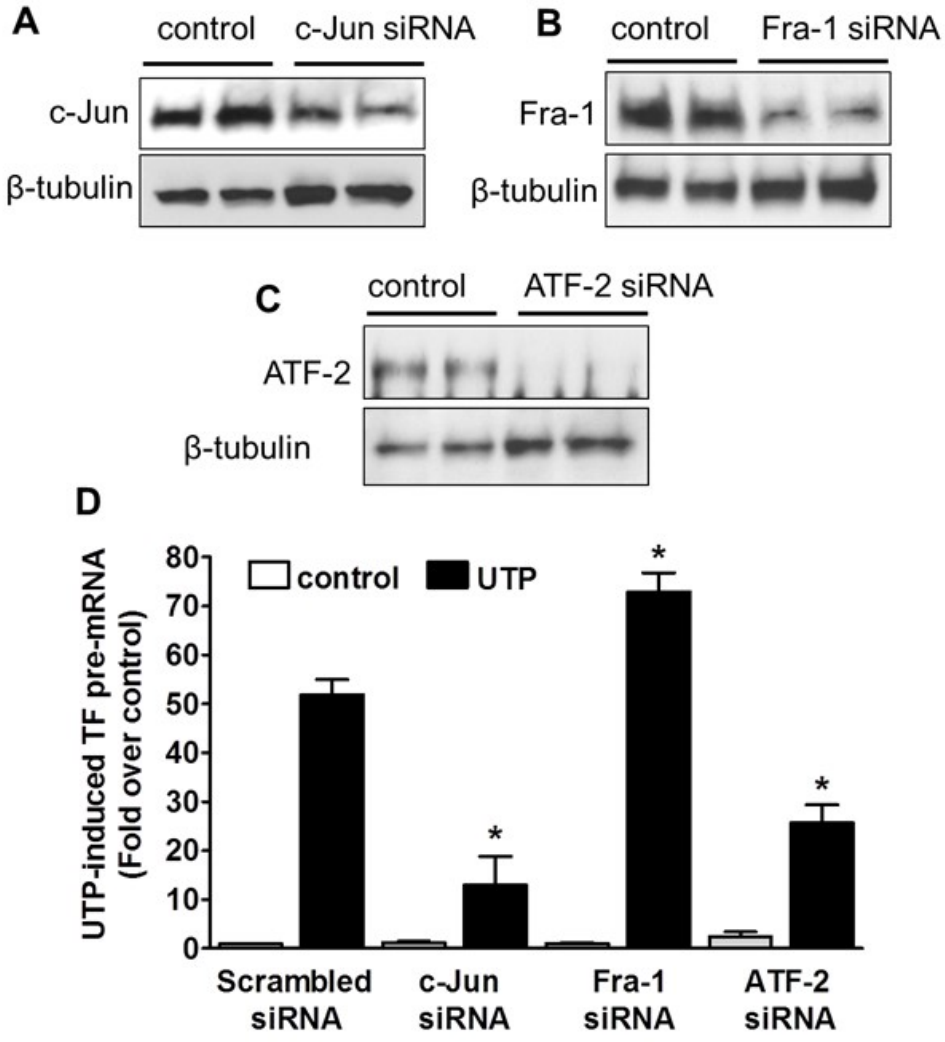
A
control
c-Jun siRNA
c-Jun
β-tubulin
B
control
Fra-1 siRNA
Fra-1
β-tubulin
C
control
ATF-2 siRNA
ATF-2
β-tubulin
D
UTP-induced TF pre-mRNA (Fold over control)
control
UTP
80
70
60
50
40
30
20
10
0
*
*
*
Scrambled siRNA
c-Jun siRNA
Fra-1 siRNA
ATF-2 siRNA

Figure 5.17. P2Y2R signaling mechanism in control of AP-1 subunits and TF gene transcription in HCAEC.

Phosphorylation levels of AP-1 subunits in response to P2Y2R activation were determined with Western blotting after HCAECs were pretreated for 1 h with the individual inhibitor for JNK (A), ERK1/2 (B), Rho kinase (C) and Src (D). TF pre-mRNA levels in response to UTP stimulation (100 μM for 30 min) were analyzed with real-time PCR after HCAECs were pretreated for 1 h with the individual inhibitor for JNK, ERK1/2, Rho kinase, and Src (E).

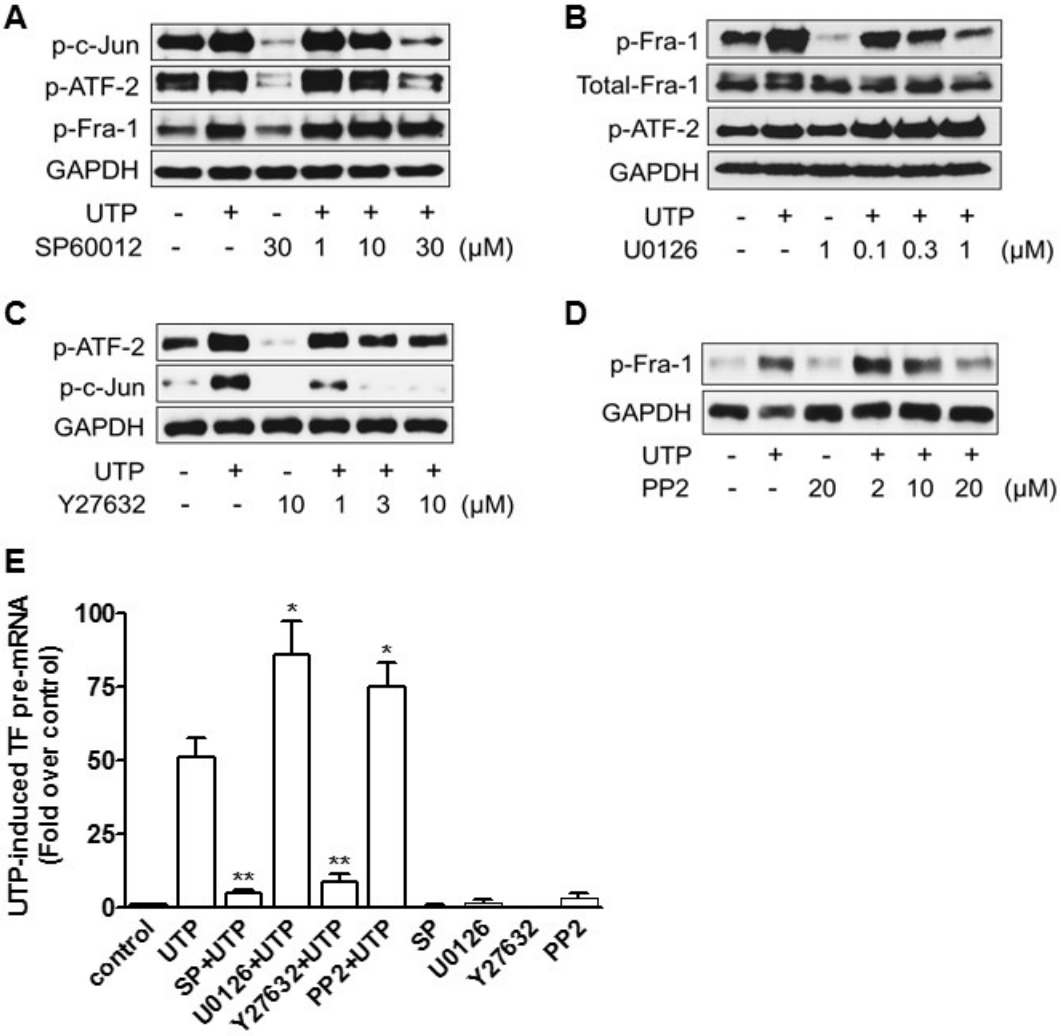
A
p-c-Jun
p-ATF-2
p-Fra-1
GAPDH
UTP - + - + + +
SP60012 - - 30 1 10 30 (μM)
B
p-Fra-1
Total-Fra-1
p-ATF-2
GAPDH
UTP - + - + + +
U0126 - - 1 0.1 0.3 1 (μM)
C
p-ATF-2
p-c-Jun
GAPDH
UTP - + - + + +
Y27632 - - 10 1 3 10 (μM)
D
p-Fra-1
GAPDH
UTP - + - + + +
PP2 - - 20 2 10 20 (μM)
E
UTP-induced TF pre-mRNA (Fold over control)
100
75
50
25
0
*
*
**
**
control
UTP
SP+UTP
U0126+UTP
Y27632+UTP
PP2+UTP
SP
U0126
Y27632
PP2

Figure 5.18. P2Y2R activation stabilizes TF mRNA in HCAEC.

(A) Quantitative data on time course change of TF pre-mRNA in response to UTP (100 μM), actinomycin D (10μg/ml), or both were determined by real-time RT-PCR. For clarity, error bars and markers for statistical analysis were omitted (n=3).

(B) TF mRNA decay curve. Quantitative data on time course change of TF mRNA in response to actinomycin D (10μg/ml) with or without UTP (100 μM) determined by real-time RT-PCR. For clarity, error bars and markers for statistical analysis were omitted (n=3).

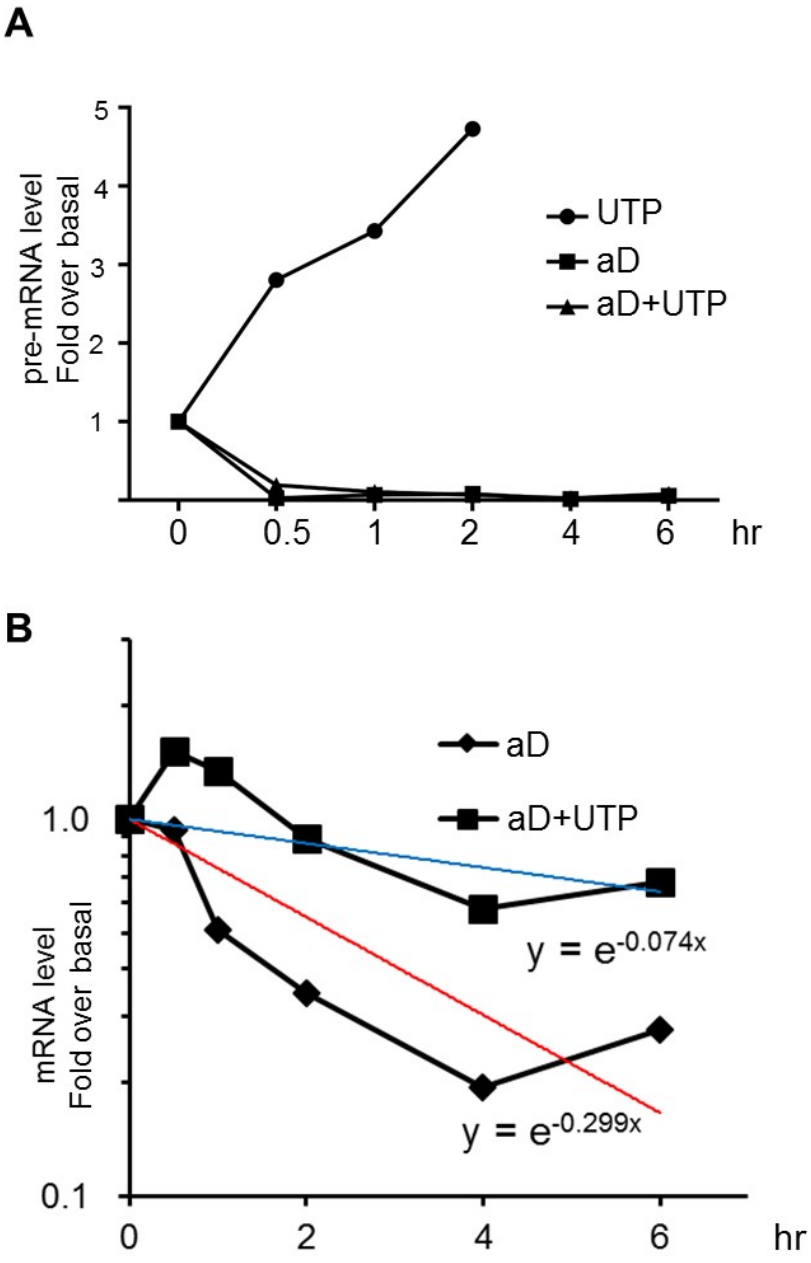
A
pre-mRNA level
Fold over basal
5
4
3
2
1
0
0.5
1
2
4
6
hr
UTP
aD
aD+UTP
B
aD
aD+UTP
1.0
0.1
mRNA level
Fold over basal
y = e-0.074x
y = e-0.299x
0
2
4
6
hr

Figure 5.19. P2Y2R activation affects mRNA stabilization pathway p38/MK-2/hsp27 in HCAEC.

(A) Schematic description of AU-rich elements (ARE) in TF mRNA 3'-UTR. ARE in three classes are colored differently: red-Class I; blue-Class II; green-Class III.

(B) Dose- and time-dependent change in MK-2 phosphorylation level under UTP stimulation demonstrated with Western blotting. Time course study (upper panel) was done with 100μM UTP. Dose response was carried out at 5 min duration. GAPDH was used as loading control.

A

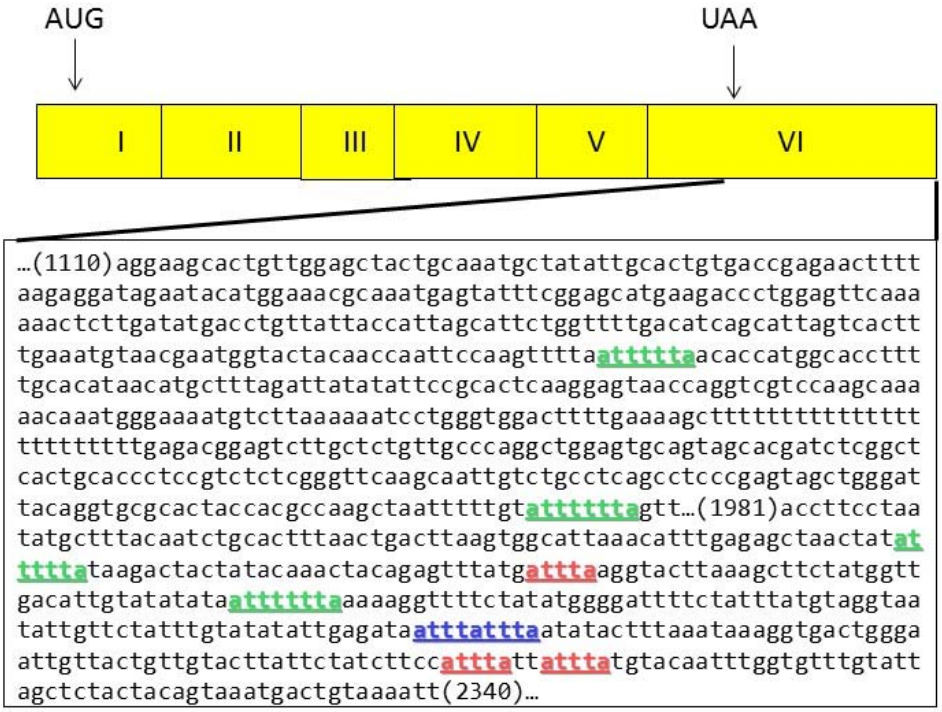
AUG
UAA
I
II
III
IV
V
VI
…(1110)aggaagcactgttggagctactgcaaatgctatattgcactgtgaccgagaacttttaagaggatagaatacatggaaacgcaaatgagtatttcggagcatgaagaccctggagttcaaaaaactcttgatatgacctgttattaccattagcattctggttttgacatcagcattagtcacttgaaatgtaacgaatggtactacaaccaattccaagtttaatttttaacaccatggcaccttttgcacataacatgctttagattatatattccgcactcaaggagtaaccaggtcgtccaagcaaaaacaaatgggaaaatgtcttaaaaaatcctgggtggacttttgaaaagctttttttttttttttttttgagacggagtcttgctctgttgcccaggctggagtgcagtagcacgatctcggctcactgcaccctccgtctctcgggttcaagcaattgtctgcctcagcctcccgagtagctgggattacaggtgcgcactaccacgccaagctaatttttgtatttttttagtt…(1981)accttcctaatatgctttacaatctgcactttaactgacttaagtggcattaaacatttgagagctaactatattttttaagactactatacaaactacagagtttatgatttaaggtacttaaagcttctatggttgacattgtatatataatttttttaaaaggttttctatatggggattttctatttatgtaggtaatattgttctatttgtatatattgagataatttatttaatatactttaaataaaggtgactgggaattgttactgttgtacttattctatcttccatttattatttatgtacaatttggtgtttgtattagctctactacagtaaatgactgtaaaatt(2340)…

B

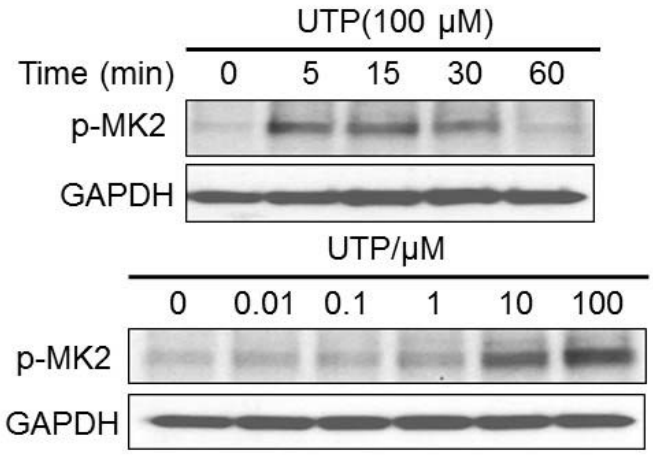
UTP(100 μM)
Time (min)
0
5
15
30
60
p-MK2
GAPDH
UTP/μM
0
0.01
0.1
1
10
100
p-MK2
GAPDH

Figure 5.20. Effect of p38 and MK-2 inhibitors on AREBP and TF mRNA stability.

(A) Phosphorylation levels of p38, MK-2 and in response to P2Y2R activation were determined with Western blotting after HCAECs were pretreated with or without MK-2 inhibitor PF3644022 (3μM) or p38 inhibitor SB203580 (30μM) for 30 min.

(B) TF mRNA levels 1.5 h after UTP and actinomycin D co-treatment in HCAEC were determined with real-time PCR after pre-treatment with or without MK-2 inhibitor PF3644022 (3μM) or p38 inhibitor SB203580 (30μM) for 30 min. (n=3, *, $p<0.05$).

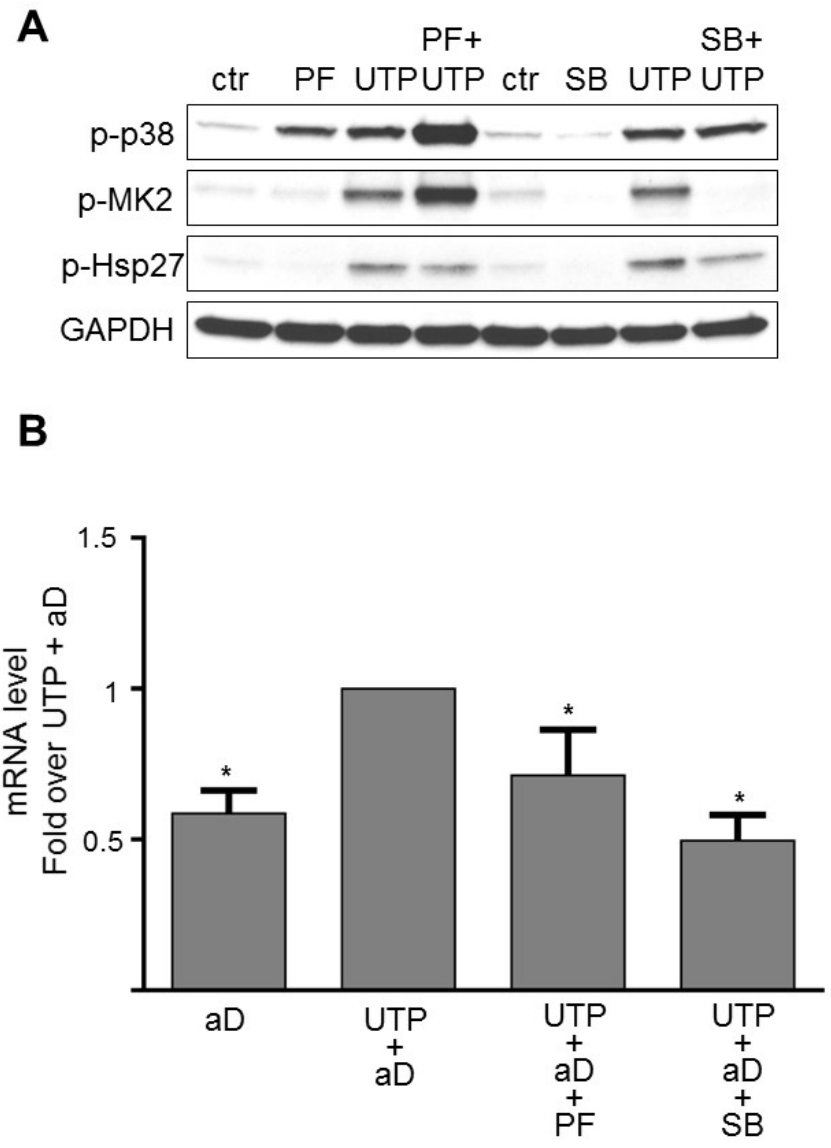
A
ctr
PF
UTP
PF+ UTP
ctr
SB
UTP
SB+ UTP
p-p38
p-MK2
p-Hsp27
GAPDH
B
mRNA level
Fold over UTP + aD
1.5
1
0.5
*
*
*
aD
UTP + aD
UTP + aD + PF
UTP + aD + SB

Figure 5.21. microRNA expression profiles in UTP treated HCAECs.

Microarray heat map of genes regulated specifically in response to UTP 100μM treatment for 1 h on HCAEC. The fold change of expression of the miRNAs compared to untreated cells is shown. Red indicates that the induction of expression while green indicates inhibition.

A

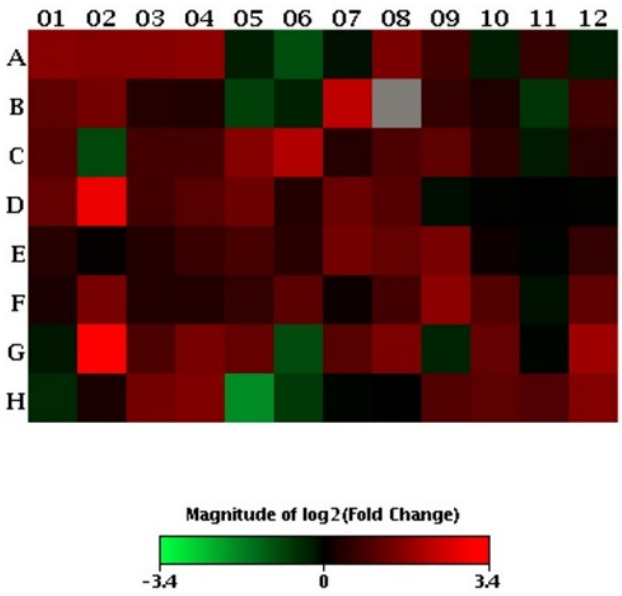
01 02 03 04 05 06 07 08 09 10 11 12
A
B
C
D
E
F
G
H
Magnitude of log2(Fold Change)
-3.4
0
3.4

B

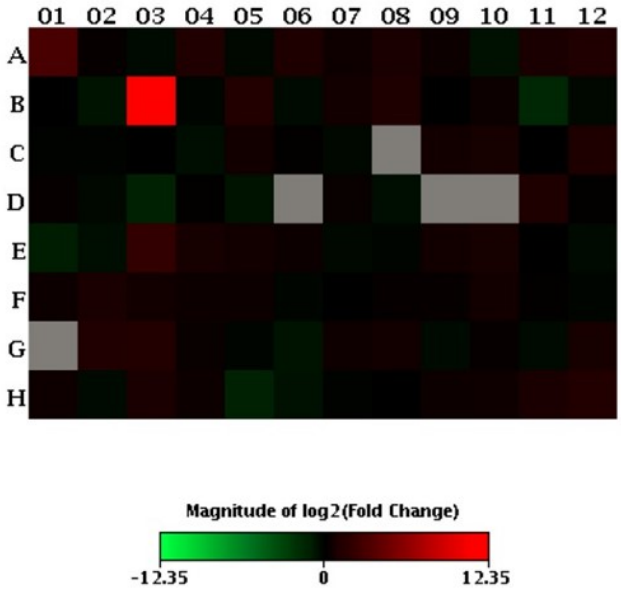
01 02 03 04 05 06 07 08 09 10 11 12
A
B
C
D
E
F
G
H
Magnitude of log2(Fold Change)
-12.35
0
12.35

C

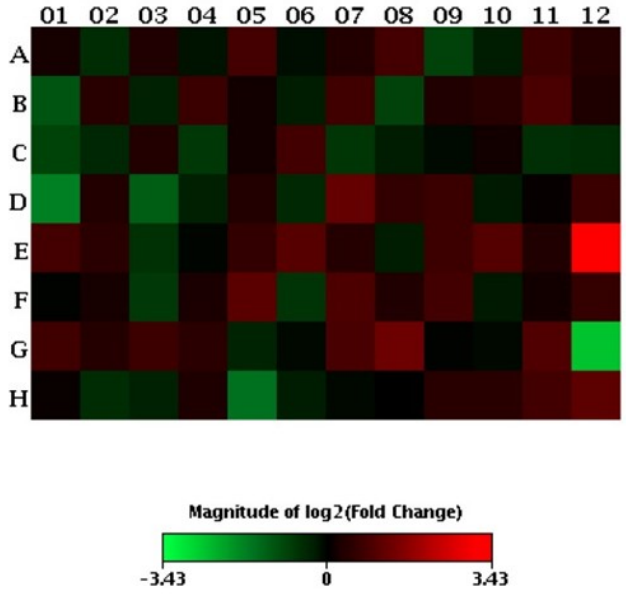
01 02 03 04 05 06 07 08 09 10 11 12
A
B
C
D
E
F
G
H
Magnitude of log2(Fold Change)
-3.43
0
3.43

D

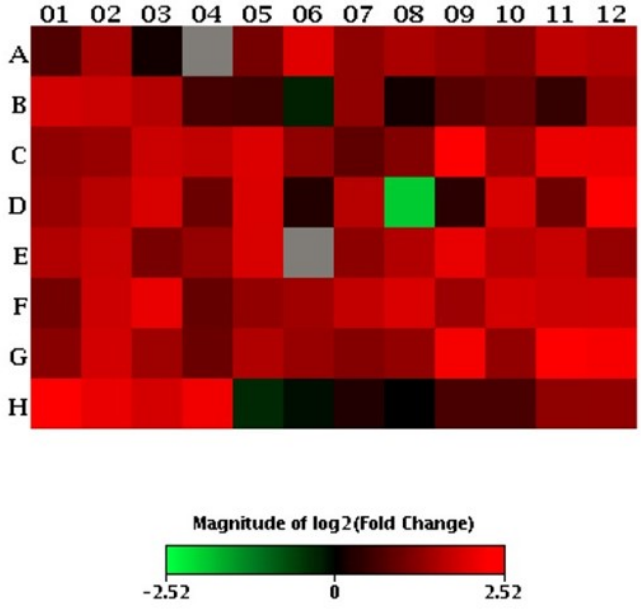
01 02 03 04 05 06 07 08 09 10 11 12
A
B
C
D
E
F
G
H
Magnitude of log2(Fold Change)
-2.52
0
2.52

E

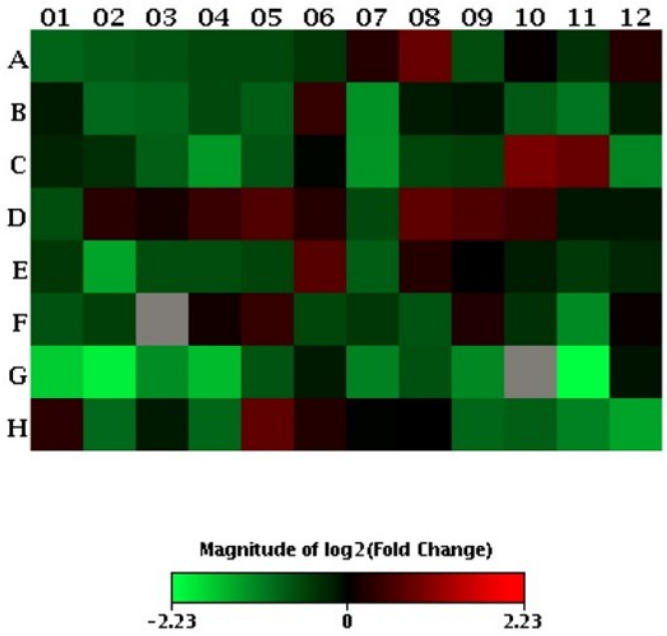
01 02 03 04 05 06 07 08 09 10 11 12
A
B
C
D
E
F
G
H
Magnitude of log2(Fold Change)
-2.23
0
2.23

F

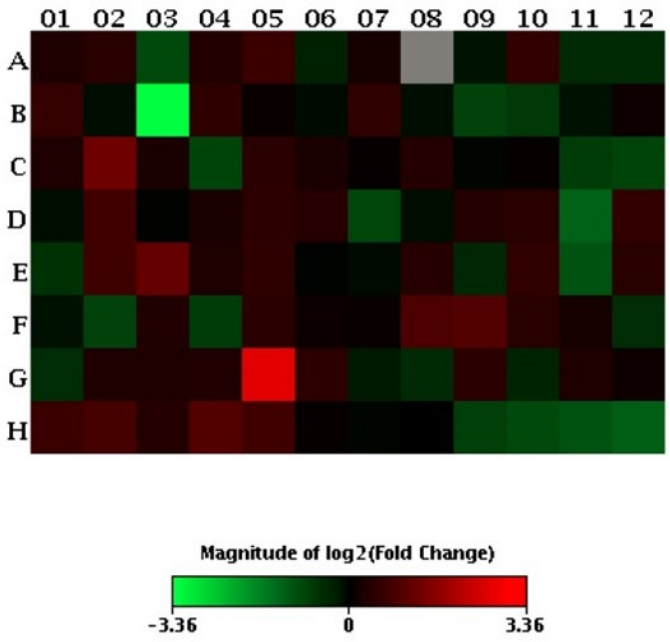
01 02 03 04 05 06 07 08 09 10 11 12
A
B
C
D
E
F
G
H
Magnitude of log2(Fold Change)
-3.36
0
3.36

G

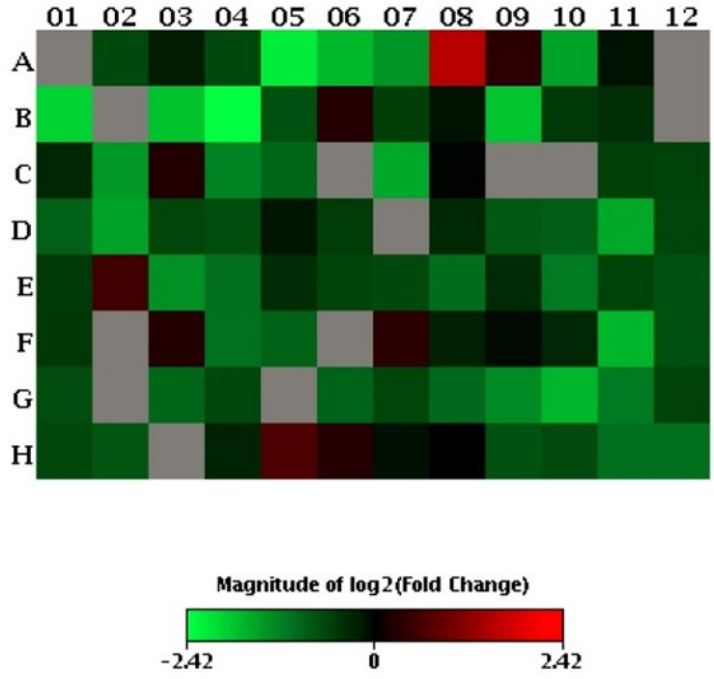
01 02 03 04 05 06 07 08 09 10 11 12
A
B
C
D
E
F
G
H
Magnitude of log2(Fold Change)
-2.42
0
2.42

H

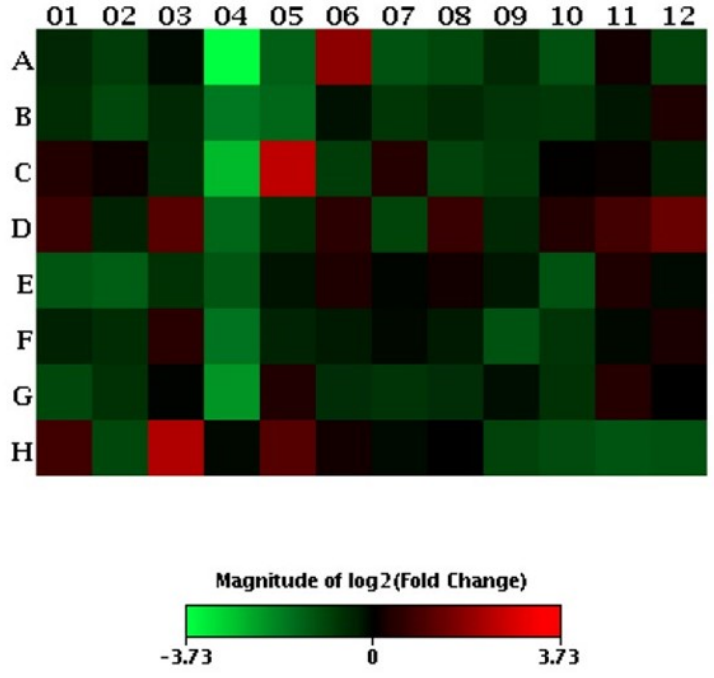
01 02 03 04 05 06 07 08 09 10 11 12
A
B
C
D
E
F
G
H
Magnitude of log2(Fold Change)
-3.73
0
3.73

Figure 5.22. MiRNA-181a was down-regulated by P2Y2R activation in HCAEC.

(A) Seed region for hsa-181a in TF mRNA 3'-UTR and it is conservativeness across multiple species.

(B) hsa-181a levels with or without 1 h 100μM UTP treatment in HCAEC determined with stem-loop RT followed by real-time PCR. (n=3, *, $p<0.05$).

A

```
            1       10        20        30        40        50
Human       TATTAGCTCTACTACAGTAAATGACTGTAAAATTGTCAGTGGCTTACAAC
Pig         CTTTTGCACATAATATTCTTGAGACTGTATGTTCTCTACATTGAGGTGAA
Cow         TAGCACACATGGAAACACAAGTGACTGTTCTGGAGCATACAGAGCCTGGG
Dog         ATTAGACACTTTGGAATGTAATGAACGTACAACCCAGTCCAAGTTTTTAA
Rat         AAGACGGTACGAAACTGAAGGTGACGGTGCTGACTGTCACACTGCCCACA
Mouse       TTAAACATTTGACAGCCAACTTCACTTTAATACGACTACAAAGAAACTAC
Chicken     ATTCAGAGGTACCTTTTGCTATGACTGTTTTAATATTTATTTTATGGATG
miR-181a                    ACCACUGACCGUAGACUGUACC
```

B

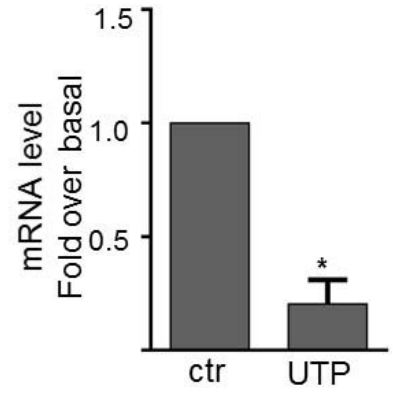

Reference

Abbracchio, M.P., Burnstock, G., Boeynaems, J.M., Barnard, E.A., Boyer, J.L., Kennedy, C., Knight, G.E., Fumagalli, M., Gachet, C., Jacobson, K.A., *et al.* (2006). International Union of Pharmacology LVIII: update on the P2Y G protein-coupled nucleotide receptors: from molecular mechanisms and pathophysiology to therapy. Pharmacological reviews *58*, 281-341.

Ahern, S.M., Miyata, T., and Sadler, J.E. (1993). Regulation of human tissue factor expression by mRNA turnover. The Journal of biological chemistry *268*, 2154-2159.

Aljada, A., Ghanim, H., Mohanty, P., Kapur, N., and Dandona, P. (2002). Insulin inhibits the pro-inflammatory transcription factor early growth response gene-1 (Egr)-1 expression in mononuclear cells (MNC) and reduces plasma tissue factor (TF) and plasminogen activator inhibitor-1 (PAI-1) concentrations. The Journal of clinical endocrinology and metabolism *87*, 1419-1422.

Ambros, V. (2004). The functions of animal microRNAs. Nature *431*, 350-355.

Anderson, T.J., Meredith, I.T., Yeung, A.C., Frei, B., Selwyn, A.P., and Ganz, P. (1995). The effect of cholesterol-lowering and antioxidant therapy on endothelium-dependent coronary vasomotion. The New England journal of medicine *332*, 488-493.

Arany, I., Megyesi, J.K., Kaneto, H., Price, P.M., and Safirstein, R.L. (2004). Cisplatin-induced cell death is EGFR/src/ERK signaling dependent in mouse proximal tubule cells. American journal of physiology Renal physiology *287*, F543-549.

Atkinson, B., Dwyer, K., Enjyoji, K., and Robson, S.C. (2006). Ecto-nucleotidases of the CD39/NTPDase family modulate platelet activation and thrombus formation: Potential as therapeutic targets. Blood cells, molecules & diseases *36*, 217-222.

Badeanlou, L., Furlan-Freguia, C., Yang, G., Ruf, W., and Samad, F. (2011). Tissue factor-protease-activated receptor 2 signaling promotes diet-induced obesity and adipose inflammation. Nat Med *17*, 1490-1497.

Bagchi, S., Liao, Z., Gonzalez, F.A., Chorna, N.E., Seye, C.I., Weisman, G.A., and Erb, L. (2005). The P2Y2 nucleotide receptor interacts with alphav integrins to activate Go and induce cell migration. The Journal of biological chemistry *280*, 39050-39057.

Baker, O.J., Camden, J.M., Rome, D.E., Seye, C.I., and Weisman, G.A. (2008). P2Y2 nucleotide receptor activation up-regulates vascular cell adhesion molecule-1 [corrected] expression and enhances lymphocyte adherence to a human submandibular gland cell line. Molecular immunology *45*, 65-75.

Barn, K., and Steinhubl, S.R. (2012). A brief review of the past and future of platelet P2Y12 antagonist. Coronary artery disease *23*, 368-374.

Bastid, J., Cottalorda-Regairaz, A., Alberici, G., Bonnefoy, N., Eliaou, J.F., and Bensussan, A. (2013). ENTPD1/CD39 is a promising therapeutic target in oncology. Oncogene *32*, 1743-1751.

Bavendiek, U., Libby, P., Kilbride, M., Reynolds, R., Mackman, N., and Schonbeck, U. (2002). Induction of tissue factor expression in human endothelial cells by CD40 ligand is mediated via activator protein 1, nuclear factor kappa B, and Egr-1. The Journal of biological chemistry *277*, 25032-25039.

Bea, F., Blessing, E., Shelley, M.I., Shultz, J.M., and Rosenfeld, M.E. (2003). Simvastatin inhibits expression of tissue factor in advanced atherosclerotic lesions of apolipoprotein E deficient mice independently of lipid lowering: potential role of simvastatin-mediated inhibition of Egr-1 expression and activation. Atherosclerosis *167*, 187-194.

Beavis, P.A., Stagg, J., Darcy, P.K., and Smyth, M.J. (2012). CD73: a potent suppressor of antitumor immune responses. Trends in immunology *33*, 231-237.

Behrendt, D., and Ganz, P. (2002). Endothelial function. From vascular biology to clinical applications. The American journal of cardiology *90*, 40L-48L.

Belguise, K., Kersual, N., Galtier, F., and Chalbos, D. (2005). FRA-1 expression level regulates proliferation and invasiveness of breast cancer cells. Oncogene *24*, 1434-1444.

Bellofatto, V., and Wilusz, J. (2011). Transcription and mRNA stability: parental guidance suggested. Cell *147*, 1438-1439.

Benbrook, D.M., and Jones, N.C. (1990). Heterodimer formation between CREB and JUN proteins. Oncogene *5*, 295-302.

Bickford, J.S., Beachy, D.E., Newsom, K.J., Barilovits, S.J., Herlihy, J.D., Qiu, X., Walters, J.N., Li, N., and Nick, H.S. (2013). A distal enhancer controls cytokine-dependent human cPLA2alpha gene expression. J Lipid Res *54*, 1915-1926.

Bodin, P., and Burnstock, G. (2001). Evidence that release of adenosine triphosphate from endothelial cells during increased shear stress is vesicular. Journal of cardiovascular pharmacology *38*, 900-908.

Bours, M.J., Swennen, E.L., Di Virgilio, F., Cronstein, B.N., and Dagnelie, P.C. (2006). Adenosine 5'-triphosphate and adenosine as endogenous signaling molecules in immunity and inflammation. Pharmacology & therapeutics *112*, 358-404.

Budagian, V., Bulanova, E., Brovko, L., Orinska, Z., Fayad, R., Paus, R., and Bulfone-Paus, S. (2003). Signaling through P2X7 receptor in human T cells involves p56lck, MAP kinases, and transcription factors AP-1 and NF-kappa B. J Biol Chem *278*, 1549-1560.

Burgos, M., Neary, J.T., and Gonzalez, F.A. (2007). P2Y2 nucleotide receptors inhibit trauma-induced death of astrocytic cells. Journal of neurochemistry *103*, 1785-1800.
Burnstock, G. (1976). Do some nerve cells release more than one transmitter? Neuroscience *1*, 239-248.

Burnstock, G. (2007). Physiology and pathophysiology of purinergic neurotransmission. Physiological reviews *87*, 659-797.

Burnstock, G. (2011). Introductory overview of purinergic signalling. Frontiers in bioscience *3*, 896-900.

Burrell, H.E., Wlodarski, B., Foster, B.J., Buckley, K.A., Sharpe, G.R., Quayle, J.M., Simpson, A.W., and Gallagher, J.A. (2005). Human keratinocytes release ATP and utilize three mechanisms for nucleotide interconversion at the cell surface. The Journal of biological chemistry *280*, 29667-29676.

Butenas, S., Orfeo, T., and Mann, K.G. (2009). Tissue factor in coagulation: Which? Where? When? Arterioscler Thromb Vasc Biol *29*, 1989-1996.

Cattaneo, M. (2011). The platelet P2Y(1)(2) receptor for adenosine diphosphate: congenital and drug-induced defects. Blood *117*, 2102-2112.

Cermak, J., Key, N.S., Bach, R.R., Balla, J., Jacob, H.S., and Vercellotti, G.M. (1993). C-reactive protein induces human peripheral blood monocytes to synthesize tissue factor. Blood *82*, 513-520.

Chalmin, F., Mignot, G., Bruchard, M., Chevriaux, A., Vegran, F., Hichami, A., Ladoire, S., Derangere, V., Vincent, J., Masson, D., *et al.* (2012). Stat3 and Gfi-1 transcription factors control Th17 cell immunosuppressive activity via the regulation of ectonucleotidase expression. Immunity *36*, 362-373.

Chen, C., Ridzon, D.A., Broomer, A.J., Zhou, Z., Lee, D.H., Nguyen, J.T., Barbisin, M., Xu, N.L., Mahuvakar, V.R., Andersen, M.R., *et al.* (2005). Real-time quantification of microRNAs by stem-loop RT-PCR. Nucleic Acids Res *33*, e179.

Chen, C.Y., and Shyu, A.B. (1995). AU-rich elements: characterization and importance in mRNA degradation. Trends Biochem Sci *20*, 465-470.

Chen, X., Clarence Yan, C., Zhang, X., Li, Z., Deng, L., Zhang, Y., and Dai, Q. (2015). RBMMMDA: predicting multiple types of disease-microRNA associations. Sci Rep *5*, 13877.

Chuang, T.D., Luo, X., Panda, H., and Chegini, N. (2012). miR-93/106b and their host gene, MCM7, are differentially expressed in leiomyomas and functionally target F3 and IL-8. Molecular endocrinology *26*, 1028-1042.

Cohen, J.D., Drury, J.H., Ostdiek, J., Finn, J., Babu, B.R., Flaker, G., Belew, K., Donohue, T., and Labovitz, A. (2000). Benefits of lipid lowering on vascular reactivity in patients with coronary artery disease and average cholesterol levels: a mechanism for reducing clinical events? American heart journal *139*, 734-738.

Colucci, M., Balconi, G., Lorenzet, R., Pietra, A., Locati, D., Donati, M.B., and Semeraro, N. (1983). Cultured human endothelial cells generate tissue factor in response to endotoxin. J Clin Invest *71*, 1893-1896.

Cornwell, T.L., Arnold, E., Boerth, N.J., and Lincoln, T.M. (1994). Inhibition of smooth muscle cell growth by nitric oxide and activation of cAMP-dependent protein kinase by cGMP. The American journal of physiology *267*, C1405-1413.

Cui, M.Z., Parry, G.C., Edgington, T.S., and Mackman, N. (1994). Regulation of tissue factor gene expression in epithelial cells. Induction by serum and phorbol 12-myristate 13-acetate. Arterioscler Thromb *14*, 807-814.

de Graaf, J.C., Banga, J.D., Moncada, S., Palmer, R.M., de Groot, P.G., and Sixma, J.J. (1992). Nitric oxide functions as an inhibitor of platelet adhesion under flow conditions. Circulation *85*, 2284-2290.

Deaglio, S., and Robson, S.C. (2011). Ectonucleotidases as regulators of purinergic signaling in thrombosis, inflammation, and immunity. Advances in pharmacology *61*, 301-332.

Dean, J.L., Sully, G., Clark, A.R., and Saklatvala, J. (2004). The involvement of AU-rich element-binding proteins in p38 mitogen-activated protein kinase pathway-mediated mRNA stabilisation. Cell Signal *16*, 1113-1121.

Di Virgilio, F., and Solini, A. (2002). P2 receptors: new potential players in atherosclerosis. Br J Pharmacol *135*, 831-842.

Ding, L., Ma, W., Littmann, T., Camp, R., and Shen, J. (2011). The P2Y(2) nucleotide receptor mediates tissue factor expression in human coronary artery endothelial cells. The Journal of biological chemistry *286*, 27027-27038.

Drake, T.A., Morrissey, J.H., and Edgington, T.S. (1989). Selective cellular expression of tissue factor in human tissues. Implications for disorders of hemostasis and thrombosis. The American journal of pathology *134*, 1087-1097.

Drury, A.N., and Szent-Gyorgyi, A. (1929). The physiological activity of adenine compounds with especial reference to their action upon the mammalian heart. The Journal of physiology *68*, 213-237.

Dwyer, K.M., Deaglio, S., Gao, W., Friedman, D., Strom, T.B., and Robson, S.C. (2007). CD39 and control of cellular immune responses. Purinergic signalling *3*, 171-180.

Elliott, M.R., Chekeni, F.B., Trampont, P.C., Lazarowski, E.R., Kadl, A., Walk, S.F., Park, D., Woodson, R.I., Ostankovich, M., Sharma, P., *et al.* (2009). Nucleotides released by apoptotic cells act as a find-me signal to promote phagocytic clearance. Nature *461*, 282-286.

Eltzschig, H.K., Eckle, T., Mager, A., Kuper, N., Karcher, C., Weissmuller, T., Boengler, K., Schulz, R., Robson, S.C., and Colgan, S.P. (2006). ATP release from activated neutrophils occurs via connexin 43 and modulates adenosine-dependent endothelial cell function. Circulation research *99*, 1100-1108.

Eltzschig, H.K., Ibla, J.C., Furuta, G.T., Leonard, M.O., Jacobson, K.A., Enjyoji, K., Robson, S.C., and Colgan, S.P. (2003). Coordinated adenine nucleotide phosphohydrolysis and nucleoside signaling in posthypoxic endothelium: role of ectonucleotidases and adenosine A2B receptors. The Journal of experimental medicine *198*, 783-796.

Eltzschig, H.K., Kohler, D., Eckle, T., Kong, T., Robson, S.C., and Colgan, S.P. (2009). Central role of Sp1-regulated CD39 in hypoxia/ischemia protection. Blood *113*, 224-232.

Enjyoji, K., Sevigny, J., Lin, Y., Frenette, P.S., Christie, P.D., Esch, J.S., 2nd, Imai, M., Edelberg, J.M., Rayburn, H., Lech, M., *et al.* (1999). Targeted disruption of cd39/ATP diphosphohydrolase results in disordered hemostasis and thromboregulation. Nat Med *5*, 1010-1017.

Essafi-Benkhadir, K., Pouyssegur, J., and Pages, G. (2010). Implication of the ERK pathway on the post-transcriptional regulation of VEGF mRNA stability. Methods Mol Biol *661*, 451-469.

Fabre, A.C., Vantourout, P., Champagne, E., Terce, F., Rolland, C., Perret, B., Collet, X., Barbaras, R., and Martinez, L.O. (2006). Cell surface adenylate kinase activity regulates the F(1)-ATPase/P2Y (13)-mediated HDL endocytosis pathway on human hepatocytes. Cellular and molecular life sciences : CMLS *63*, 2829-2837.

Falati, S., Gross, P., Merrill-Skoloff, G., Furie, B.C., and Furie, B. (2002). Real-time in vivo imaging of platelets, tissue factor and fibrin during arterial thrombus formation in the mouse. Nat Med *8*, 1175-1181.

Falati, S., Liu, Q., Gross, P., Merrill-Skoloff, G., Chou, J., Vandendries, E., Celi, A., Croce, K., Furie, B.C., and Furie, B. (2003). Accumulation of tissue factor into developing thrombi in vivo is dependent upon microparticle P-selectin glycoprotein ligand 1 and platelet P-selectin. The Journal of experimental medicine *197*, 1585-1598.

Farooq, V., Serruys, P.W., Zhang, Y., Mack, M., Stahle, E., Holmes, D.R., Feldman, T., Morice, M.C., Colombo, A., Bourantas, C.V., *et al.* (2013). Short-term and long-term clinical impact of stent thrombosis and graft occlusion in the SYNTAX trial at 5 years: Synergy Between Percutaneous Coronary Intervention with Taxus and Cardiac Surgery trial. Journal of the American College of Cardiology *62*, 2360-2369.

Fears, S., Mathieu, C., Zeleznik-Le, N., Huang, S., Rowley, J.D., and Nucifora, G. (1996). Intergenic splicing of MDS1 and EVI1 occurs in normal tissues as well as in myeloid leukemia and produces a new member of the PR domain family. Proceedings of the National Academy of Sciences of the United States of America *93*, 1642-1647.

Fields, R.D., and Burnstock, G. (2006). Purinergic signalling in neuron-glia interactions. Nature reviews Neuroscience *7*, 423-436.

Fleck, R.A., Rao, L.V., Rapaport, S.I., and Varki, N. (1990). Localization of human tissue factor antigen by immunostaining with monospecific, polyclonal anti-human tissue factor antibody. Thrombosis research *59*, 421-437.

Furie, B., and Furie, B.C. (2008). Mechanisms of thrombus formation. The New England journal of medicine *359*, 938-949.

Gachet, C. (2006). Regulation of platelet functions by P2 receptors. Annual review of pharmacology and toxicology *46*, 277-300.

Gauthier, T.W., Scalia, R., Murohara, T., Guo, J.P., and Lefer, A.M. (1995). Nitric oxide protects against leukocyte-endothelium interactions in the early stages of hypercholesterolemia. Arterioscler Thromb Vasc Biol *15*, 1652-1659.

Gavala, M.L., Hill, L.M., Lenertz, L.Y., Karta, M.R., and Bertics, P.J. (2010). Activation of the transcription factor FosB/activating protein-1 (AP-1) is a prominent downstream signal of the extracellular nucleotide receptor P2RX7 in monocytic and osteoblastic cells. J Biol Chem *285*, 34288-34298.

Gebhard, C., Holy, E.W., Camici, G.G., Akhmedov, A., Stampfli, S.F., Stahli, B.E., von Rickenbach, B., Breitenstein, A., Greutert, H., Yang, Z., *et al.* (2012). Caffeine induces endothelial tissue factor expression via phosphatidylinositol 3-kinase inhibition. Thromb Haemost *107*, 884-894.

Gerasimovskaya, E.V., Ahmad, S., White, C.W., Jones, P.L., Carpenter, T.C., and Stenmark, K.R. (2002). Extracellular ATP is an autocrine/paracrine regulator of hypoxia-induced adventitial fibroblast growth. Signaling through extracellular signal-regulated kinase-1/2 and the Egr-1 transcription factor. The Journal of biological chemistry *277*, 44638-44650.

Gerrits, A.J., Koekman, C.A., van Haeften, T.W., and Akkerman, J.W. (2011). Increased tissue factor expression in diabetes mellitus type 2 monocytes caused by insulin resistance. J Thromb Haemost *9*, 873-875.

Gerrits, A.J., Koekman, C.A., Yildirim, C., Nieuwland, R., and Akkerman, J.W. (2009). Insulin inhibits tissue factor expression in monocytes. J Thromb Haemost *7*, 198-205.

Ghiringhelli, F., Bruchard, M., Chalmin, F., and Rebe, C. (2012). Production of adenosine by ectonucleotidases: a key factor in tumor immunoescape. Journal of biomedicine & biotechnology *2012*, 473712.

Giesen, P.L., Rauch, U., Bohrmann, B., Kling, D., Roque, M., Fallon, J.T., Badimon, J.J., Himber, J., Riederer, M.A., and Nemerson, Y. (1999). Blood-borne tissue factor: another view of thrombosis. Proceedings of the National Academy of Sciences of the United States of America *96*, 2311-2315.

Glover, J.N., and Harrison, S.C. (1995). Crystal structure of the heterodimeric bZIP transcription factor c-Fos-c-Jun bound to DNA. Nature *373*, 257-261.

Goyama, S., Yamamoto, G., Shimabe, M., Sato, T., Ichikawa, M., Ogawa, S., Chiba, S., and Kurokawa, M. (2008). Evi-1 is a critical regulator for hematopoietic stem cells and transformed leukemic cells. Cell Stem Cell *3*, 207-220.

Guha, M., and Mackman, N. (2002). The phosphatidylinositol 3-kinase-Akt pathway limits lipopolysaccharide activation of signaling pathways and expression of inflammatory mediators in human monocytic cells. The Journal of biological chemistry *277*, 32124-32132.

Guha, M., O'Connell, M.A., Pawlinski, R., Hollis, A., McGovern, P., Yan, S.F., Stern, D., and Mackman, N. (2001). Lipopolysaccharide activation of the MEK-ERK1/2 pathway in human monocytic cells mediates tissue factor and tumor necrosis factor alpha expression by inducing Elk-1 phosphorylation and Egr-1 expression. Blood *98*, 1429-1439.

Guns, P.J., Hendrickx, J., Van Assche, T., Fransen, P., and Bult, H. (2010). P2Y receptors and atherosclerosis in apolipoprotein E-deficient mice. Br J Pharmacol *159*, 326-336.

Guzman-Aranguez, A., and Pintor, J. (2012). Focus on molecules: purinergic P2Y(2) receptor. Experimental eye research *105*, 83-84.

Habermacher, C., Dunning, K., Chataigneau, T., and Grutter, T. (2015). Molecular structure and function of P2X receptors. Neuropharmacology.

Halees, A.S., El-Badrawi, R., and Khabar, K.S. (2008). ARED Organism: expansion of ARED reveals AU-rich element cluster variations between human and mouse. Nucleic Acids Res *36*, D137-140.

He, M., He, X., Xie, Q., Chen, F., and He, S. (2006). Angiotensin II induces the expression of tissue factor and its mechanism in human monocytes. Thrombosis research *117*, 579-590.

Hechler, B., Freund, M., Ravanat, C., Magnenat, S., Cazenave, J.P., and Gachet, C. (2008). Reduced atherosclerotic lesions in P2Y1/apolipoprotein E double-knockout mice: the contribution of non-hematopoietic-derived P2Y1 receptors. Circulation *118*, 754-763.

Hechler, B., and Gachet, C. (2015). Purinergic Receptors in Thrombosis and Inflammation. Arterioscler Thromb Vasc Biol.

Heidenreich, P.A., Trogdon, J.G., Khavjou, O.A., Butler, J., Dracup, K., Ezekowitz, M.D., Finkelstein, E.A., Hong, Y., Johnston, S.C., Khera, A., *et al.* (2011). Forecasting the

future of cardiovascular disease in the United States: a policy statement from the American Heart Association. Circulation *123*, 933-944.

Heine, P., Braun, N., Sevigny, J., Robson, S.C., Servos, J., and Zimmermann, H. (2001). The C-terminal cysteine-rich region dictates specific catalytic properties in chimeras of the ectonucleotidases NTPDase1 and NTPDase2. European journal of biochemistry / FEBS *268*, 364-373.

Hess, J., Angel, P., and Schorpp-Kistner, M. (2004). AP-1 subunits: quarrel and harmony among siblings. J Cell Sci *117*, 5965-5973.

Heuts, D.P., Weissenborn, M.J., Olkhov, R.V., Shaw, A.M., Gummadova, J., Levy, C., and Scrutton, N.S. (2012). Crystal structure of a soluble form of human CD73 with ecto-5'-nucleotidase activity. Chembiochem : a European journal of chemical biology *13*, 2384-2391.

Hirata, Y., Masuda, Y., Kakutani, H., Higuchi, T., Takada, K., Ito, A., Nakagawa, Y., and Ishii, H. (2008). Sp1 is an essential transcription factor for LPS-induced tissue factor expression in THP-1 monocytic cells, and nobiletin represses the expression through inhibition of NF-kappaB, AP-1, and Sp1 activation. Biochemical pharmacology *75*, 1504-1514.

Holzmuller, H., Moll, T., Hofer-Warbinek, R., Mechtcheriakova, D., Binder, B.R., and Hofer, E. (1999). A transcriptional repressor of the tissue factor gene in endothelial cells. Arterioscler Thromb Vasc Biol *19*, 1804-1811.

Homolya, L., Steinberg, T.H., and Boucher, R.C. (2000). Cell to cell communication in response to mechanical stress via bilateral release of ATP and UTP in polarized epithelia. The Journal of cell biology *150*, 1349-1360.

Houston, P., Dickson, M.C., Ludbrook, V., White, B., Schwachtgen, J.L., McVey, J.H., Mackman, N., Reese, J.M., Gorman, D.G., Campbell, C., *et al.* (1999). Fluid shear stress induction of the tissue factor promoter in vitro and in vivo is mediated by Egr-1. Arterioscler Thromb Vasc Biol *19*, 281-289.

Iqbal, M.B., Johns, M., Cao, J., Liu, Y., Yu, S.C., Hyde, G.D., Laffan, M.A., Marchese, F.P., Cho, S.H., Clark, A.R., *et al.* (2014). PARP-14 combines with tristetraprolin in the selective posttranscriptional control of macrophage tissue factor expression. Blood *124*, 3646-3655.

Jacob, F., Perez Novo, C., Bachert, C., and Van Crombruggen, K. (2013). Purinergic signaling in inflammatory cells: P2 receptor expression, functional effects, and modulation of inflammatory responses. Purinergic signalling *9*, 285-306.

Jacobson, K.A., Paoletta, S., Katritch, V., Wu, B., Gao, Z.G., Zhao, Q., Stevens, R.C., and Kiselev, E. (2015). Nucleotides Acting at P2Y Receptors: Connecting Structure and Function. Molecular pharmacology *88*, 220-230.

Jarvis, B., and Simpson, K. (2000). Clopidogrel: a review of its use in the prevention of atherothrombosis. Drugs *60*, 347-377.

Jin, J., Dasari, V.R., Sistare, F.D., and Kunapuli, S.P. (1998). Distribution of P2Y receptor subtypes on haematopoietic cells. British journal of pharmacology *123*, 789-794.

Johnson-Tidey, R.R., McGregor, J.L., Taylor, P.R., and Poston, R.N. (1994). Increase in the adhesion molecule P-selectin in endothelium overlying atherosclerotic plaques. Coexpression with intercellular adhesion molecule-1. The American journal of pathology *144*, 952-961.

Kapojos, J.J., van den Berg, A., Borghuis, T., Banas, B., Huitema, S., Poelstra, K., and Bakker, W.W. (2004). Enhanced ecto-apyrase activity of stimulated endothelial or mesangial cells is downregulated by glucocorticoids in vitro. European journal of pharmacology *501*, 191-198.

Kappetein, A.P., Feldman, T.E., Mack, M.J., Morice, M.C., Holmes, D.R., Stahle, E., Dawkins, K.D., Mohr, F.W., Serruys, P.W., and Colombo, A. (2011). Comparison of coronary bypass surgery with drug-eluting stenting for the treatment of left main and/or three-vessel disease: 3-year follow-up of the SYNTAX trial. European heart journal *32*, 2125-2134.

Kellerman, D., Rossi Mospan, A., Engels, J., Schaberg, A., Gorden, J., and Smiley, L. (2008). Denufosol: a review of studies with inhaled P2Y(2) agonists that led to Phase 3. Pulm Pharmacol Ther *21*, 600-607.

Knapp, K., Zebisch, M., Pippel, J., El-Tayeb, A., Muller, C.E., and Strater, N. (2012). Crystal structure of the human ecto-5'-nucleotidase (CD73): insights into the regulation of purinergic signaling. Structure *20*, 2161-2173.

Krikun, G., Schatz, F., Mackman, N., Guller, S., Demopoulos, R., and Lockwood, C.J. (2000). Regulation of tissue factor gene expression in human endometrium by transcription factors Sp1 and Sp3. Molecular endocrinology *14*, 393-400.

Kubes, P., Suzuki, M., and Granger, D.N. (1991). Nitric oxide: an endogenous modulator of leukocyte adhesion. Proceedings of the National Academy of Sciences of the United States of America *88*, 4651-4655.

Lau, O.C., Samarawickrama, C., and Skalicky, S.E. (2014). P2Y2 receptor agonists for the treatment of dry eye disease: a review. Clin Ophthalmol *8*, 327-334.

Lazarowski, E.R., and Boucher, R.C. (2009). Purinergic receptors in airway epithelia. Current opinion in pharmacology *9*, 262-267.

Lazarowski, E.R., Boucher, R.C., and Harden, T.K. (2000). Constitutive release of ATP and evidence for major contribution of ecto-nucleotide pyrophosphatase and nucleoside diphosphokinase to extracellular nucleotide concentrations. The Journal of biological chemistry *275*, 31061-31068.

Lazarowski, E.R., Boucher, R.C., and Harden, T.K. (2003). Mechanisms of release of nucleotides and integration of their action as P2X- and P2Y-receptor activating molecules. Molecular pharmacology *64*, 785-795.

Lee, R., Williams, J.C., and Mackman, N. (2012). P2X7 regulation of macrophage tissue factor activity and microparticle generation. Journal of thrombosis and haemostasis : JTH *10*, 1965-1967.

Lennon, P.F., Taylor, C.T., Stahl, G.L., and Colgan, S.P. (1998). Neutrophil-derived 5'-adenosine monophosphate promotes endothelial barrier function via CD73-mediated conversion to adenosine and endothelial A2B receptor activation. The Journal of experimental medicine *188*, 1433-1443.

Leon, C., Ravanat, C., Freund, M., Cazenave, J.P., and Gachet, C. (2003). Differential involvement of the P2Y1 and P2Y12 receptors in platelet procoagulant activity. Arterioscler Thromb Vasc Biol *23*, 1941-1947.

Ley, K., and Tedder, T.F. (1995). Leukocyte interactions with vascular endothelium. New insights into selectin-mediated attachment and rolling. Journal of immunology *155*, 525-528.

Li, S., Chen, H., Ren, J., Geng, Q., Song, J., Lee, C., Cao, C., Zhang, J., and Xu, N. (2014a). MicroRNA-223 inhibits tissue factor expression in vascular endothelial cells. Atherosclerosis *237*, 514-520.

Li, S., Ren, J., Xu, N., Zhang, J., Geng, Q., Cao, C., Lee, C., Song, J., Li, J., and Chen, H. (2014b). MicroRNA-19b functions as potential anti-thrombotic protector in patients with unstable angina by targeting tissue factor. Journal of molecular and cellular cardiology *75*, 49-57.

Li, Y.D., Ye, B.Q., Zheng, S.X., Wang, J.T., Wang, J.G., Chen, M., Liu, J.G., Pei, X.H., Wang, L.J., Lin, Z.X., *et al.* (2009). NF-kappaB transcription factor p50 critically regulates tissue factor in deep vein thrombosis. The Journal of biological chemistry *284*, 4473-4483.

Liao, Z., Seye, C.I., Weisman, G.A., and Erb, L. (2007). The P2Y2 nucleotide receptor requires interaction with alpha v integrins to access and activate G12. Journal of cell science *120*, 1654-1662.

Libby, P. (2001). Current concepts of the pathogenesis of the acute coronary syndromes. Circulation *104*, 365-372.

Liu, J., Liao, Z., Camden, J., Griffin, K.D., Garrad, R.C., Santiago-Perez, L.I., Gonzalez, F.A., Seye, C.I., Weisman, G.A., and Erb, L. (2004). Src homology 3 binding sites in the P2Y2 nucleotide receptor interact with Src and regulate activities of Src, proline-rich tyrosine kinase 2, and growth factor receptors. The Journal of biological chemistry *279*, 8212-8218.

Lohman, A.W., Billaud, M., and Isakson, B.E. (2012). Mechanisms of ATP release and signalling in the blood vessel wall. Cardiovascular research *95*, 269-280.

Lundy, D.J., and Trzeciak, S. (2009). Microcirculatory dysfunction in sepsis. Critical care clinics *25*, 721-731, viii.

Luscinskas, F.W., Kansas, G.S., Ding, H., Pizcueta, P., Schleiffenbaum, B.E., Tedder, T.F., and Gimbrone, M.A., Jr. (1994). Monocyte rolling, arrest and spreading on IL-4-activated vascular endothelium under flow is mediated via sequential action of L-selectin, beta 1-integrins, and beta 2-integrins. The Journal of cell biology *125*, 1417-1427.

Ma, W., Liu, Y., Ellison, N., and Shen, J. (2013). Induction of C-X-C Chemokine Receptor Type 7 (CXCR7) Switches Stromal Cell-Derived Factor-1 (SDF-1) Signaling and Phagocytic Activity in Macrophages Linked to Atherosclerosis. The Journal of biological chemistry.

Mach, F., Schonbeck, U., Bonnefoy, J.Y., Pober, J.S., and Libby, P. (1997). Activation of monocyte/macrophage functions related to acute atheroma complication by ligation of CD40: induction of collagenase, stromelysin, and tissue factor. Circulation *96*, 396-399.

Mackman, N. (1996). Regulation of tissue factor gene expression in human monocytic and endothelial cells. Haemostasis *26 Suppl 1*, 17-19.

Mackman, N., Fowler, B.J., Edgington, T.S., and Morrissey, J.H. (1990). Functional analysis of the human tissue factor promoter and induction by serum. Proceedings of the National Academy of Sciences of the United States of America *87*, 2254-2258.

Mackman, N., Morrissey, J.H., Fowler, B., and Edgington, T.S. (1989). Complete sequence of the human tissue factor gene, a highly regulated cellular receptor that initiates the coagulation protease cascade. Biochemistry *28*, 1755-1762.

Mallat, Z., Benamer, H., Hugel, B., Benessiano, J., Steg, P.G., Freyssinet, J.M., and Tedgui, A. (2000). Elevated levels of shed membrane microparticles with procoagulant potential in the peripheral circulating blood of patients with acute coronary syndromes. Circulation *101*, 841-843.

Mancini, G.B., Henry, G.C., Macaya, C., O'Neill, B.J., Pucillo, A.L., Carere, R.G., Wargovich, T.J., Mudra, H., Luscher, T.F., Klibaner, M.I., *et al.* (1996). Angiotensin-converting enzyme inhibition with quinapril improves endothelial vasomotor dysfunction in patients with coronary artery disease. The TREND (Trial on Reversing ENdothelial Dysfunction) Study. Circulation *94*, 258-265.

Mangano, D.T., and Multicenter Study of Perioperative Ischemia Research, G. (2002). Aspirin and mortality from coronary bypass surgery. The New England journal of medicine *347*, 1309-1317.

Matys, V., Fricke, E., Geffers, R., Gossling, E., Haubrock, M., Hehl, R., Hornischer, K., Karas, D., Kel, A.E., Kel-Margoulis, O.V., *et al.* (2003). TRANSFAC: transcriptional regulation, from patterns to profiles. Nucleic Acids Res *31*, 374-378.

Meisel, S.R., Xu, X.P., Edgington, T.S., Dimayuga, P., Kaul, S., Lee, S., Fishbein, M.C., Cercek, B., and Shah, P.K. (2002). Differentiation of adherent human monocytes into macrophages markedly enhances tissue factor protein expression and procoagulant activity. Atherosclerosis *161*, 35-43.

Meszaros, K., Aberle, S., Dedrick, R., Machovich, R., Horwitz, A., Birr, C., Theofan, G., and Parent, J.B. (1994). Monocyte tissue factor induction by lipopolysaccharide (LPS): dependence on LPS-binding protein and CD14, and inhibition by a recombinant fragment of bactericidal/permeability-increasing protein. Blood *83*, 2516-2525.

Mizumoto, N., Kumamoto, T., Robson, S.C., Sevigny, J., Matsue, H., Enjyoji, K., and Takashima, A. (2002). CD39 is the dominant Langerhans cell-associated ecto-NTPDase: modulatory roles in inflammation and immune responsiveness. Nat Med *8*, 358-365.

Moll, T., Czyz, M., Holzmuller, H., Hofer-Warbinek, R., Wagner, E., Winkler, H., Bach, F.H., and Hofer, E. (1995). Regulation of the tissue factor promoter in endothelial cells. Binding of NF kappa B-, AP-1-, and Sp1-like transcription factors. J Biol Chem *270*, 3849-3857.

Molliver, D.C., Cook, S.P., Carlsten, J.A., Wright, D.E., and McCleskey, E.W. (2002). ATP and UTP excite sensory neurons and induce CREB phosphorylation through the metabotropic receptor, P2Y2. The European journal of neuroscience *16*, 1850-1860.

Morishita, K., Parganas, E., Douglass, E.C., and Ihle, J.N. (1990). Unique expression of the human Evi-1 gene in an endometrial carcinoma cell line: sequence of cDNAs and structure of alternatively spliced transcripts. Oncogene *5*, 963-971.

North, R.A., and Verkhratsky, A. (2006). Purinergic transmission in the central nervous system. Pflugers Archiv : European journal of physiology *452*, 479-485.

O'Reilly, F.M., Casper, K.A., Otto, K.B., Sexton, S.A., and Swerlick, R.A. (2003). Regulation of tissue factor in microvascular dermal endothelial cells. J Invest Dermatol *120*, 489-494.

Obenauf, A.C., Zou, Y., Ji, A.L., Vanharanta, S., Shu, W., Shi, H., Kong, X., Bosenberg, M.C., Wiesner, T., Rosen, N., *et al.* (2015). Therapy-induced tumour secretomes promote resistance and tumour progression. Nature.

Oeth, P., Parry, G.C., and Mackman, N. (1997). Regulation of the tissue factor gene in human monocytic cells. Role of AP-1, NF-kappa B/Rel, and Sp1 proteins in uninduced and lipopolysaccharide-induced expression. Arterioscler Thromb Vasc Biol *17*, 365-374.

Oliveira, A.G., Marques, P.E., Amaral, S.S., Quintao, J.L., Cogliati, B., Dagli, M.L., Rogiers, V., Vanhaecke, T., Vinken, M., and Menezes, G.B. (2013). Purinergic signalling during sterile liver injury. Liver international : official journal of the International Association for the Study of the Liver *33*, 353-361.

Orriss, I.R., Burnstock, G., and Arnett, T.R. (2010). Purinergic signalling and bone remodelling. Current opinion in pharmacology *10*, 322-330.

Oury, C., Lecut, C., Hego, A., Wera, O., and Delierneux, C. (2015). Purinergic control of inflammation and thrombosis: Role of P2X1 receptors. Computational and structural biotechnology journal *13*, 106-110.

Palmer, R.M., Ashton, D.S., and Moncada, S. (1988). Vascular endothelial cells synthesize nitric oxide from L-arginine. Nature *333*, 664-666.

Parry, G.C., and Mackman, N. (1995). Transcriptional regulation of tissue factor expression in human endothelial cells. Arterioscler Thromb Vasc Biol *15*, 612-621.

Pendurthi, U.R., Williams, J.T., and Rao, L.V. (1997). Inhibition of tissue factor gene activation in cultured endothelial cells by curcumin. Suppression of activation of transcription factors Egr-1, AP-1, and NF-kappa B. Arterioscler Thromb Vasc Biol *17*, 3406-3413.

Peterson, T.S., Camden, J.M., Wang, Y., Seye, C.I., Wood, W.G., Sun, G.Y., Erb, L., Petris, M.J., and Weisman, G.A. (2010). P2Y2 nucleotide receptor-mediated responses in brain cells. Molecular neurobiology *41*, 356-366.

Poston, R.N., Haskard, D.O., Coucher, J.R., Gall, N.P., and Johnson-Tidey, R.R. (1992). Expression of intercellular adhesion molecule-1 in atherosclerotic plaques. The American journal of pathology *140*, 665-673.

Prandoni, P. (2009). Venous and arterial thrombosis: Two aspects of the same disease? Clinical epidemiology *1*, 1-6.

Proctor, R.A., Denlinger, L.C., Leventhal, P.S., Daugherty, S.K., van de Loo, J.W., Tanke, T., Firestein, G.S., and Bertics, P.J. (1994). Protection of mice from endotoxic death by 2-methylthio-ATP. Proceedings of the National Academy of Sciences of the United States of America *91*, 6017-6020.

Pudusseri, A., Shameem, R., and Spyropoulos, A.C. (2013). A new paradigm shift in antithrombotic therapy. Frontiers in pharmacology *4*, 133.

Qawi, I., and Robson, S.C. (2000). New developments in anti-platelet therapies: potential use of CD39/vascular ATP diphosphohydrolase in thrombotic disorders. Current drug targets *1*, 285-296.

Rajasekaran, S., Vaz, M., and Reddy, S.P. (2012). Fra-1/AP-1 transcription factor negatively regulates pulmonary fibrosis in vivo. PLoS One *7*, e41611.

Ransohoff, R.M., and Perry, V.H. (2009). Microglial physiology: unique stimuli, specialized responses. Annual review of immunology *27*, 119-145.

Reddy, K.V., Bhattacharjee, G., Schabbauer, G., Hollis, A., Kempf, K., Tencati, M., O'Connell, M., Guha, M., and Mackman, N. (2004). Dexamethasone enhances LPS

induction of tissue factor expression in human monocytic cells by increasing tissue factor mRNA stability. J Leukoc Biol *76*, 145-151.

Regateiro, F.S., Howie, D., Nolan, K.F., Agorogiannis, E.I., Greaves, D.R., Cobbold, S.P., and Waldmann, H. (2011). Generation of anti-inflammatory adenosine by leukocytes is regulated by TGF-beta. European journal of immunology *41*, 2955-2965.

Robson, S.C., Kaczmarek, E., Siegel, J.B., Candinas, D., Koziak, K., Millan, M., Hancock, W.W., and Bach, F.H. (1997). Loss of ATP diphosphohydrolase activity with endothelial cell activation. The Journal of experimental medicine *185*, 153-163.

Robson, S.C., Wu, Y., Sun, X., Knosalla, C., Dwyer, K., and Enjyoji, K. (2005). Ectonucleotidases of CD39 family modulate vascular inflammation and thrombosis in transplantation. Seminars in thrombosis and hemostasis *31*, 217-233.

Ruepp, A., Kowarsch, A., Schmidl, D., Buggenthin, F., Brauner, B., Dunger, I., Fobo, G., Frishman, G., Montrone, C., and Theis, F.J. (2010). PhenomiR: a knowledgebase for microRNA expression in diseases and biological processes. Genome Biol *11*, R6.

Ruf, W., Disse, J., Carneiro-Lobo, T.C., Yokota, N., and Schaffner, F. (2011). Tissue factor and cell signalling in cancer progression and thrombosis. J Thromb Haemost *9 Suppl 1*, 306-315.

Sambola, A., Osende, J., Hathcock, J., Degen, M., Nemerson, Y., Fuster, V., Crandall, J., and Badimon, J.J. (2003). Role of risk factors in the modulation of tissue factor activity and blood thrombogenicity. Circulation *107*, 973-977.

Schreck, I., Al-Rawi, M., Mingot, J.M., Scholl, C., Diefenbacher, M.E., O'Donnell, P., Bohmann, D., and Weiss, C. (2011). c-Jun localizes to the nucleus independent of its phosphorylation by and interaction with JNK and vice versa promotes nuclear accumulation of JNK. Biochemical and biophysical research communications *407*, 735-740.

Schror, K. (1997). Aspirin and platelets: the antiplatelet action of aspirin and its role in thrombosis treatment and prophylaxis. Seminars in thrombosis and hemostasis *23*, 349-356.

Schwiebert, E.M., and Fitz, J.G. (2008). Purinergic signaling microenvironments: An introduction. Purinergic signalling *4*, 89-92.

Seifert, R., and Schultz, G. (1989). Involvement of pyrimidinoceptors in the regulation of cell functions by uridine and by uracil nucleotides. Trends in pharmacological sciences *10*, 365-369.

Seye, C.I., Agca, Y., Agca, C., and Derbigny, W. (2012). P2Y2 receptor-mediated lymphotoxin-alpha secretion regulates intercellular cell adhesion molecule-1 expression in vascular smooth muscle cells. J Biol Chem *287*, 10535-10543.

Seye, C.I., Kong, Q., Yu, N., Gonzalez, F.A., Erb, L., and Weisman, G.A. (2007). P2 receptors in atherosclerosis and postangioplasty restenosis. Purinergic signalling *3*, 153-162.

Seye, C.I., Yu, N., Jain, R., Kong, Q., Minor, T., Newton, J., Erb, L., Gonzalez, F.A., and Weisman, G.A. (2003). The P2Y2 nucleotide receptor mediates UTP-induced vascular cell adhesion molecule-1 expression in coronary artery endothelial cells. The Journal of biological chemistry *278*, 24960-24965.

Shen, J., Seye, C.I., Wang, M., Weisman, G.A., Wilden, P.A., and Sturek, M. (2004). Cloning, up-regulation, and mitogenic role of porcine P2Y2 receptor in coronary artery smooth muscle cells. Molecular pharmacology *66*, 1265-1274.

Shen, Z.J., and Malter, J.S. (2015). Regulation of AU-Rich Element RNA Binding Proteins by Phosphorylation and the Prolyl Isomerase Pin1. Biomolecules *5*, 412-434.

Sikka, P., and Bindra, V.K. (2010). Newer antithrombotic drugs. Indian journal of critical care medicine : peer-reviewed, official publication of Indian Society of Critical Care Medicine *14*, 188-195.

Simic, I., Pecin, I., Tedeschi-Reiner, E., Zrinscak, O., Sucur, N., and Reiner, Z. (2013). Risk factors for microvascular atherosclerotic changes in patients with type 2 diabetes mellitus. Collegium antropologicum *37*, 783-787.

Smith, T.M., and Kirley, T.L. (1998). Cloning, sequencing, and expression of a human brain ecto-apyrase related to both the ecto-ATPases and CD39 ecto-apyrases1. Biochimica et biophysica acta *1386*, 65-78.

Soltoff, S.P., Avraham, H., Avraham, S., and Cantley, L.C. (1998). Activation of P2Y2 receptors by UTP and ATP stimulates mitogen-activated kinase activity through a pathway that involves related adhesion focal tyrosine kinase and protein kinase C. The Journal of biological chemistry *273*, 2653-2660.

Sorensen, C.E., and Novak, I. (2001). Visualization of ATP release in pancreatic acini in response to cholinergic stimulus. Use of fluorescent probes and confocal microscopy. The Journal of biological chemistry *276*, 32925-32932.

Sprague, R.S., Stephenson, A.H., and Ellsworth, M.L. (2007). Red not dead: signaling in and from erythrocytes. Trends in endocrinology and metabolism: TEM *18*, 350-355.

Springer, T.A. (1994). Traffic signals for lymphocyte recirculation and leukocyte emigration: the multistep paradigm. Cell *76*, 301-314.

Stary, H.C., Chandler, A.B., Dinsmore, R.E., Fuster, V., Glagov, S., Insull, W., Jr., Rosenfeld, M.E., Schwartz, C.J., Wagner, W.D., and Wissler, R.W. (1995). A definition of advanced types of atherosclerotic lesions and a histological classification of atherosclerosis. A report from the Committee on Vascular Lesions of the Council on Arteriosclerosis, American Heart Association. Circulation *92*, 1355-1374.

Steffel, J., Luscher, T.F., and Tanner, F.C. (2006). Tissue factor in cardiovascular diseases: molecular mechanisms and clinical implications. Circulation *113*, 722-731.

Strater, N. (2006). Ecto-5'-nucleotidase: Structure function relationships. Purinergic signalling *2*, 343-350.

Synnestvedt, K., Furuta, G.T., Comerford, K.M., Louis, N., Karhausen, J., Eltzschig, H.K., Hansen, K.R., Thompson, L.F., and Colgan, S.P. (2002). Ecto-5'-nucleotidase (CD73) regulation by hypoxia-inducible factor-1 mediates permeability changes in intestinal epithelia. J Clin Invest *110*, 993-1002.

Taylor, F.B., Jr., Chang, A., Ruf, W., Morrissey, J.H., Hinshaw, L., Catlett, R., Blick, K., and Edgington, T.S. (1991). Lethal E. coli septic shock is prevented by blocking tissue factor with monoclonal antibody. Circulatory shock *33*, 127-134.

Terasawa, K., Okazaki, K., and Nishida, E. (2003). Regulation of c-Fos and Fra-1 by the MEK5-ERK5 pathway. Genes Cells *8*, 263-273.

Thompson, L.F., Eltzschig, H.K., Ibla, J.C., Van De Wiele, C.J., Resta, R., Morote-Garcia, J.C., and Colgan, S.P. (2004). Crucial role for ecto-5'-nucleotidase (CD73) in vascular leakage during hypoxia. The Journal of experimental medicine *200*, 1395-1405.

Tomiyama, H., Kimura, Y., Mitsuhashi, H., Kinouchi, T., Yoshida, H., Kushiro, T., and Doba, N. (1998). Relationship between endothelial function and fibrinolysis in early hypertension. Hypertension *31*, 321-327.

Uehata, A., Lieberman, E.H., Gerhard, M.D., Anderson, T.J., Ganz, P., Polak, J.F., Creager, M.A., and Yeung, A.C. (1997). Noninvasive assessment of endothelium-dependent flow-mediated dilation of the brachial artery. Vascular medicine *2*, 87-92.

van Dam, H., and Castellazzi, M. (2001). Distinct roles of Jun : Fos and Jun : ATF dimers in oncogenesis. Oncogene *20*, 2453-2464.

Van Kolen, K., and Slegers, H. (2006). Integration of P2Y receptor-activated signal transduction pathways in G protein-dependent signalling networks. Purinergic signalling *2*, 451-469.

VanderLaan, P.A., Reardon, C.A., and Getz, G.S. (2004). Site specificity of atherosclerosis: site-selective responses to atherosclerotic modulators. Arterioscler Thromb Vasc Biol *24*, 12-22.

Vassort, G. (2001). Adenosine 5'-triphosphate: a P2-purinergic agonist in the myocardium. Physiological reviews *81*, 767-806.

Verheugt, F.W. (2013). Antithrombotic therapy during and after percutaneous coronary intervention in patients with atrial fibrillation. Circulation *128*, 2058-2061.

Viles-Gonzalez, J.F., Fuster, V., and Badimon, J.J. (2004). Atherothrombosis: a widespread disease with unpredictable and life-threatening consequences. European heart journal *25*, 1197-1207.

Wada, H., Kaneko, T., Wakita, Y., Minamikawa, K., Nagaya, S., Tamaki, S., Deguchi, K., and Shirakawa, S. (1994). Effect of lipoproteins on tissue factor activity and PAI-II antigen in human monocytes and macrophages. International journal of cardiology *47*, S21-25.

Wagner, B., Natarajan, A., Grunaug, S., Kroismayr, R., Wagner, E.F., and Sibilia, M. (2006). Neuronal survival depends on EGFR signaling in cortical but not midbrain astrocytes. The EMBO journal *25*, 752-762.

Washburn, K.B., and Neary, J.T. (2006). P2 purinergic receptors signal to STAT3 in astrocytes: Difference in STAT3 responses to P2Y and P2X receptor activation. Neuroscience *142*, 411-423.

Weiss, N., Keller, C., Hoffmann, U., and Loscalzo, J. (2002). Endothelial dysfunction and atherothrombosis in mild hyperhomocysteinemia. Vascular medicine *7*, 227-239.

Wilcox, J.N., Smith, K.M., Schwartz, S.M., and Gordon, D. (1989). Localization of tissue factor in the normal vessel wall and in the atherosclerotic plaque. Proceedings of the National Academy of Sciences of the United States of America *86*, 2839-2843.

Wiley, S.R., Schooley, K., Smolak, P.J., Din, W.S., Huang, C.P., Nicholl, J.K., Sutherland, G.R., Smith, T.D., Rauch, C., Smith, C.A., *et al.* (1995). Identification and characterization of a new member of the TNF family that induces apoptosis. Immunity *3*, 673-682.

Wilusz, C.J., Wormington, M., and Peltz, S.W. (2001). The cap-to-tail guide to mRNA turnover. Nat Rev Mol Cell Biol *2*, 237-246.

Wolberg, A.S., Aleman, M.M., Leiderman, K., and Machlus, K.R. (2012). Procoagulant activity in hemostasis and thrombosis: Virchow's triad revisited. Anesthesia and analgesia *114*, 275-285.

Wong, C.W., Christen, T., Roth, I., Chadjichristos, C.E., Derouette, J.P., Foglia, B.F., Chanson, M., Goodenough, D.A., and Kwak, B.R. (2006). Connexin37 protects against atherosclerosis by regulating monocyte adhesion. Nat Med *12*, 950-954.

Wu, X., and Brewer, G. (2012). The regulation of mRNA stability in mammalian cells: 2.0. Gene *500*, 10-21.

Yan, J., Wang, K., Dong, L., Liu, H., Chen, W., Xi, W., Ding, Q., Kieffer, N., Caen, J.P., Chen, S., *et al.* (2010). PML/RARalpha fusion protein transactivates the tissue factor promoter through a GAGC-containing element without direct DNA association. Proceedings of the National Academy of Sciences of the United States of America *107*, 3716-3721.

Yan, S.F., Zou, Y.S., Gao, Y., Zhai, C., Mackman, N., Lee, S.L., Milbrandt, J., Pinsky, D., Kisiel, W., and Stern, D. (1998). Tissue factor transcription driven by Egr-1 is a critical mechanism of murine pulmonary fibrin deposition in hypoxia. Proc Natl Acad Sci U S A *95*, 8298-8303.

Yegutkin, G.G. (2008). Nucleotide- and nucleoside-converting ectoenzymes: Important modulators of purinergic signalling cascade. Biochimica et biophysica acta *1783*, 673-694.

Yegutkin, G.G., Wieringa, B., Robson, S.C., and Jalkanen, S. (2012). Metabolism of circulating ADP in the bloodstream is mediated via integrated actions of soluble adenylate kinase-1 and NTPDase1/CD39 activities. FASEB journal : official publication of the Federation of American Societies for Experimental Biology *26*, 3875-3883.

Yu, G., Li, H., Wang, X., Wu, T., Zhu, J., Huang, S., Wan, Y., and Tang, J. (2013a). MicroRNA-19a targets tissue factor to inhibit colon cancer cells migration and invasion. Molecular and cellular biochemistry *380*, 239-247.

Yu, N., Erb, L., Shivaji, R., Weisman, G.A., and Seye, C.I. (2008). Binding of the P2Y2 nucleotide receptor to filamin A regulates migration of vascular smooth muscle cells. Circulation research *102*, 581-588.

Yu, Y.H., Wu, D.S., Huang, F.F., Zhang, Z., Liu, L.X., Zhang, J., Zhan, H.E., Peng, M.Y., Zeng, H., and Chen, F.P. (2013b). MicroRNA-20b and ERK1/2 pathway independently regulate the expression of tissue factor in hematopoietic and trophoblastic differentiation of human embryonic stem cells. Stem cell research & therapy *4*, 121.

Zahno, A., Brecht, K., Bodmer, M., Bur, D., Tsakiris, D.A., and Krahenbuhl, S. (2010). Effects of drug interactions on biotransformation and antiplatelet effect of clopidogrel in vitro. British journal of pharmacology *161*, 393-404.

Zhou, L.Y., Chen, F.Y., Shen, L.J., Wan, H.X., and Zhong, J.H. (2014). Arsenic trioxide induces apoptosis in the THP1 cell line by downregulating EVI-1. Exp Ther Med *8*, 85-90.

Zimmermann, H. (1999). Two novel families of ectonucleotidases: molecular structures, catalytic properties and a search for function. Trends in pharmacological sciences *20*, 231-236.

Appendix

Table 6.1. microRNA expression profiles in HCAEC treated with/without UTP

PCR array catalog number: MAH-100

Position	Gene	Ct in control cells	Ct in UTP treated cells	ΔCt	Fold change
1-A01	miR-142-5p	34.76	34.99	0.23	3.0951
1-A02	miR-16	17.85	18.14	0.29	2.969
1-A03	miR-142-3p	34.73	35	0.27	3.0105
1-A04	miR-21	15.09	15.26	0.17	3.2266
1-A05	miR-15a	23.77	25.91	2.14	0.8236
1-A06	miR-29b	27.26	30.15	2.89	0.4897
1-A07	let-7a	20.97	23	2.03	0.8888
1-A08	miR-126	14.57	14.95	0.38	2.7895
1-A09	miR-143	32.84	33.95	1.11	1.6818
1-A10	let-7b	23.12	25.25	2.13	0.8293
1-A11	miR-27a	18.21	19.46	1.25	1.5263
1-A12	let-7f	29.52	31.65	2.13	0.8293
1-B01	miR-9	32.12	32.86	0.74	2.1735
1-B02	miR-26a	19.73	20.21	0.48	2.6027
1-B03	miR-24	18.26	19.76	1.5	1.2834
1-B04	miR-30e	23.77	25.37	1.6	1.1975
1-B05	miR-181a	24.79	27.44	2.65	0.5783
1-B06	miR-29a	21.3	23.5	2.2	0.79
1-B07	miR-124	30.86	30.49	-0.37	4.6913
1-B08	miR-144	35	35	0	3.6301
1-B09	miR-30d	22.27	23.55	1.28	1.4948
1-B10	miR-19b	20.67	22.29	1.62	1.181
1-B11	miR-22	21.39	23.89	2.5	0.6417
1-B12	miR-122	32.94	34.07	1.13	1.6586
1-C01	miR-150	26.1	26.95	0.85	2.0139
1-C02	miR-32	27.51	30.3	2.79	0.5249
1-C03	miR-155	25.7	26.76	1.06	1.7411

1-C04	miR-140-5p	23.7	24.76	1.06	1.7411
1-C05	miR-125b	17.43	17.68	0.25	3.0525
1-C06	miR-141	35	34.78	-0.22	4.2281
1-C07	miR-92a	20.74	22.25	1.51	1.2746
1-C08	miR-424	20.41	21.36	0.95	1.879
1-C09	miR-191	20.86	21.59	0.73	2.1886
1-C10	miR-17	19.64	20.97	1.33	1.4439
1-C11	miR-130a	25.12	27.22	2.1	0.8467
1-C12	miR-20a	19.18	20.57	1.39	1.3851
1-D01	miR-27b	21.16	21.82	0.66	2.2974
1-D02	miR-26b	23.86	22.86	-1	7.2602
1-D03	miR-146a	25.56	26.64	1.08	1.7171
1-D04	miR-200c	29.88	30.69	0.81	2.0705
1-D05	miR-99a	19.76	20.32	0.56	2.4623
1-D06	miR-19a	20.6	22.17	1.57	1.2226
1-D07	miR-23a	17.66	18.25	0.59	2.4116
1-D08	miR-30a	20.8	21.65	0.85	2.0139
1-D09	let-7i	22.48	24.46	1.98	0.9202
1-D10	miR-93	20.5	22.4	1.9	0.9727
1-D11	let-7c	25.28	27.13	1.85	1.007
1-D12	miR-106b	21.8	23.68	1.88	0.9862
1-E01	miR-101	24.1	25.56	1.46	1.3195
1-E02	let-7g	23.06	24.86	1.8	1.0425
1-E03	miR-425	22.98	24.52	1.54	1.2483
1-E04	miR-15b	21.47	22.7	1.23	1.5476
1-E05	miR-28-5p	22.47	23.5	1.03	1.7777
1-E06	miR-18a	22.56	24	1.44	1.3379
1-E07	miR-25	20.53	21	0.47	2.6208
1-E08	miR-23b	21.13	21.81	0.68	2.2658
1-E09	miR-302a	31.74	32.17	0.43	2.6945
1-E10	miR-186	22.46	24.19	1.73	1.0943
1-E11	miR-29c	23.82	25.72	1.9	0.9727
1-E12	miR-7	24.43	25.7	1.27	1.5052
1-F01	let-7d	26.54	28.19	1.65	1.1567
1-F02	miR-30c	20.84	21.27	0.43	2.6945
1-F03	miR-181b	23.37	24.94	1.57	1.2226
1-F04	miR-223	31.21	32.74	1.53	1.257
1-F05	miR-320a	23.07	24.34	1.27	1.5052
1-F06	miR-374a	21.78	22.57	0.79	2.0994
1-F07	let-7e	22.35	24.09	1.74	1.0867

1-F08	miR-151-5p	19.75	20.8	1.05	1.7532
1-F09	miR-374b	23.66	23.83	0.17	3.2266
1-F10	miR-196b	29.48	30.36	0.88	1.9725
1-F11	miR-140-3p	23.54	25.56	2.02	0.895
1-F12	miR-100	16.98	17.69	0.71	2.2191
1-G01	miR-103	21	23.06	2.06	0.8706
1-G02	miR-96	34.8	33.26	-1.54	10.5561
1-G03	miR-302b	33.19	34.15	0.96	1.8661
1-G04	miR-194	26.25	26.66	0.41	2.7321
1-G05	miR-125a-5p	18.5	19.17	0.67	2.2815
1-G06	miR-423-5p	26.94	29.79	2.85	0.5035
1-G07	miR-376c	22.32	23.13	0.81	2.0705
1-G08	miR-195	19.28	19.65	0.37	2.8089
1-G09	miR-222	21.38	23.65	2.27	0.7526
1-G10	miR-28-3p	23.74	24.39	0.65	2.3134
1-G11	miR-128	24.49	26.39	1.9	0.9727
1-G12	miR-302c	34.99	34.95	-0.04	3.7321
1-H01	miR-423-3p	21.72	24.05	2.33	0.722
1-H02	miR-185	23.85	25.49	1.64	1.1647
1-H03	miR-30b	21.16	21.63	0.47	2.6208
1-H04	miR-210	27.93	28.27	0.34	2.8679
1-H05	SNORD48	24.85	28.6	3.75	0.2698
1-H06	SNORD47	22.28	24.87	2.59	0.6029
1-H07	SNORD44	19.22	21.13	1.91	0.9659
1-H08	RNU6-2	21.03	22.89	1.86	1
1-H09	miRTC	18.37	19.23	0.86	2
1-H10	miRTC	18.19	18.95	0.76	2.1435
1-H11	PPC	17.4	18.29	0.89	1.9588
1-H12	PPC	17.4	17.7	0.3	2.9485
2-A01	miR-375	35	32.98	-2.02	8.7543
2-A02	miR-182	34.08	35	0.92	1.1408
2-A03	miR-196a	33.55	35	1.45	0.79
2-A04	miR-10a	21.79	21.91	0.12	1.9862
2-A05	miR-324-5p	25.76	27.13	1.37	0.8351
2-A06	miR-137	24.71	24.98	0.27	1.7901
2-A07	miR-378	26.03	26.65	0.62	1.4044
2-A08	miR-135b	30.47	30.78	0.31	1.7411
2-A09	miR-342-3p	25.13	25.82	0.69	1.3379
2-A10	miR-205	32.95	34.66	1.71	0.6598
2-A11	miR-192	28.07	28.44	0.37	1.6702

2-A12	miR-10b	23.03	23.19	0.16	1.9319
2-B01	miR-744	26.66	27.74	1.08	1.021
2-B02	miR-363	32.95	34.75	1.8	0.6199
2-B03	miR-503	27.3	16.06	-11.24	5220.6003
2-B04	miR-130b	26	27.29	1.29	0.8827
2-B05	miR-151-3p	22.38	22.45	0.07	2.0562
2-B06	miR-214	33.09	34.62	1.53	0.7474
2-B07	miR-454	24.48	24.98	0.5	1.5263
2-B08	miR-379	26.83	27.06	0.23	1.8404
2-B09	miR-301a	26.99	28.09	1.1	1.007
2-B10	miR-98	30.01	30.77	0.76	1.2746
2-B11	miR-34a	25.9	28.69	2.79	0.3121
2-B12	miR-33a	31.95	33.33	1.38	0.8293
2-C01	miR-339-3p	26.01	27.21	1.2	0.9395
2-C02	miR-301b	27.29	28.46	1.17	0.9593
2-C03	miR-193b	24.69	25.81	1.12	0.9931
2-C04	miR-652	26.89	28.48	1.59	0.717
2-C05	miR-20b	23.7	24.23	0.53	1.4948
2-C06	miR-138	33.72	34.72	1	1.0792
2-C07	miR-199a-3p	32.55	33.96	1.41	0.8123
2-C08	miR-183	35	35	0	2.1585
2-C09	miR-134	27.41	27.94	0.53	1.4948
2-C10	miR-132	27.22	27.66	0.44	1.5911
2-C11	miR-148a	29.27	30.41	1.14	0.9794
2-C12	miR-218	26.12	26.33	0.21	1.8661
2-D01	miR-365	23.73	24.67	0.94	1.1251
2-D02	miR-339-5p	25.85	27.26	1.41	0.8123
2-D03	miR-497	26.8	29.06	2.26	0.4506
2-D04	miR-193a-5p	24.82	25.79	0.97	1.1019
2-D05	miR-625	29.7	31.48	1.78	0.6285
2-D06	miR-488	35	35	0	2.1585
2-D07	miR-129-5p	30.91	31.73	0.82	1.2226
2-D08	miR-345	26.26	27.87	1.61	0.7071
2-D09	miR-518b	35	35	0	2.1585
2-D10	miR-517a	35	35	0	2.1585
2-D11	miR-421	25.57	25.85	0.28	1.7777
2-D12	miR-197	25.99	27.02	1.03	1.057
2-E01	miR-17*	28.63	30.74	2.11	0.5
2-E02	miR-18b	29.48	31.09	1.61	0.7071
2-E03	miR-335	29.76	28.78	-0.98	4.2575

2-E04	miR-376a	25.37	25.82	0.45	1.5801
2-E05	miR-361-5p	25.59	26.16	0.57	1.454
2-E06	miR-505	26.28	27.04	0.76	1.2746
2-E07	miR-877	28.12	29.5	1.38	0.8293
2-E08	miR-203	33.74	35	1.26	0.9013
2-E09	miR-411	26.38	26.9	0.52	1.5052
2-E10	miR-152	24.55	24.95	0.4	1.6358
2-E11	miR-532-5p	26.12	27.19	1.07	1.0281
2-E12	miR-342-5p	29.96	31.44	1.48	0.7738
2-F01	miR-373	34.29	35	0.71	1.3195
2-F02	miR-135a	34.05	34.37	0.32	1.7291
2-F03	miR-202	28.92	29.43	0.51	1.5157
2-F04	miR-340	28.23	28.95	0.72	1.3104
2-F05	miR-139-5p	26.95	27.7	0.75	1.2834
2-F06	miR-129-3p	33.65	35	1.35	0.8467
2-F07	miR-545	33.68	34.8	1.12	0.9931
2-F08	miR-338-3p	26.77	27.64	0.87	1.181
2-F09	miR-127-3p	24.81	25.68	0.87	1.181
2-F10	miR-455-3p	24.71	25.23	0.52	1.5052
2-F11	miR-484	25.05	26.11	1.06	1.0353
2-F12	miR-500	26.97	28.32	1.35	0.8467
2-G01	miR-518c	35	35	0	2.1585
2-G02	miR-1	34.84	35	0.16	1.9319
2-G03	miR-590-3p	26.77	26.7	-0.07	2.2658
2-G04	miR-372	31.72	32.5	0.78	1.257
2-G05	miR-148b	28.24	29.56	1.32	0.8645
2-G06	miR-181c	28.48	30.29	1.81	0.6156
2-G07	miR-188-5p	31.3	31.89	0.59	1.434
2-G08	miR-149	29.31	29.83	0.52	1.5052
2-G09	miR-410	29.11	30.63	1.52	0.7526
2-G10	miR-431	27.8	28.72	0.92	1.1408
2-G11	miR-331-3p	26.49	27.97	1.48	0.7738
2-G12	miR-548c-5p	29.2	29.61	0.41	1.6245
2-H01	miR-486-5p	27.85	28.45	0.6	1.4241
2-H02	miR-34c-5p	31.96	33.42	1.46	0.7846
2-H03	miR-629	31.66	32.03	0.37	1.6702
2-H04	miR-452	33.33	34.05	0.72	1.3104
2-H05	SNORD48	27.4	29.68	2.28	0.4444
2-H06	SNORD47	24.31	25.98	1.67	0.6783
2-H07	SNORD44	20.92	22.08	1.16	0.9659

2-H08	RNU6-2	22.76	23.87	1.11	1
2-H09	miRTC	19.8	20.49	0.69	1.3379
2-H10	miRTC	19.39	20.01	0.62	1.4044
2-H11	PPC	18.45	18.77	0.32	1.7291
2-H12	PPC	18.7	18.7	0	2.1585
3-A01	miR-574-5p	25.74	27.07	1.33	1.1408
3-A02	miR-184	29.24	31.31	2.07	0.683
3-A03	miR-660	24.59	25.84	1.25	1.2058
3-A04	miR-337-5p	31.99	33.69	1.7	0.8827
3-A05	miR-146b-5p	29.08	29.79	0.71	1.7532
3-A06	miR-432	29.13	30.78	1.65	0.9138
3-A07	miR-370	27.33	28.52	1.19	1.257
3-A08	miR-95	32.5	33.22	0.72	1.7411
3-A09	miR-206	32.65	35	2.35	0.5625
3-A10	miR-873	33.07	34.85	1.78	0.8351
3-A11	miR-532-3p	25.41	26.23	0.82	1.6245
3-A12	miR-139-3p	28.23	29.36	1.13	1.3104
3-B01	miR-524-5p	32.36	35	2.64	0.4601
3-B02	miR-188-3p	26.95	28.04	1.09	1.3472
3-B03	miR-590-5p	26.01	27.87	1.86	0.79
3-B04	miR-455-5p	24.93	25.77	0.84	1.6021
3-B05	miR-331-5p	29.47	30.83	1.36	1.1173
3-B06	miR-429	33.21	35	1.79	0.8293
3-B07	miR-362-5p	26.43	27.2	0.77	1.6818
3-B08	miR-525-3p	32.42	34.78	2.36	0.5586
3-B09	miR-493	29.78	31.03	1.25	1.2058
3-B10	miR-526b	33.78	34.86	1.08	1.3566
3-B11	miR-190	30.93	31.55	0.62	1.8661
3-B12	miR-515-5p	33.72	35	1.28	1.181
3-C01	miR-665	26.49	28.86	2.37	0.5548
3-C02	miR-147	30.59	32.58	1.99	0.722
3-C03	miR-361-3p	25.01	26.23	1.22	1.2311
3-C04	miR-514	32.77	35	2.23	0.6113
3-C05	miR-376b	27.52	28.88	1.36	1.1173
3-C06	miR-582-5p	27.91	28.66	0.75	1.7053
3-C07	miR-187	28.2	30.39	2.19	0.6285
3-C08	miR-671-5p	31.69	33.49	1.8	0.8236
3-C09	miR-487b	27.76	29.39	1.63	0.9266
3-C10	miR-651	32.78	34.15	1.37	1.1096
3-C11	miR-219-5p	31.6	33.72	2.12	0.6598

3-C12	miR-299-3p	30.99	33.06	2.07	0.683
3-D01	miR-449a	29.35	32.6	3.25	0.3015
3-D02	miR-369-3p	26	27.23	1.23	1.2226
3-D03	miR-219-2-3p	32.06	34.82	2.76	0.4234
3-D04	miR-105	33.12	34.94	1.82	0.8123
3-D05	miR-551b	32.64	33.87	1.23	1.2226
3-D06	miR-542-5p	31.91	33.91	2	0.717
3-D07	miR-542-3p	27.39	27.7	0.31	2.3134
3-D08	miR-618	34.08	35	0.92	1.5157
3-D09	miR-502-3p	27.17	28.02	0.85	1.5911
3-D10	miR-519a	33.16	34.92	1.76	0.8467
3-D11	miR-181d	27.45	28.91	1.46	1.0425
3-D12	miR-382	25.7	26.56	0.86	1.5801
3-E01	miR-508-3p	34.3	35	0.7	1.7654
3-E02	miR-450a	25.25	26.31	1.06	1.3755
3-E03	miR-127-5p	30.8	32.94	2.14	0.6507
3-E04	miR-523	33.43	35	1.57	0.9659
3-E05	miR-589	29.9	30.84	0.94	1.4948
3-E06	miR-369-5p	29.16	29.64	0.48	2.0562
3-E07	miR-615-3p	33.84	35	1.16	1.2834
3-E08	miR-527	33.2	35	1.8	0.8236
3-E09	miR-576-3p	30.04	30.86	0.82	1.6245
3-E10	miR-337-3p	24.14	24.64	0.5	2.0279
3-E11	miR-362-3p	26	27.25	1.25	1.2058
3-E12	miR-515-3p	35	33.09	-1.91	10.7779
3-F01	miR-518a-3p	30.91	32.47	1.56	0.9727
3-F02	miR-885-5p	28.78	30.11	1.33	1.1408
3-F03	miR-433	29.41	31.66	2.25	0.6029
3-F04	miR-512-3p	30.47	31.77	1.3	1.1647
3-F05	miR-548d-5p	29.87	30.31	0.44	2.114
3-F06	miR-133b	32.83	35	2.17	0.6373
3-F07	miR-296-5p	34.12	34.72	0.6	1.8921
3-F08	miR-371-3p	33.75	35	1.25	1.2058
3-F09	miR-330-3p	26.06	26.8	0.74	1.7171
3-F10	miR-329	29.25	31.02	1.77	0.8409
3-F11	miR-495	25.28	26.64	1.36	1.1173
3-F12	miR-450b-5p	29.91	30.8	0.89	1.5476
3-G01	miR-758	29.57	30.33	0.76	1.6935
3-G02	miR-522	33.82	35	1.18	1.2658
3-G03	miR-323-3p	25.88	26.7	0.82	1.6245

3-G04	miR-889	29.71	30.76	1.05	1.3851
3-G05	miR-208b	33.09	35	1.91	0.7631
3-G06	miR-487a	30.58	32.19	1.61	0.9395
3-G07	miR-628-3p	28.58	29.23	0.65	1.8277
3-G08	miR-628-5p	28.86	29.07	0.21	2.4794
3-G09	miR-671-3p	27.75	29.31	1.56	0.9727
3-G10	miR-485-3p	27.41	29.01	1.6	0.9461
3-G11	miR-548d-3p	30.21	30.76	0.55	1.9588
3-G12	miR-383	30.9	34.99	4.09	0.1684
3-H01	miR-548b-3p	31.66	33.11	1.45	1.0497
3-H02	miR-215	32.95	35	2.05	0.6926
3-H03	miR-520d-5p	33.17	35	1.83	0.8066
3-H04	miR-520d-3p	33.71	35	1.29	1.1728
3-H05	SNORD48	26.82	29.87	3.05	0.3463
3-H06	SNORD47	23.76	25.56	1.8	0.8236
3-H07	SNORD44	20.16	21.77	1.61	0.9395
3-H08	RNU6-2	22.15	23.67	1.52	1
3-H09	miRTC	19.01	20.11	1.1	1.3379
3-H10	miRTC	18.78	19.86	1.08	1.3566
3-H11	PPC	17.87	18.62	0.75	1.7053
3-H12	PPC	17.91	18.34	0.43	2.1287
4-A01	miR-584	29.83	30.34	0.51	1.6358
4-A02	miR-513a-5p	33.56	33.31	-0.25	2.7702
4-A03	miR-579	31.67	32.78	1.11	1.0792
4-A04	miR-498	35	35	0	2.3295
4-A05	miR-550	29.87	30.05	0.18	2.0562
4-A06	miR-556-5p	31.75	31.01	-0.74	3.8906
4-A07	miR-380	35	34.96	-0.04	2.395
4-A08	miR-491-3p	31.26	30.98	-0.28	2.8284
4-A09	miR-576-5p	29.68	29.55	-0.13	2.5491
4-A10	miR-597	34.31	34.38	0.07	2.2191
4-A11	miR-504	34.05	33.6	-0.45	3.1821
4-A12	miR-520g	34.07	33.71	-0.36	2.9897
4-B01	miR-642	34.18	33.57	-0.61	3.5554
4-B02	miR-875-5p	33.74	33.18	-0.56	3.4343
4-B03	miR-875-3p	33.66	33.29	-0.37	3.0105
4-B04	miR-501-5p	27.68	28.31	0.63	1.5052
4-B05	miR-501-3p	26.98	27.67	0.69	1.4439
4-B06	miR-544	33.46	34.89	1.43	0.8645
4-B07	miR-548a-5p	31.97	31.91	-0.06	2.4284

4-B08	miR-548a-3p	31.16	32.27	1.11	1.0792
4-B09	miR-422a	26.68	27.13	0.45	1.7053
4-B10	miR-489	29.25	29.56	0.31	1.879
4-B11	miR-636	23.95	24.71	0.76	1.3755
4-B12	miR-198	32.76	32.61	-0.15	2.5847
4-C01	miR-496	29.7	29.64	-0.06	2.4284
4-C02	miR-518d-3p	32.27	32.15	-0.12	2.5315
4-C03	miR-524-3p	33.72	33.17	-0.55	3.4105
4-C04	miR-519b-5p	32.67	32.21	-0.46	3.2043
4-C05	miR-519c-3p	34.52	33.8	-0.72	3.8371
4-C06	miR-516a-3p	33.77	33.72	-0.05	2.4116
4-C07	miR-502-5p	32.77	33.16	0.39	1.7777
4-C08	miR-512-5p	33.86	33.94	0.08	2.2038
4-C09	miR-566	33.38	32.08	-1.3	5.7358
4-C10	miR-548c-3p	33.96	33.81	-0.15	2.5847
4-C11	miR-555	34.18	33.3	-0.88	4.2871
4-C12	miR-492	33.97	33.12	-0.85	4.1989
4-D01	miR-638	26.49	26.37	-0.12	2.5315
4-D02	miR-412	31.86	31.48	-0.38	3.0314
4-D03	miR-588	34.68	34	-0.68	3.7321
4-D04	miR-650	33.14	33.41	0.27	1.9319
4-D05	miR-619	33.75	33.06	-0.69	3.7581
4-D06	miR-543	27.99	28.99	1	1.1647
4-D07	miR-643	33.61	33.22	-0.39	3.0525
4-D08	miR-603	31.8	35	3.2	0.2535
4-D09	miR-602	25.39	26.28	0.89	1.257
4-D10	miR-563	33.65	32.98	-0.67	3.7064
4-D11	miR-558	33.83	34.06	0.23	1.9862
4-D12	miR-657	34.37	33.16	-1.21	5.3889
4-E01	miR-511	33.58	33.25	-0.33	2.9282
4-E02	miR-595	32.19	31.68	-0.51	3.3173
4-E03	miR-613	32.88	33.04	0.16	2.0849
4-E04	miR-802	34.57	34.47	-0.1	2.4967
4-E05	miR-583	35	34.32	-0.68	3.7321
4-E06	miR-384	35	35	0	2.3295
4-E07	miR-611	32.3	32.27	-0.03	2.3784
4-E08	miR-575	30.95	30.61	-0.34	2.9485
4-E09	miR-658	33.56	32.72	-0.84	4.1699
4-E10	miR-637	30.68	30.29	-0.39	3.0525
4-E11	miR-580	33.93	33.42	-0.51	3.3173

4-E12	miR-564	29.53	29.43	-0.1	2.4967
4-F01	miR-610	31.41	31.6	0.19	2.042
4-F02	miR-633	34.74	34.16	-0.58	3.4822
4-F03	miR-562	33.7	32.85	-0.85	4.1989
4-F04	miR-614	27.64	27.97	0.33	1.8532
4-F05	miR-325	34.91	34.83	-0.08	2.4623
4-F06	miR-600	33.13	32.92	-0.21	2.6945
4-F07	miR-630	33.54	33.06	-0.48	3.249
4-F08	miR-298	33.84	33.15	-0.69	3.7581
4-F09	miR-622	30.76	30.6	-0.16	2.6027
4-F10	miR-626	33.71	33.07	-0.64	3.6301
4-F11	miR-659	29.61	29.06	-0.55	3.4105
4-F12	miR-585	33.65	33.07	-0.58	3.4822
4-G01	miR-639	30.33	30.34	0.01	2.3134
4-G02	miR-220c	34.1	33.48	-0.62	3.5801
4-G03	miR-211	34.17	33.98	-0.19	2.6574
4-G04	miR-623	33.47	33.74	0.27	1.9319
4-G05	miR-641	32.89	32.56	-0.33	2.9282
4-G06	miR-557	34.34	34.21	-0.13	2.5491
4-G07	miR-212	29.11	29.16	0.05	2.2501
4-G08	miR-632	32.73	32.65	-0.08	2.4623
4-G09	miR-567	34.45	33.47	-0.98	4.5948
4-G10	miR-605	33.67	33.58	-0.09	2.4794
4-G11	miR-208a	33.72	32.65	-1.07	4.8906
4-G12	miR-448	33.56	32.56	-1	4.6589
4-H01	miR-621	34.33	33.22	-1.11	5.0281
4-H02	miR-648	33.09	32.23	-0.86	4.2281
4-H03	miR-190b	33.39	32.75	-0.64	3.6301
4-H04	miR-587	34.61	33.68	-0.93	4.4383
4-H05	SNORD48	26.94	28.51	1.57	0.7846
4-H06	SNORD47	23.78	25.09	1.31	0.9395
4-H07	SNORD44	20.26	21.29	1.03	1.1408
4-H08	RNU6-2	22.1	23.32	1.22	1
4-H09	miRTC	19.22	19.8	0.58	1.5583
4-H10	miRTC	18.79	19.37	0.58	1.5583
4-H11	PPC	17.96	17.92	-0.04	2.395
4-H12	PPC	17.93	17.86	-0.07	2.4453

PCR array catalog number: MAH-200

1-A01	let-7a*	24.21	24.18	0.325335	0.5471
1-A02	let-7a-2*	26.82	26.71	0.05329	0.5783
1-A03	let-7b*	27.87	27.68	0.025737	0.6113
1-A04	let-7d*	24.04	23.76	0.366021	0.6507
1-A05	let-7f-1*	29	28.72	0.01176	0.6507
1-A06	let-7f-2*	29.39	28.93	0.008974	0.7371
1-A07	let-7g*	30.46	29.34	0.004275	1.1647
1-A08	let-7i*	31.15	29.44	0.00265	1.7532
1-A09	miR-103-as	33.46	33.23	0.000534	0.6285
1-A10	miR-106b*	27.96	27.03	0.024181	1.021
1-A11	miR-10b*	31.45	30.96	0.002152	0.7526
1-A12	miR-125b-1*	31.49	30.36	0.002093	1.1728
1-B01	miR-125b-2*	29.05	28.31	0.011359	0.895
1-B02	miR-126*	16.83	16.85	54.1917	0.5285
1-B03	miR-130b*	24.46	24.44	0.273573	0.5434
1-B04	miR-133a	31.82	31.55	0.001665	0.6462
1-B05	miR-138-1*	28.75	28.65	0.013985	0.5743
1-B06	miR-138-2*	28.24	26.93	0.019915	1.3287
1-B07	miR-141*	26.98	27.38	0.047696	0.4061
1-B08	miR-145	31.51	30.77	0.002064	0.895
1-B09	miR-153	35	34.22	0.000184	0.9202
1-B10	miR-15b*	24.97	24.85	0.192109	0.5824
1-B11	miR-181a*	25.56	25.7	0.127627	0.4863
1-B12	miR-18a*	26.81	26.08	0.05366	0.8888
1-C01	miR-193a-3p	28.65	28	0.014989	0.8409
1-C02	miR-193b*	24.69	24.17	0.233258	0.7684
1-C03	miR-199a-5p	31.96	31.89	0.001511	0.5625
1-C04	miR-146b-3p	32.64	33.08	0.000943	0.395
1-C05	miR-19a*	33.62	33.46	0.000478	0.5987
1-C06	miR-19b-2*	34.97	34.1	0.000188	0.9794
1-C07	miR-200a	34.59	35	0.000244	0.4033
1-C08	miR-200a*	31.61	31.3	0.001926	0.6643
1-C09	miR-297	33.97	33.6	0.000375	0.6926
1-C10	miR-21*	28.09	26.24	0.022097	1.9319
1-C11	miR-216a	27.21	25.5	0.040667	1.7532
1-C12	miR-216b	28.93	29.22	0.012344	0.4383
1-D01	miR-217	20.04	19.83	5.856343	0.6199
1-D02	miR-22*	26.26	25.08	0.078563	1.2142
1-D03	miR-221	22.79	21.77	0.870551	1.0867
1-D04	miR-224	31.61	30.29	0.001926	1.3379

1-D05	miR-24-1*	31.9	30.37	0.001575	1.5476
1-D06	miR-24-2*	26.52	25.37	0.065607	1.1892
1-D07	miR-25*	30.14	29.87	0.005336	0.6462
1-D08	miR-27a*	24.22	22.58	0.323088	1.6702
1-D09	miR-29a*	28.59	27.07	0.015625	1.5369
1-D10	miR-29b-1*	27.66	26.3	0.02977	1.3755
1-D11	miR-29b-2*	29.61	28.85	0.007705	0.9075
1-D12	miR-29c*	28.39	27.63	0.017948	0.9075
1-E01	miR-302a*	34.17	33.73	0.000327	0.727
1-E02	miR-302c*	33.31	33.85	0.000593	0.3686
1-E03	miR-302d*	34.03	33.8	0.00036	0.6285
1-E04	miR-30a*	24.57	24.34	0.25349	0.6285
1-E05	miR-30c-1*	33.38	33.06	0.000565	0.669
1-E06	miR-30c-2*	31.91	30.33	0.001565	1.6021
1-E07	miR-30e*	25.06	24.96	0.180491	0.5743
1-E08	miR-31	21.96	20.82	1.547565	1.181
1-E09	miR-324-3p	27.72	26.82	0.028557	1
1-E10	miR-326	27.8	27.08	0.027017	0.8827
1-E11	miR-328	29.09	28.67	0.011049	0.717
1-E12	miR-33b	34.38	33.76	0.000282	0.8236
1-F01	miR-346	29.94	29.76	0.00613	0.6071
1-F02	miR-323-5p	27	26.63	0.047039	0.6926
1-F03	miR-367*	35	35	0.000184	0.5359
1-F04	miR-374b*	29.75	28.74	0.006992	1.0792
1-F05	miR-381	29.35	28.04	0.009227	1.3287
1-F06	miR-409-3p	25.21	24.9	0.162668	0.6643
1-F07	miR-409-5p	27.79	27.35	0.027205	0.727
1-F08	miR-411*	28.93	28.77	0.012344	0.5987
1-F09	miR-424*	27.32	26.24	0.037681	1.1329
1-F10	miR-425*	27.62	27.13	0.030607	0.7526
1-F11	miR-431*	30.41	30.73	0.004425	0.4293
1-F12	miR-451	34.68	33.72	0.000229	1.0425
1-G01	miR-483-3p	32.5	33.36	0.001039	0.2952
1-G02	miR-486-3p	33.54	34.7	0.000506	0.2398
1-G03	miR-490-3p	32.38	32.74	0.00113	0.4175
1-G04	miR-506	33.95	34.68	0.00038	0.3231
1-G05	miR-509-3-5p	33.63	33.47	0.000475	0.5987
1-G06	miR-509-5p	33.95	33.21	0.00038	0.895
1-G07	miR-510	33.3	33.56	0.000597	0.4475
1-G08	miR-516b	32.87	32.67	0.000804	0.6156

1-G09	miR-518a-5p	34.56	34.87	0.000249	0.4323
1-G10	miR-518f	35	35	0.000184	0.5359
1-G11	miR-9*	31.91	33.24	0.001565	0.2132
1-G12	miR-92a-1*	30.62	29.85	0.003826	0.9138
1-H01	miR-92a-2*	35	33.78	0.000184	1.2483
1-H02	miR-93*	25.94	25.96	0.098073	0.5285
1-H03	miR-99b*	27.01	26.26	0.046714	0.9013
1-H04	miR-99b	20.15	20.15	5.426417	0.5359
1-H05	SNORD48	27.41	25.75	0.035403	1.6935
1-H06	SNORD47	24.26	23.17	0.314253	1.1408
1-H07	SNORD44	20.77	19.88	3.530812	0.9931
1-H08	RNU6-2	22.59	21.69	1	1
1-H09	miRTC	19.26	19.25	10.056107	0.5396
1-H10	miRTC	19.08	19.01	11.392402	0.5625
1-H11	PPC	18.01	18.24	23.917588	0.4569
1-H12	PPC	17.98	18.51	24.420147	0.3711
2-A01	miR-129*	35	33.33	0.000171	1.1892
2-A02	miR-136*	27.84	25.99	0.024518	1.3472
2-A03	miR-145*	33.68	33.2	0.000428	0.5212
2-A04	miR-132*	30.52	28.78	0.003826	1.2483
2-A05	miR-1908	28.36	26.29	0.017098	1.5692
2-A06	miR-191*	28.93	27.82	0.011518	0.8066
2-A07	miR-200b*	32.76	31.16	0.00081	1.1329
2-A08	miR-202*	35	35	0.000171	0.3737
2-A09	miR-20a*	26.95	25.72	0.045437	0.8766
2-A10	miR-219-1-3p	31.32	29.32	0.002197	1.4948
2-A11	miR-220b	34.49	33.56	0.000244	0.712
2-A12	miR-221*	24.23	23.3	0.29937	0.712
2-B01	miR-31*	29.19	27.16	0.009618	1.5263
2-B02	miR-299-5p	30.13	28.85	0.005013	0.9075
2-B03	miR-300	33.06	35	0.000658	0.0974
2-B04	miR-302b*	34.37	32.42	0.000265	1.4439
2-B05	miR-30b*	32.12	30.61	0.001262	1.0644
2-B06	miR-320b	26.77	25.46	0.051474	0.9266
2-B07	miR-320c	31.06	29.08	0.002631	1.4743
2-B08	miR-320d	30.15	28.85	0.004944	0.9202
2-B09	miR-224*	32.28	31.68	0.00113	0.5664
2-B10	miR-340*	27.93	27.22	0.023035	0.6113
2-B11	miR-34b	31.12	29.87	0.002524	0.8888
2-B12	miR-34b*	34.33	32.77	0.000273	1.1019

2-C01	miR-135b*	32.75	31.09	0.000816	1.181
2-C02	miR-363*	34.01	31.27	0.000341	2.4967
2-C03	miR-371-5p	32.29	30.67	0.001122	1.1487
2-C04	miR-373*	21.64	21.08	1.802501	0.551
2-C05	miR-376a*	29.83	27.97	0.006172	1.3566
2-C06	miR-377*	33.61	31.97	0.000449	1.1647
2-C07	miR-378*	31.2	29.74	0.002388	1.0281
2-C08	miR-380*	30.31	28.56	0.004425	1.257
2-C09	miR-432*	32.11	30.73	0.001271	0.9727
2-C10	miR-449b	32.9	31.42	0.000735	1.0425
2-C11	miR-452*	33.35	32.66	0.000538	0.6029
2-C12	miR-454*	27.53	26.97	0.030395	0.551
2-D01	miR-485-5p	27.53	26.24	0.030395	0.9138
2-D02	miR-488*	33.4	31.25	0.00052	1.6586
2-D03	miR-500*	28.1	26.7	0.020475	0.9862
2-D04	miR-577	35	33.37	0.000171	1.1567
2-D05	miR-513a-3p	34.54	32.63	0.000236	1.4044
2-D06	miR-513b	35	33.19	0.000171	1.3104
2-D07	miR-513c	35	34.48	0.000171	0.5359
2-D08	miR-517b	35	33.71	0.000171	0.9138
2-D09	miR-518c*	33.83	32.06	0.000386	1.2746
2-D10	miR-518f*	33.78	31.93	0.000399	1.3472
2-D11	miR-519d	33.24	33.1	0.000581	0.4118
2-D12	miR-519e	34.91	32.91	0.000182	1.4948
2-E01	miR-519e*	34.18	33.37	0.000303	0.6552
2-E02	miR-520e	35	32.87	0.000171	1.6358
2-E03	miR-520f	34.74	32.14	0.000205	2.2658
2-E04	miR-521	34.66	33.01	0.000217	1.1728
2-E05	miR-526b*	35	33.06	0.000171	1.434
2-E06	miR-539	32.06	30.67	0.001316	0.9794
2-E07	miR-549	33.64	32.32	0.00044	0.933
2-E08	miR-550*	31.99	30.18	0.001381	1.3104
2-E09	miR-551a	26.99	26.02	0.044194	0.732
2-E10	miR-554	30.62	28.65	0.00357	1.4641
2-E11	miR-559	29.67	29.32	0.006896	0.4763
2-E12	miR-561	34.5	32.66	0.000242	1.3379
2-F01	miR-570	31.92	30.65	0.00145	0.9013
2-F02	miR-571	30.32	29.72	0.004395	0.5664
2-F03	miR-572	26.65	24.97	0.055939	1.1975
2-F04	miR-574-3p	22.13	21.46	1.283426	0.5946

2-F05	miR-578	35	33.13	0.000171	1.366
2-F06	miR-581	35	33.48	0.000171	1.0718
2-F07	miR-609	35	33.49	0.000171	1.0644
2-F08	miR-591	34.79	32.47	0.000198	1.8661
2-F09	miR-607	35	32.6	0.000171	1.9725
2-F10	miR-608	30.08	28.25	0.00519	1.3287
2-F11	miR-612	30.83	29.23	0.003086	1.1329
2-F12	miR-616*	29.42	28.56	0.008201	0.6783
2-G01	miR-624*	29.49	28.62	0.007812	0.683
2-G02	miR-635	34.33	32.66	0.000273	1.1892
2-G03	miR-627	30.7	29.04	0.003377	1.181
2-G04	miR-646	30.1	28.42	0.005119	1.1975
2-G05	miR-647	35	30.9	0.000171	6.4086
2-G06	miR-649	34.35	32.43	0.000269	1.4142
2-G07	miR-662	29.09	27.91	0.010309	0.8467
2-G08	miR-708	31.15	30.24	0.002472	0.7022
2-G09	miR-708*	35	33.13	0.000171	1.366
2-G10	miR-766	26.83	25.77	0.049378	0.7792
2-G11	miR-767-5p	33.32	31.65	0.000549	1.1892
2-G12	miR-769-5p	27.82	26.28	0.024861	1.0867
2-H01	miR-92b*	27.72	25.65	0.026645	1.5692
2-H02	miR-450b-3p	34.78	32.55	0.0002	1.7532
2-H03	miR-491-5p	29.01	27.25	0.010896	1.2658
2-H04	miR-573	35	32.6	0.000171	1.9725
2-H05	SNORD48	27.11	24.95	0.040667	1.6702
2-H06	SNORD47	24.2	22.73	0.30566	1.0353
2-H07	SNORD44	20.76	19.4	3.317278	0.9593
2-H08	RNU6-2	22.49	21.07	1	1
2-H09	miRTC	19.46	18.84	8.168097	0.5743
2-H10	miRTC	19	18.53	11.235559	0.5176
2-H11	PPC	18.17	17.82	19.973289	0.4763
2-H12	PPC	18.02	17.85	22.161751	0.4204
3-A01	miR-1178	35	35	0.000198	0.5783
3-A02	miR-1179	31.05	30.95	0.003065	0.6199
3-A03	miR-1180	28.52	27.92	0.017701	0.8766
3-A04	miR-1181	20.48	20.38	4.658934	0.6199
3-A05	miR-1182	31.86	33.3	0.001748	0.2132
3-A06	miR-1183	30.98	31.94	0.003217	0.2973
3-A07	miR-1184	32.17	32.81	0.00141	0.3711
3-A08	miR-1185	35	32.67	0.000198	2.9079

3-A09	miR-1201	24.06	22.9	0.389582	1.2924
3-A10	miR-1202	30.91	31.68	0.003377	0.3392
3-A11	miR-1203	29.67	29.02	0.007977	0.9075
3-A12	miR-1204	35	35	0.000198	0.5783
3-B01	miR-1205	33.81	35	0.000452	0.2535
3-B02	miR-1206	35	35	0.000198	0.5783
3-B03	miR-1207-3p	33.96	35	0.000408	0.2813
3-B04	miR-1207-5p	28.31	29.94	0.020475	0.1869
3-B05	miR-1208	25.96	25.92	0.104386	0.5946
3-B06	miR-1224-3p	34.59	33.56	0.000263	1.181
3-B07	miR-1224-5p	28.19	27.95	0.022251	0.683
3-B08	miR-1225-3p	23.3	22.65	0.659754	0.9075
3-B09	miR-1225-5p	29.86	30.92	0.006992	0.2774
3-B10	miR-1226	30.38	30.11	0.004876	0.6974
3-B11	miR-135a*	23.51	23.14	0.570382	0.7474
3-B12	miR-144*	35	35	0.000198	0.5783
3-C01	miR-143*	34.78	34.29	0.000231	0.8123
3-C02	miR-185*	32.29	32.97	0.001298	0.361
3-C03	miR-186*	34.91	33.91	0.000211	1.1567
3-C04	miR-205*	34.52	35	0.000277	0.4147
3-C05	miR-222*	29.94	30.12	0.006615	0.5105
3-C06	miR-146a*	35	35	0.000198	0.5783
3-C07	miR-148a*	34.19	35	0.000348	0.3299
3-C08	miR-379*	31.77	31	0.001861	0.9862
3-C09	miR-499-3p	35	35	0.000198	0.5783
3-C10	miR-499-5p	35	35	0.000198	0.5783
3-C11	miR-541	33.61	33.38	0.00052	0.6783
3-C12	miR-541*	33.87	33.69	0.000434	0.6552
3-D01	miR-548e	29.94	30.07	0.006615	0.5285
3-D02	miR-548h	32.31	33.05	0.00128	0.3463
3-D03	miR-548i	29.31	29.16	0.010237	0.6417
3-D04	miR-548j	31.66	31.61	0.002008	0.5987
3-D05	miR-548k	30.65	30.01	0.004044	0.9013
3-D06	miR-548l	30.66	30.4	0.004016	0.6926
3-D07	miR-548m	35	35	0.000198	0.5783
3-D08	miR-548o	31.06	30.61	0.003044	0.79
3-D09	miR-548p	32.2	32.25	0.001381	0.5586
3-D10	miR-548g	34.9	35	0.000213	0.5396
3-D11	miR-20b*	32.33	33.14	0.001262	0.3299
3-D12	miR-593	31.89	31.74	0.001712	0.6417

3-E01	miR-148b*	31.87	31.59	0.001736	0.7022
3-E02	miR-154*	28.4	27.09	0.019237	1.434
3-E03	miR-155*	28.22	28.82	0.021793	0.3816
3-E04	miR-629*	28.42	28.69	0.018972	0.4796
3-E05	miR-653	31.98	31.59	0.001609	0.7579
3-E06	miR-654-3p	31.51	31.34	0.002228	0.6507
3-E07	miR-663	25.91	25.81	0.108067	0.6199
3-E08	miR-663b	28.61	28.87	0.016631	0.483
3-E09	miR-664	25.61	25.19	0.133046	0.7738
3-E10	miR-675	27.76	28.15	0.029977	0.4414
3-E11	miR-675*	28.65	28.46	0.016176	0.6598
3-E12	miR-720	20.57	20.55	4.377175	0.5864
3-F01	miR-760	28.11	27.82	0.023519	0.7071
3-F02	miR-767-3p	35	35	0.000198	0.5783
3-F03	miR-769-3p	35	33.99	0.000198	1.1647
3-F04	miR-770-5p	28.73	29.03	0.015303	0.4698
3-F05	miR-220a	34.86	35	0.000219	0.5249
3-F06	miR-876-3p	35	35	0.000198	0.5783
3-F07	miR-886-3p	32.7	31.59	0.000977	1.2483
3-F08	miR-886-5p	27.22	26.66	0.043586	0.8526
3-F09	miR-888	33.76	33.05	0.000468	0.9461
3-F10	miR-888*	32.1	31.62	0.00148	0.8066
3-F11	miR-892a	34.06	35	0.00038	0.3015
3-F12	miR-195*	28.1	28.06	0.023683	0.5946
3-G01	miR-891a	32.73	32.67	0.000956	0.6029
3-G02	miR-891b	35	35	0.000198	0.5783
3-G03	miR-920	34.18	34.38	0.00035	0.5035
3-G04	miR-922	33.66	33.54	0.000502	0.6285
3-G05	miR-223*	35	35	0.000198	0.5783
3-G06	miR-335*	25.65	25.8	0.129408	0.5212
3-G07	miR-935	26.05	25.91	0.098073	0.6373
3-G08	miR-936	30.54	30.75	0.004364	0.5
3-G09	miR-937	30.92	31.45	0.003354	0.4005
3-G10	miR-938	32.65	33.59	0.001011	0.3015
3-G11	miR-939	32.49	32.87	0.00113	0.4444
3-G12	miR-940	18.48	18.27	18.635737	0.669
3-H01	miR-942	29.49	29.36	0.009037	0.6329
3-H02	miR-943	26.79	26.82	0.05872	0.5664
3-H03	miR-944	35	35	0.000198	0.5783
3-H04	miR-548n	32.14	31.63	0.00144	0.8236

3-H05	SNORD48	27.54	26.1	0.034915	1.5692
3-H06	SNORD47	24.57	23.52	0.273573	1.1975
3-H07	SNORD44	21.09	20.42	3.052518	0.9202
3-H08	RNU6-2	22.7	21.91	1	1
3-H09	miRTC	19.58	19.57	8.693879	0.5824
3-H10	miRTC	19.27	19.19	10.777869	0.6113
3-H11	PPC	18.39	18.67	19.835323	0.4763
3-H12	PPC	18.34	18.62	20.534814	0.4763
4-A01	let-7c*	32.39	32.33	0.000627	0.722
4-A02	let-7e*	26.12	26.4	0.048361	0.5704
4-A03	miR-103-2*	28.32	27.91	0.010525	0.9202
4-A04	miR-105*	31.8	35	0.000943	0.0754
4-A05	miR-106a*	34.15	35	0.000185	0.3842
4-A06	miR-1197	34.58	32.21	0.000137	3.5801
4-A07	miR-122*	33.75	34.42	0.000244	0.4353
4-A08	miR-1227	31.17	31.67	0.00146	0.4897
4-A09	miR-1228	23.11	23.12	0.389582	0.6878
4-A10	miR-1229	29.1	29.73	0.00613	0.4475
4-A11	miR-1231	28.49	27.77	0.009355	1.1408
4-A12	miR-1233	29.27	29.64	0.005448	0.5359
4-B01	miR-1234	20.97	21.02	1.717131	0.669
4-B02	miR-1236	31.13	31.63	0.001501	0.4897
4-B03	miR-1237	24.75	24.76	0.125	0.6878
4-B04	miR-1238	28.8	30.03	0.007546	0.2952
4-B05	miR-124*	32.65	33.64	0.000523	0.3487
4-B06	miR-1243	34.67	34.31	0.000129	0.8888
4-B07	miR-1244	33.82	34.01	0.000233	0.6071
4-B08	miR-1245	31.8	31.8	0.000943	0.6926
4-B09	miR-1246	17.1	17.27	25.106691	0.6156
4-B10	miR-1247	22.9	23.13	0.450625	0.5905
4-B11	miR-1249	29.96	29.65	0.003377	0.8586
4-B12	miR-1250	30.71	29.91	0.002008	1.2058
4-C01	miR-1251	32.93	32.07	0.000431	1.257
4-C02	miR-1252	33.78	33.09	0.000239	1.1173
4-C03	miR-1253	29.71	29.73	0.004016	0.683
4-C04	miR-1258	30.83	33	0.001848	0.1539
4-C05	miR-1259	27.13	24.14	0.024014	5.5022
4-C06	miR-1260	19.05	19.34	6.498019	0.5664
4-C07	miR-1471	31.85	30.92	0.000911	1.3195
4-C08	miR-1262	33.58	33.97	0.000275	0.5285

4-C09	miR-1263	32.14	32.37	0.000745	0.5905
4-C10	miR-1264	32.44	31.88	0.000605	1.021
4-C11	miR-1265	33.98	33.37	0.000208	1.057
4-C12	miR-1266	30.93	30.76	0.001724	0.7792
4-D01	miR-18b*	31.49	30.26	0.001169	1.6245
4-D02	miR-192*	31.97	31.81	0.000838	0.7738
4-D03	miR-194*	33.74	32.08	0.000246	2.1886
4-D04	miR-1267	28.64	29.59	0.008431	0.3585
4-D05	miR-196b*	29.69	29.74	0.004072	0.669
4-D06	miR-1268	26.68	25.65	0.032804	1.4142
4-D07	miR-218-1*	32.77	33.22	0.000482	0.507
4-D08	miR-218-2*	29.26	28.02	0.005486	1.6358
4-D09	miR-1269	32.92	32.89	0.000434	0.7071
4-D10	miR-1270	33.78	32.94	0.000239	1.2397
4-D11	miR-23a*	33.16	31.78	0.000367	1.8025
4-D12	miR-23b*	32.07	30.17	0.000782	2.5847
4-E01	miR-26a-1*	29.05	29.77	0.006346	0.4204
4-E02	miR-26a-2*	26.97	27.78	0.02683	0.395
4-E03	miR-32*	33	33.14	0.000411	0.6285
4-E04	miR-1273	32.61	33.33	0.000538	0.4204
4-E05	miR-33a*	31.02	30.7	0.00162	0.8645
4-E06	miR-33b*	31	30.22	0.001642	1.1892
4-E07	miR-34a*	26.43	25.97	0.03901	0.9526
4-E08	miR-365*	29.55	28.84	0.004487	1.1329
4-E09	miR-374a*	27.03	26.73	0.025737	0.8526
4-E10	miR-449b*	27.87	28.54	0.014378	0.4353
4-E11	miR-497*	33.28	32.5	0.000338	1.1892
4-E12	miR-505*	28.8	28.38	0.007546	0.9266
4-F01	miR-545*	28.22	28.07	0.011281	0.7684
4-F02	miR-1254	31.63	31.69	0.001061	0.6643
4-F03	miR-1255a	34.95	33.94	0.000106	1.3947
4-F04	miR-556-3p	30.52	31.68	0.002291	0.3099
4-F05	miR-569	34.84	34.74	0.000115	0.7423
4-F06	miR-596	23.58	23.3	0.281265	0.8409
4-F07	miR-1271	26.79	26.36	0.030395	0.933
4-F08	miR-599	33.92	33.66	0.000217	0.8293
4-F09	miR-601	27.41	28.09	0.019777	0.4323
4-F10	miR-606	33.78	33.96	0.000239	0.6113
4-F11	miR-615-5p	28.18	27.74	0.011598	0.9395
4-F12	miR-620	33.84	33.09	0.000229	1.1647

4-G01	miR-625*	24.8	25.29	0.120742	0.4931
4-G02	miR-631	29.8	29.95	0.003773	0.6242
4-G03	miR-634	32.28	31.79	0.000676	0.9727
4-G04	miR-1272	33.33	35	0.000327	0.2176
4-G05	miR-655	27.29	26.48	0.021493	1.2142
4-G06	miR-656	25.91	25.99	0.055939	0.6552
4-G07	miR-661	29.38	29.55	0.005048	0.6156
4-G08	miR-664*	32.69	32.78	0.000509	0.6507
4-G09	miR-7-1*	27.77	27.4	0.01541	0.895
4-G10	miR-7-2*	31.55	31.68	0.001122	0.6329
4-G11	miR-1275	28.11	27.17	0.012174	1.3287
4-G12	miR-933	32	31.47	0.000821	1
4-H01	miR-99a*	30.32	28.98	0.002631	1.7532
4-H02	miR-96*	34.33	34.81	0.000163	0.4965
4-H03	miR-1256	34.77	31.95	0.00012	4.8906
4-H04	miR-1257	30.45	30	0.002405	0.9461
4-H05	SNORD48	26.71	25.06	0.032129	2.1735
4-H06	SNORD47	23.48	22.76	0.301452	1.1408
4-H07	SNORD44	19.85	19.45	3.732132	0.9138
4-H08	RNU6-2	21.75	21.22	1	1
4-H09	miRTC	18.47	18.86	9.713559	0.5285
4-H10	miRTC	18.11	18.65	12.466633	0.4763
4-H11	PPC	17.2	17.89	23.425371	0.4293
4-H12	PPC	17.22	17.86	23.102867	0.4444